Neurobehavioural correlates of magnetoreception in rainbow trout (*Oncorhynchus mykiss*)

Von der Fakultät für Mathematik und Naturwissenschaften
der Carl von Ossietzky Universität Oldenburg

zur Erlangung des Grades und Titels eines
Doktor der Naturwissenschaften (Dr. rer. Nat.)

angenommene Dissertation

von Frau Laura Ziegenbalg
geboren am 31.08.1988 in Bremen

Gutachter: Prof. Dr. Michael Winklhofer

Weitere Gutachter:in: Prof. Dr. Gabriele Gerlach

Prof. Dr. Arne Nolte

Tag der Disputation: 20.11.2023

Content

List of Figures

List of Tables

Abbreviations

ABC	Avidin-biotin-peroxidase complex
BAP	Bacterial Alkaline Phosphatase
BORIS	Behavioural Observation Research Interactive Software
CN	Correct negatives
Conc.	Concentration
CP	Correct positives
Cry	Cryptochrome
CS / S+	Conditioned stimulus
DAB	3’3-diaminobenzidine
DiI	1,1'-Dioctadecyl-3,3,3',3'-Tetramethylindocarbocyanine Perchlorate
DMEM	Dulbeccos Modified Eagle Serum
DV	Descending trigeminal root
ECL	Enhanced chemifluorescence
EDTA	Ethylenediaminetetraacetic acid
FBS	Fetal bovine serum
FN	False negatives
FP	False positives
GLM	Generalized linear model
gt	Goat
HRP	Horseradish Peroxidase
IEG	Immediate Early Genes
LVII	Lobus facialis
Mc	Monoclonal
MFN	Medial funicular nucleus
MO	Medulla oblongata
ms	Mouse
MS-222	Ethyl-3-aminobenzoat -methansulfonat
NA	Numerical aperture
NDV	Sensory nucleus
NGS	Normal goat serum
NHS	Normal horse serum
NV	Primary sensory trigeminal nucleus
NVmd	Trigeminal motor nucleus, dorsal part

NVmv	Trigeminal motor nucleus, ventral part
OM	Oncorhynchus mykiss
PBS	Phosphate-buffered saline
PBS-T	Phosphate-buffered saline – Triton X100
pc	Polyclonal
PFA	Paraformaldehyde
PLL	Poly-L-lysine
PrV	Principal trigeminal nuclei
rb	Rabbit
rosV	Trigeminal nerve's ramus opthalmicus superior
S-	Non-reinforced condition
SPE	Solid Phase Extraction
SpV	Spinal trigeminal nuclei
TBS-T	Tris-buffered saline – Triton x100
US	Unconditioned stimulus (such as food)
V1	Trigeminal nerve
ZMF	Zero magnetic field

Summary

Magnetic conditioning in teleost fish

A key objective of the thesis was to establish a behavioural assay that allows for quantifying magnetosensitivity in fish under controlled conditions in the laboratory throughout the year without having to rely on a specific season or stage in the life cycle where ecologically meaningful spontaneous orientation tendencies might occur in the lab species available. Therefore, I used an operant conditioning approach in order to train trout to respond to magnetic field changes in the vertical and horizontal components. Rainbow trout (*Oncorhynchus mykiss*) was chosen as a model species because it had previously proved amenable to operant magnetic conditioning (Shcherbakov et al., 2005; Walker et al., 1997). However, the readout in previous operant conditioning attempts was the striking rate at the feeder, but fish were not discouraged from waiting around the feeder and therefore did not have to invest energy to get to it, which can explain why the striking rate differed only by 20% between reinforced and non-reinforced stimulus. To overcome this problem, we have designed a fully-automated Horner-type shuttle box with two compartments separated by a hurdle (Horner et al., 1961; Portavella, 2004), with a feeder over each compartment, forcing the fish to shuttle across when the conditioned stimulus occurs. Shuttling between the two compartments is registered with a light barrier. Both the magnetic stimulus (changing magnetic field, superimposed on the ambient geomagnetic field), which was to be reinforced with a food reward to become the conditioned stimulus (S+/CS), and the non-reinforced condition (S-, ambient field only) are applied with a computer-controlled sequence. Food reward as a positive reinforcement in a Horner-type shuttle box is a novel approach to studying magnetosensitivity in fish. The protocol consists of several training sessions with reinforcement, followed by recall performances without positive reinforcement.

Naïve rainbow trout were trained to respond to a ±100 µT oscillating magnetic field either in the vertical or horizontal component. In the training phase, S+ was the oscillating magnetic field, and S- were oscillating currents producing no oscillating field (magnetic sham control). In both cases, a light stimulus was co-administered to indicate the start of a trial to the fish. All four fish learned to respond significantly more often to the magnetic field stimulus than sham and maintained the discrimination performance in test trials (without reinforcement) after training. Putting correct and false positive rates in relation to one another, the correct positive responses to the magnetic field stimulus are higher than the 50% level of guessing by chance. Using statistical tests for count data or for proportions (χ^2-test), the ratios are significantly different at a level of $p > 10^{-4}$.

With the setup and paradigm having been established and successfully tested here, it can now be used to study important aspects such as threshold sensitivity and stimulus generalisation, i.e. does a fish trained to respond to one kind of magnetic stimulus also respond to a different kind, and if so, how different can these magnetic stimuli be?

Neuroanatomical basis of magnetoreception

In songbirds, a number of candidate brain areas have been identified in magnetic field perception, such as Cluster N for the light-dependent inclination compass (Zapka et al., 2009) or trigeminal nuclei for map information (Heyers et al., 2010). Key experiments by (Hellinger & Hoffmann, 2012) on rainbow trout also point to the trigeminal system as a site for magnetic intensity and inclination perception. Further, they found that conditioned responses to a 90° direction change persist in darkness, suggesting that compass information in fish – unlike birds – is conveyed through a light-independent pathway. Recent experiments on juvenile medaka (Myklatun et al., 2018) point to an involvement of the lateral hindbrain, from where all cranial sensory nerves emerge, except for the I. (olfactory) and II. (optical) nerve. There are few hints toward the location and internal structure of candidate magnetoreceptor cells, their afferent nerves, and central projections in the brain. Earlier reports of candidate receptor cells in trigeminally innervated, lateral parts of the olfactory organ (Walker et al., 1997) have not stood up to the acid test of independent replication.

A brain atlas for rainbow trout is not available, which would otherwise facilitate studies of brain activity under magnetic stimulation. To identify the key brain areas connected to the trigeminal system, I applied DiI stain crystals on the trigeminal nerve and traced its projections into the brain. These results can now be used to verify the brain areas which, under magnetic stimulation, have differential expression of immediate early genes (IEG) as a proxy for neuronal activity.
While IEG expression studies have been immensely useful in studying magnetic activation patterns in bird brains (Elbers et al., 2017; Heyers et al., 2010; Kobylkov et al., 2020; Zapka et al., 2009), the protocols cannot be transferred to fish brains without first testing if available IEG antibodies against cfos or ZENK also recognise the fish-specific IEG homologues.

For *in vitro* validation of the cFos antibody, I have expressed the cFos homolog from rainbow trout in HEK cells and quantified antibody binding in western blots. In addition, I established a histochemical staining protocol (DAB) to label primary antibodies against IEGs (cFos) for rainbow trout and used it for visualising neuronal activity in stimulus-specific processing regions. When it comes to molecular mapping of behaviour with IEGs, the animal has to be stimulated for up to an hour. During this time, the animal should be as calm as possible to minimise noise in brain activity. I established a free

cortisol ELISA assay as a non-invasive stress indicator for lab fish and recorded the daily variation in cortisol production of (unstimulated) trout to find a suitable time of day for the stimulation experiments. The endocrinological proxy for physiological activity was in turn validated by analysis of video-recorded behaviour at different times of the day, confirming the correlation between low motional activity and low cortisol levels.

Zusammenfassung

Magnetische Konditionierung in Teleost-Fischen

Ein Hauptziel dieser Arbeit war es, einen Verhaltenstest zu etablieren, der es ermöglicht, die Magnetosensitivität von Fischen unter kontrollierten Bedingungen im Labor das ganze Jahr über zu quantifizieren, ohne dabei auf eine bestimmte Jahreszeit oder ein bestimmtes Stadium im Lebenszyklus angewiesen zu sein. Bei den zur Verfügung stehenden Tierarten im Labor könnten ökologisch sinnvolle spontane Orientierungstendenzen auftreten, deren Einfluss auf die Versuche schwer einzuschätzen wären. Daher verwendete ich einen operanten Konditionierungsansatz, um Forellen auf Magnetfeldänderungen in der vertikalen und horizontalen Komponente zu trainieren. Die Regenbogenforelle (*Oncorhynchus mykiss*) wurde als Modellart gewählt, weil sie sich zuvor als zugänglich für operante magnetische Konditionierung erwiesen hatte (Shcherbakov et al., 2005; Walker et al., 1997). Bei früheren Versuchen zur operanten Konditionierung wurde jedoch die Schlagrate am Futterautomaten gemessen. Die Fische wurden allerdings nicht davon abgehalten, in der Nähe des Futterautomaten zu warten, und mussten daher keine Energie aufwenden, um zum Futterautomaten zu gelangen, was erklären könnte, warum sich die Schlagrate zwischen dem verstärkten und dem nicht verstärkten Reiz nur um 20 % unterschied. Um dieses Problem aus dem Weg zu gehen, haben wir eine vollautomatische Shuttlebox nach Horner (Horner et al., 1961; Portavella, 2004) mit zwei durch eine Hürde getrennten Kammern konstruiert. Überhalb jeder Kammer befindet sich ein Futterautomat, der die Fische auffordert, zwischen den beiden Kammern hin und her zu pendeln, wenn der konditionierte Reiz auftritt. Das Hin- und Herpendeln zwischen den beiden Kammern wird mit einer Lichtschranke registriert. Sowohl der magnetische Reiz (wechselndes Magnetfeld, das dem umgebenden geomagnetischen Feld überlagert wird), welcher mit einer Futterbelohnung verstärkt wird, um zum konditionierten Reiz (S+/CS) zu werden, als auch die nicht verstärkte Bedingung (S-, nur Umgebungsfeld) werden in einer computergesteuerten Abfolge angewendet. Die Futterbelohnung als positive Verstärkung in einem Horner-Shuttlebox ist ein neuartiger Ansatz zur Untersuchung der Magnetosensitivität bei Fischen. Das Protokoll besteht aus mehreren Trainingssitzungen mit Verstärkung, gefolgt von Rückrufaktionen ohne positive Verstärkung.

Naïve Regenbogenforellen wurden darauf trainiert, auf ein ±100 µT oszillierendes Magnetfeld entweder in der vertikalen oder horizontalen Komponente zu reagieren. In der Trainingsphase war S+ das oszillierende Magnetfeld, und S- waren oszillierende Ströme, die kein oszillierendes Feld erzeugten (magnetische Scheinkontrolle). In beiden Fällen wurde gleichzeitig ein Lichtreiz verabreicht, um den Fischen den Beginn eines Versuchs anzuzeigen. Alle vier Fische lernten,

signifikant häufiger auf den Magnetfeldreiz zu reagieren als auf den Scheinreiz und behielten die Unterscheidungsleistung in Testversuchen (ohne Verstärkung) nach dem Training bei. Setzt man richtige und falsch-positive Raten in Relation zueinander, so liegen die richtigen positiven Reaktionen auf den Magnetfeldreiz über dem 50%-Niveau des Zufallsniveaus. Unter Verwendung statistischer Tests für Zähldaten oder für Proportionen (χ2-Test) sind die Verhältnisse auf einem Niveau von $p> 10^{-4}$ signifikant unterschiedlich.
Nachdem der Aufbau und das Paradigma hier etabliert und erfolgreich getestet wurden, können nun wichtige Aspekte wie Schwellenempfindlichkeit und Reizgeneralisierung untersucht werden, d.h. reagiert ein Fisch, der auf einen bestimmten magnetischen Reiz trainiert wurde, auch auf einen anderen, und wenn ja, wie unterschiedlich können diese magnetischen Reize sein?

Neuroanatomische Grundlage der Magnetorezeption

Bei Singvögeln wurde eine Reihe von Hirnarealen identifiziert, die für die Magnetfeldwahrnehmung in Frage kommen, z. B. Cluster N für den lichtabhängigen Neigungskompass (Zapka et al., 2009) oder Trigeminalkerne für Karteninformationen (Heyers et al., 2010). Zentrale Experimente von (Hellinger & Hoffmann, 2012) an Regenbogenforellen deuten ebenfalls auf das trigeminale System als Ort für die Verarbeitung von magnetischer Intensität und Neigung hin. Darüber hinaus fanden sie heraus, dass konditionierte Reaktionen auf eine Richtungsänderung von 90° auch in der Dunkelheit bestehen bleiben, was bedeutet, dass die Kompassinformationen bei Fischen - anders als bei Vögeln - über einen lichtunabhängigen Weg übermittelt werden. Aktuelle Experimente an juvenilen Medakas (Myklatun et al., 2018) deuten auf eine Beteiligung des lateralen Hinterhirns hin, von dem alle sensorischen Hirnnerven ausgehen, mit Ausnahme des I. (Geruchs-) und II. ("Seh-") Nerv. Es gibt nur wenige Hinweise auf die Lage und den inneren Aufbau der Kandidaten-Magnetorezeptorzellen, ihrer afferenten Nerven und zentralen Projektionen im Gehirn. Frühere Berichte über Kandidatenrezeptorzellen in trigeminal innervierten, lateralen Teilen des Riechorgans (Walker et al., 1997) haben dem Härtetest der unabhängigen Replikation nicht standgehalten.
Es gibt keinen Gehirnatlas für Regenbogenforellen, der die Untersuchung der Gehirnaktivität unter Magnetstimulation erleichtern würde. Um die wichtigsten mit dem Trigeminussystem verbundenen Hirnareale zu identifizieren, habe ich DiI-Färbekristalle auf den Trigeminusnerv aufgebracht und seine Projektionen ins Gehirn verfolgt. Diese Ergebnisse können nun verwendet werden, um die Hirnareale zu verifizieren, die unter magnetischer Stimulation eine unterschiedliche Expression von "immediate early genes" (IEG) aufweisen, die stellvertretend für die neuronale Aktivität stehen.

Während IEG-Expressionsstudien bei der Untersuchung von magnetischen Aktivierungsmustern in Vogelgehirnen von großem Nutzen waren (Elbers et al., 2017; Heyers et al., 2010; Kobylkov et al.,

2020; Zapka et al., 2009), können die Protokolle nicht auf Fischgehirne übertragen werden, ohne vorher zu testen, ob verfügbare IEG-Antikörper gegen cfos oder ZENK auch die fischspezifischen IEG-Homologe erkennen.

Zur *In-vitro*-Validierung des cFos-Antikörpers habe ich das cFos-Homolog der Regenbogenforelle in HEK-Zellen exprimiert und die Antikörperbindung in Western Blots quantifiziert. Außerdem habe ich ein histochemisches Färbeprotokoll (DAB) zur Markierung von primären Antikörpern gegen IEGs (cFos) für Regenbogenforellen erstellt und zur Visualisierung der neuronalen Aktivität in reizspezifischen Verarbeitungsregionen verwendet. Für die molekulare Kartierung des Verhaltens mit IEGs muss das Tier bis zu einer Stunde lang stimuliert werden. Während dieser Zeit sollte das Tier so ruhig wie möglich sein, um das Aktivitätsrauschen im Gehirn zu minimieren. Ich habe einen ELISA-Test für freies Cortisol als nicht-invasiven Stressindikator für Laborfische etabliert und die täglichen Schwankungen der Cortisolproduktion von (nicht stimulierten) Forellen aufgezeichnet, um eine geeignete Tageszeit für die Stimulationsversuche zu finden. Der endokrinologische Richtwert für die physiologische Aktivität wurde wiederum durch die Analyse des auf Video aufgezeichneten Verhaltens zu verschiedenen Tageszeiten validiert, wodurch der Zusammenhang zwischen geringer Bewegungsaktivität und niedrigen Cortisolwerten bestätigt wurde.

1. Introduction

1.1 Geomagnetic Field

The Earth generates its own magnetic field, also referred to as the geomagnetic field, which is mostly caused by electric currents in the liquid outer core of the Earth (the “dynamo effect”), with minor contributions from magnetised rocks in the Earth’s crust. Before the advent of satellite-based global positioning systems, human navigators relied heavily on the Earth's magnetic field, which provides a constant source of directional and latitudinal information anywhere on the globe. This is due to the predominant dipolar character of the geomagnetic field since a dipolar field has two convenient properties: first, its field lines have rotational symmetry about the dipolar axis, so that a compass needle at any location always points to the magnetic pole. Second, both the field intensity and the inclination angle between the field lines and the horizontal vary systematically with the distance from the pole. That is, the magnetic vector is directed upwards in the southern hemisphere (negative inclination), downwards in the northern hemisphere (positive inclination), and parallel to the Earth's surface at the magnetic equator (zero inclination) (Fig. 1). The geomagnetic dipole axis is tilted by ca. 10 degrees from the rotational axis of the Earth, so that most of the magnetic field lines leave the Earth’s surface near the geographic South pole and re-enter antipodally near the geographic North pole. Therefore, geomagnetic north and geographic north do not strictly coincide, with the deviation, called declination, being quite large near the magnetic poles. However, usually less than 20° at lower latitudes, so magnetic field lines run roughly north-south in most parts of the world (see chart (Winklhofer, 2010)). The total magnetic field strength gradually decreases - roughly symmetrically in both hemispheres - from a maximum of about 60,000 nT at the poles to about 30,000 nT near the magnetic equator. The geomagnetic field undergoes temporal variations on various time scales, ranging from daily over secular to geological time scales. The latter two types of changes are so slow that they have to be taken into account only in evolutionary considerations. The regular daily variations, in contrast, mostly in the range 30–100 nT, and irregular fluctuations associated with magnetic storms are important for all considerations of a navigational ‘map’ (see below) but are negligible for magnetic compass orientation. A detailed description of the geomagnetic field and its variations in time and space were given by (Skiles, 1985).

Despite its temporal variations, the geomagnetic field represents a very reliable, omnipresent source of information. The magnetic vector provides directional information, and the spatial distribution of factors such as total intensity and inclination may provide information about position. Indeed, the use of magnetic information in bird orientation was discussed in the 19th century, when Viguier suggested that displaced pigeons use total magnetic intensity and inclination to determine their

home direction (Viguier, 1882). However, it was not until about 50 years ago that the first systematic experiments were conducted to investigate magnetic orientation in animals (Keeton, 1971; Lindauer & Martin, 1968; Merkel, Fredrick Wilhelm & Wiltschko, Wolfgang, 1965; Walcott & Green, 1974; W. Wiltschko & Wiltschko, 1972), which culminated in two major discoveries: the inclination compass in songbirds (W. Wiltschko & Wiltschko, 1972) and magnetotaxis in a group of bacteria that biomineralise an intracellular magnetic compass needle made of magnetite particles, which aligns their cell body with the magnetic fieldlines (R. Blakemore, 1975). Since this thesis is focused on magnetic field perception in teleost fish, the following section features some key behavioural studies on magnetic orientation and magnetic field sensitivity in fish.

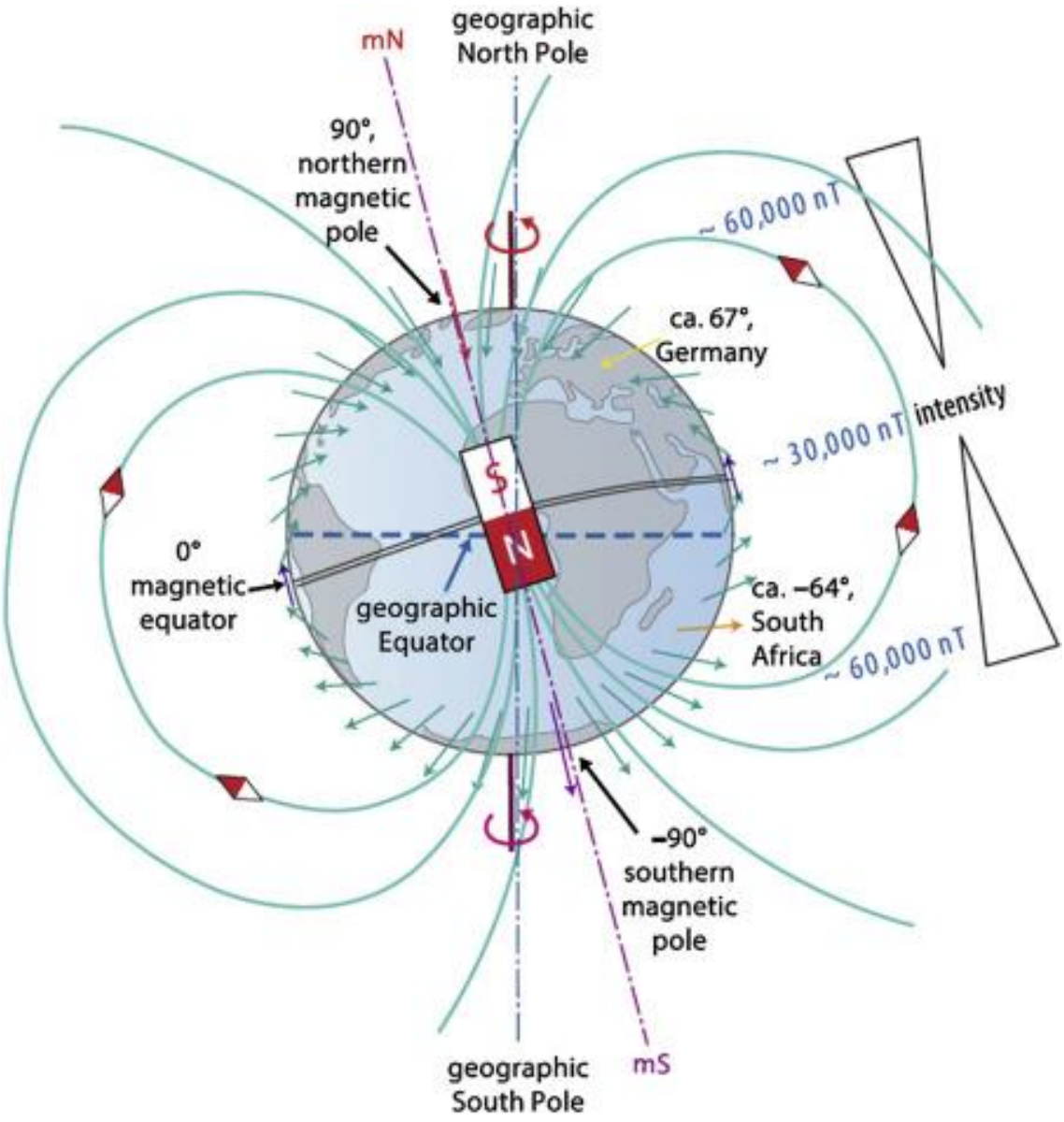

Figure 1: Key features of the Earth's dipolar magnetic field as relevant for magnetic orientation.

By and large, the geomagnetic field can be approximated by that of a giant bar magnet in the middle of the Earth but tilted by ca. 10 degrees about the rotational axis. Therefore, *the southern and northern magnetic poles and the magnetic equator do not coincide with the geographical poles and the geographic equator.* The *magnetic field lines intersect the Earth's surface at different angles depending on the magnetic latitude (blue-green lines and vectors). The intersection angle is called the magnetic inclination. Magnetic inclination is +90° at the Magnetic North Pole (red vector),* ca. *+67° at the latitude of Germany (yellow vector), 0° at the magnetic equator (dark blue vectors), ca. −64° at the latitude of South Africa (orange vector), and −90° at the Magnetic South Pole (magenta vector)* the magnetic intensity varies from ca. *60,000 nT near the magnetic poles to ca. 30,000 nT along the magnetic equator.*
(Mouritsen, 2022)

1.2 Magnetic field perception in teleostei

A great deal of behavioural research into teleost magnetoreception focused on well known migratory fish such as eels and salmons, which would greatly benefit from a keen magnetic sense when navigating over long distances in the mostly featureless ocean. In one of the first studies, concerned with magnetic field perceptions in teleost fish, Tesch (1974) used an indoor saltwater tank equipped with Helmholtz coils to monitor spontaneous directional preferences of European eel (*Anguilla anguilla*) in the silver eel stage (migratory adult) during their outbound migration from the river Elbe estuary into the North Sea. When the horizontal component of the geomagnetic field was compensated to zero so that magnetic directional information was no longer available, silver eels were found to change their preferred direction from north or south to east (Tesch, 1974). However, it has remained unclear why eels oriented in a condition where any magnetic compass would be disoriented, and, despite numerous efforts, it was not until forty years later that evidence for magnetic compass orientation in the European eel was presented (Durif et al., 2013) and glass eel stage (Cresci et al., 2019).

In the early 1980s, Quinn and coworkers conducted a series of successful magnetic compass experiments on juvenile Pacific salmon, showing that sockeye salmon (*Oncorhynchus nerka*) can use the Earth's magnetic field for orientation during downstream migration to the ocean: sockeye fry tested in a circular tank had a clear preference for the naturally given direction of migration; after an artificial change of magnetic field direction by 90°, the directional preference of fry shifted accordingly, even when they had access to the starry sky (Quinn, 1980). In contrast, after the parr-to-smolt transition, juvenile salmon was only oriented in the magnetic field when celestial cues were absent (Quinn & Brannon, 1982). To find out if salmon fry have an inclination compass as reported for birds (W. Wiltschko & Wiltschko, 1972), Quinn et al. 1981 tested their orientation in a magnetic field whose vertical component was reversed but found no difference relative to the normal field, which is consistent with a polarity compass (Quinn, 1980; Quinn et al., 1981; Quinn & Brannon, 1982). In other species of Pacific salmon (*genus Oncorhynchus*), magnetic orientation was also demonstrated in juvenile chinook salmon (*O. tschawytscha),* reorienting by 96° in a 90° shifted magnetic field (Taylor, 1986), while no significant reorientation was observed in chum salmon (*O. keta*) (Quinn & Groot, 1983). Recent research tested if salmon could use spatial variations of the geomagnetic field to derive magnetic factors for map navigation (Putman et al., 2020; Putman, Jenkins, et al., 2014; Putman, Meinke, et al., 2014; Putman, Scanlan, et al., 2014). For this purpose, juvenile salmon at the rearing site were virtually translocated by exposing them to magnetic field parameters (inclination and intensity) that would occur at remote sites in the open Pacific Ocean and reorientation after virtual displacement were taken as evidence for an innate magnetic map (Putman et al., 2020; Putman, Meinke, et al., 2014).

Spontaneous behavioural tendencies of fish recorded in tanks typically have a large scatter about the group preference direction, which may be due to a lack of motivation of animals tested in an artificial test environment to display the same orientation behaviour as in their natural habitat. Using reinforcement as a method to control motivation, several attempts were made to train fish to respond to specific magnetic field conditions in order to demonstrate magnetic field sensitivity. Walker (1984) reported that juvenile yellowfin tuna (*Thunnus albacares*), a pelagic long-distance migrant, can learn to discriminate between the absence and presence of a spatially nonuniform field ("magnetic anomaly") produced with a coil behind the feeder. Food was delivered only when the fish struck the feeder in one magnetic field condition (reinforced stimulus, S+). However, not in the other (non-reinforced stimulus, S-), and the striking rate under S+ became 20% higher compared to S- (Walker, 1984). In order to find a laboratory fish model more suitable for magnetoreception studies, Walker looked for a fish that was not only easily accessible and easy to maintain, but also had a long history of being a prime model for learning and memory in fish. However, the magnetic conditioning attempts on goldfish were unsuccessful, irrespective of whether positive or negative reinforcement was used (Walker & Bitterman, 1986). It was not until 1997, when Walker (Walker et al., 1997) eventually established a convenient fish model for studying magnetic perception at all levels, from anatomy to behaviour: the rainbow trout (*O. mykiss*) in its nonanadromous form, which in earlier studies was found to no longer orient in a magnetically shielded environment in the absence of visual and olfactory cues (Chew & Brown, 1989). Using the operant conditioning paradigm established on tuna (Walker et al. 1984), the Walker team was able to train juvenile rainbow trout to discriminate between the presence and absence of a magnetic anomaly (Walker et al., 1997) (see (Haugh & Walker, 1998) for a complete description of the conditioning experiments). Shcherbakov et al. (2005) succeeded in reproducing conditioned responses to magnetic stimuli in rainbow trout, with response rates to the reinforced stimulus (change in magnetic field from 40 to 150 μT) being on average ca. 15-20% greater compared to a non-reinforced stimulus.

In follow up studies presented in the same paper, (Shcherbakov et al., 2005) were the first to report a successful magnetic operant conditioning paradigm with negative reinforcement, where a magnetic stimulus signified an aversive stimulus, which the fish could actively avoid by shuttling from one compartment to another within 10 seconds after the onset of the magnetic stimulus. Failure to perform a timely response entailed a mild electric shock, which in turn could be aborted by shuttling, so that the animal always had the opportunity to learn from the outcome of its behaviour. Indeed, adult Mozambique tilapia (*Oreochromis mossambicus*) was found to shuttle consistently more often (25%) in response to the negatively reinforced magnetic stimulus compared to the control, while adult zebrafish (*Danio rerio*) showed less robust responses, varying between 0 and 20% among the

training sessions (Shcherbakov et al., 2005). Thereafter, a number of orientation experiments have demonstrated that adult zebrafish can orient by the magnetic field (Krylov et al., 2016; Myklatun et al., 2018; Osipova et al., 2016; Takebe et al., 2012), but again, with significant directional scatter.

As opposed to operant conditioning, where a behavioural response is reinforced, a few studies have used Pavlovian fear conditioning to magnetic stimuli, where a magnetic stimulus is paired with an aversive stimulus without reinforcing a behaviour, but using heartbeat responses as readout. Nishi (2004) applied this paradigm to Japanese eel (*Anguilla japonica*), a catadromous long-distant migrant like the European eel, using a flash of light as an aversive stimulus, which can be seen in an electrocardiogram as an interval lengthening between two heartbeats. After the conditioning phase, where each increase in magnetic field intensity was coupled with a flash of light, the magnetic field stimulus alone elicits prolongation of heartbeat intervals (Nishi et al., 2004), demonstrating magnetic sensitivity in eels. Heartbeat conditioning was also used to demonstrate that rainbow trout can perceive purely horizontal field (declination) changes as well as combined changes in inclination/intensity (Hellinger & Hoffmann, 2009).

1.3 Putative magnetoreception mechanisms

1.3.1. Electromagnetic induction

The cartilaginous fish (chondrichthyians) – chimaeras and elasmobranch fish (rays, skates and sharks) – are known for their highly sensitive electric organs, called Ampullae of Lorenzini, which allow for the detection of weak biogenic electric fields (Murray, 1960), e.g., due to smooth muscle contractions of prey buried in the seafloor (Kalmijn, 1971). The head of a shark or the wings of a ray are covered with many pores (e.g. see (Johnsen & Lohmann, 2005)), each extending as ampulla deep under the skin onto the electric sensory epithelium. The ampulla are filled with a gelly like substance of high electrical conductance. Animals with these ampullae can perceive electric fields of the order of 1 mV/km or 0.01 V/cm (Helfman et al., 2009). It is widely believed that sharks, rays, and skates can use these ampullary receptors also to perceive information from the Earth's magnetic field, making use of the Lorentz force, which can separate charges (ions) in the gelly and thus induce a voltage difference that can, in turn, be detected. For this purpose, the animal has to be moving across the field lines, because the Lorentz force can only act on moving charged particles (ions) on condition that the magnetic field has a perpendicular component to the axis of movement (Kalmijn, 1971; Paulin, 1995). Although theoretically feasible, this hypothesis has not been tested directly but rests on indirect evidence (Akoev et al., 1976; Andrianov et al., 1974; Kalmijn, 1982). Meyer (Meyer et al., 2005) reported successful magnetic conditioning experiments on sharks, but there was no follow up to determine if they detect magnetic fields with the ampullary electroreceptors.

For vertebrates that do not have Ampullae of Lorenzini, (Jungerman & Rosenblum, 1980) suggested another accessory organ for the induction mechanism: semicircular canals in the vestibular system, which can be thought of as a triaxial set of induction loops. This hypothesis, which had long been considered as too speculative (Winklhofer, 2019), has recently gained experimental support. Replicating an earlier finding that changing magnetic fields induce neuronal activity in the vestibular brain stem of head-fixed pigeons (Wu & Dickman, 2011), Nimpf (Nimpf et al., 2019) could also show that cells from the sensory epithelium of the pigeon semicircular canals express a voltage-gated ion channel that was demonstrated earlier (Bellono, Bayrer, et al., 2017) to be responsible for the high sensitivity of the ampullary electroreceptors of skates.

1.3.2. Radical-pair based magnetoreception

There is good evidence that amphibians and birds require short wavelength light for magnetic orientation (Phillips & Borland, 1992). Wiltschko et al. (2005) suggesting the involvement of photosensitive molecules, according to the radical-pair mechanism of magnetoreception proposed by (Schulten et al., 1978). When such a molecule is excited by light, it can form intermediate states with different electron spins – singlet and triplet – instead of immediately returning to the ground state. The axial orientation of the magnetic field modulates the natural singlet to triplet interconversion in a radical pair driven by nuclear spins (Ritz et al., 2000; Schulten et al., 1978) and can thereby affect the reaction kinetics of a radical pair. The fact that not the magnetic polarity but instead the axial orientation of the external magnetic field has an influence on the reaction readily explains a key feature of the inclination compass of birds. Indeed, experiments conducted with a chemical model system (the "carotenoid-porphyrin fullerene model") demonstrate that an axial magnetic compass can be realised based on the radical-pair mechanism (Maeda et al., 2008).
When Schulten et al., 1978 laid the foundations of the radical-pair mechanism, there was no known vertebrate molecule suitable to host a radical-pair mechanism. The situation changed in the 1990s, when the protein cryptochrome was discovered (Ahmad & Cashmore, 1993), a blue-light photoreceptor with molecular similarity to 6’,4’-photolyases, i.e. DNA-repair enzymes that can form radical pairs upon light excitation (Giovani et al., 2003; Sancar & Sancar, 1988). Ritz (Ritz et al., 2000), in their influential paper, proposed cryptochrome as a candidate molecule for detecting the magnetic field in a light-dependent fashion. According to the model of Ritz et al., magnetosensitive cryptochromes distributed over the retinal hemisphere would modulate visual inputs systematically, making the magnetic field axis practically visible to migratory birds. Animal type II cryptochromes in the vertebrate retina were proposed to be photoreceptors, with roles in nonvisual photoentrainment in mammals (Van Gelder et al., 2003), (Sancar, 2004) or in light-dependent magnetoreception in birds (Liedvogel et al., 2007; Mouritsen et al., 2004; Nießner et al., 2011). There is now broad consensus

that the animal type II cryptochromes (e.g., Cry1, Cry2 in mammals) play a crucial, but light-independent role in regulating circadian rhythms through transcriptional feedback loops (Takahashi, 2017). An excellent candidate for radical-pair based magnetoreception in vertebrates are animal-type IV cryptochromes, with European robin Cry4, which is highly expressed in double cones (Günther et al., 2018), showing magnetic effects in near-earth magnetic field strengths (Xu et al., 2021).

Although it remains to be demonstrated that Cry4 forms the sensory molecule of the magnetic compass of birds, key evidence of birds using the radical-pair mechanism for orientation comes from experiments with weak radio-frequency magnetic fields, which were found to disturb the inclination compass (e.g., (Leberecht et al., 2023)).

In contrast to birds and amphibians, the light dependence of magnetic orientation in teleost fish has yet to be systematically explored. However, magnetic compass responses in adult zebrafish were found to change from axial under full spectrum (white) light to polar under near-infrared light (Myklatun et al., 2018). This may hint towards an involvement of the radical-pair mechanism under white light. Also, zebrafish Cry4 is known to produce radical pairs under shortwave-light (Ozturk et al., 2009) and is expressed in the retina (Balay et al., 2020; Haug et al., 2015).

1.3.3. Biogenic magnetite

The discovery of magnetotactic bacteria (R. Blakemore, 1975), which make membrane-bound iron-rich magnetic particles called magnetosomes, greatly impacted research into animal magnetoreception. It showed that the ferrimagnetic mineral magnetite can be synthesised biologically with great precision as magnetic single domains and used for navigation along magnetic field lines (R. P. Blakemore, 1982; Frankel et al., 1979). Provided that vertebrates, too, have the genetic machinery for magnetite biomineralisation, they could realise a conceptually simple mechanism to detect the Earth's magnetic field. In effect, a chain of single-domain magnetite (Fe_3O_4) particles acts as a compass needle, which has the tendency to align with the magnetic field, although other arrangements of magnetic crystals could also work as a magnetic field detector (J. L. Kirschvink et al., 2010). However, for the torque acting on the magnetic particles to be converted into a cellular response, they have to have a connection to a mechanotransduction structure, either by being directly anchored to a mechanosensitive ion channel or indirectly, via cell membrane or cytoskeleton (Winklhofer & Kirschvink, 2010). Accordingly, opening and closing of ion channels depends on the magnetic field direction and intensity, so that a change in the electrical potential of the cell would provide information about the magnetic field (J. Kirschvink, 2001; Nordmann et al., 2017; Walker et al., 2002).

A candidate anatomical structure containing reflective particles, probably magnetite, was described in the lamina propria (connective tissue) of the olfactory rosette of rainbow trout (Bellinger et al., 2022; Diebel et al., 2000; Walker et al., 1997). However, while the olfactory lamina propria is innervated by nerve endings of rosV (Walker et al., 1997), the cell containing the candidate structure was not further characterised, so it remains unclear if it is neuronal. Apart from that, single-domain magnetic particles, indistinguishable from bacterial magnetosomes, were found in magnetic extracts in homogenated head tissue from tuna (Walker, 1984) and sockeye salmon (Walker et al., 1988), but without knowing the original anatomical context of the particles, it is not clear if they were used in magnetoreception or were of external origin (Curdt et al., 2022).

1.4 Trigeminal involvement in magnetoreception

Initial research on the distribution of biogenic magnetite in fish (yellowfin tuna, *Thunnus albacares*) revealed high concentrations of single-domain particles of magnetite in the dermethmoid tissue of the skull and suggested the involvement of supraophthalmic trunk nerve in magnetoreception, which carries branches of the trigeminal, facial, and anterior lateral line nerves and which ramifies in the ethmoid region (Walker, 1984). The first functional study suggesting that magnetic map information is transmitted through a specific branch of the trigeminal nerve was conducted on caged Bobolinks (*Dolichonyx oryzivorous*) (Beason & Semm, 1996), where an anaesthetic applied to the ophthalmic branch suppressed the effect of a short, strong magnetic pulse on bird orientation.

1.4.1 Trigeminal involvement in magnetoreception in fish

The rainbow trout (*O. mykiss)* has been a key model for studies on the structure and function of the vertebrate magnetic sense. From electrophysiological recordings, Walker et al. (1997) identified magnetically sensitive units in the ramus opthalmicus superior of the trigeminal nerve (rosV), which increased their firing rate upon stimulation with a change in magnetic field intensity. In the innervation area of rosV, traced anterogradely with a lipophilic dye from the recording site, iron rich crystals could be detected (Walker et al., 1997), which in a follow up study turned out to have magnetic properties consistent with biogenic magnetite, Fe_3O_4 (Diebel et al., 2000). While the electrophysiological and structural findings reported in the two Nature papers (Diebel et al., 2000; Walker et al., 1997) still await independent replication, some studies support them.

A conditioning study (Hellinger & Hoffmann, 2012) found that local anaesthesia of the rosV branch abolishes conditioned heartbeat responses to inclination/intensity changes, but not to declination changes, which suggests that inclination/intensity changes are adequate magnetic stimuli for the magnetic sense organ associated with rosV and thus corroborates the electrophysiological results by Walker et al. 1997. Interestingly, conditioned heartbeat responses to both declination and

inclination/intensity changes persisted in darkness or in red light, which speaks against a light-dependent radical-pair based magnetoreception mechanism in trout.

1.4.2 Trigeminal involvement in magnetoreception in birds

While there is now strong evidence for a light-dependent radical-pair mechanism in magnetic compass orientation of birds, which is not connected to the trigeminal nerve (Zapka et al., 2009), the original suggestion that the ophthalmic branch of the trigeminal nerve (V1) in migratory birds is involved in detection of magnetic map factors (Beason & Semm, 1996) has also been supported in fieldwork exploring the effects of V1 sectioning on displaced birds (Kishkinev et al., 2013). An indoor study showed that V1 transmits magnetic information to the principal and spinal trigeminal nuclei (PrV and SpV) in the bird's hindbrain, using immediate early gene expression as a proxy for neuronal activity in the hindbrain (Heyers et al., 2010). However, the V1 based sense is insufficient to orient European robins in orientation cages and is not likely associated with magnetic compass orientation (Heyers et al., 2010; Zapka et al., 2009). Suggestions have been made that this V1-dependent magnetic sense may be linked to primary sensors located in the upper beak, which are based on iron minerals (Fleissner et al., 2007), but in follow up work, no such iron minerals were histologically detectable in V1-traced upper beaks (Curdt et al., 2022). Nonetheless, further studies on the trigeminal involvement in magnetoreception have shown that the magnetically stimulated region of the trigeminal brainstem of migrating Eurasian blackcaps (*Sylvia atricapilla*) constitutes a morphologically distinct population of neurons in the ventral part of PrV, termed PrVv, which has an exclusive, previously unidentified projection towards the telencephalographic frontal nidopalla. This finding is a novel projection in the otherwise well-known trigeminal somatosensory pathway (Kobylkov et al., 2020).

2. Motivation, Aims and Scope

As emphasised in the introduction, the rainbow trout is a highly suitable fish model for holistic research into vertebrate magnetoreception from neuroanatomy to behaviour. The key objective of this thesis is to methodologically establish rainbow trout in our lab, replicate previous findings, and gain further insights into the magnetic sense. Instead of the anadromous form of rainbow trout (steelhead), which is not readily available here, we use non-anadromous forms from local fish farms and study learned behavioural responses to magnetic fields rather than innate magnetic compass orientation. For this purpose, it is necessary, first and foremost, to establish an effective conditioning paradigm and replicate previous findings on conditioned magnetic responses in trout before advancing with studies on threshold sensitivity and stimulus generalisation.

Aim 1: Design of setup and operant conditioning paradigm for training fish to respond to magnetic field stimuli and testing their recall performance.

The main research question to be addressed here is: Can rainbow trout learn to show *robust* responses to magnetic field stimuli?

Although rainbow trout have previously been reported to be amenable to operant magnetic conditioning (Haugh & Walker, 1998; Shcherbakov et al., 2005), the responses were not highly significantly different from chance level, with p-values just below 0.05. We have identified two major problems with the previous approaches that we aim at improving here. (1) The behavioural readout used previously was the striking rate at a single feeder placed in a test tank, with feeder usage getting reinforced with a food reward if the conditioned magnetic field condition was presented. However, since fish were not discouraged from waiting around the feeder, they would not have to invest much energy to get to the feeder in case the non-reinforced stimulus was presented, which may well explain why the observed difference in striking rate between reinforced and non-reinforced stimulus was not higher than 20%. In fact, motivation and cost efficiency have an important role in the outcome of operant conditioning. Therefore, we will adapt the Horner-shuttle box setup (Horner et al., 1961; Portavella, 2004), where fish, in order to obtain the food reward, have to actively shuttle from one compartment over a hurdle to the other to obtain a food reward, thereby discouraging fish from randomly shuttling. (2) Previous attempts had a pre-set number of training sessions and grouped responses of individuals according to session number for the statistical analysis. However, this approach implicitly assumes similar learning rates among individuals, which often is not the case and thus may have been another reason for the small effect sizes observed. To account for individual differences in learning performance, we will apply a predefined learning criterion that a fish had to

reach in order to be counted as successfully trained and to advance to follow-up session where the recall performance is tested without reinforcement. These extra tests will provide an independent means of assessing the robustness of the conditioned responses and the chances of surviving the process of scientific scrutiny over time.

Aim 2: Design of behavioural molecular mapping experiments to study the brain activity of rainbow trout under magnetic stimulation, using immediate early gene (IEG) expression as a proxy for brain activity.

Behavioural molecular mapping has been proven a valuable tool for guiding the discovery of new sensory perception and informational processing pathways, also in the context of the magnetic sense, in mammals (Nemec et al. 1999) as well in birds (Elbers et al., 2017; Heyers et al., 2010; Kobylkov et al., 2020; Zapka et al., 2009), but not in fish.
Therefore, the ultimate scope of this project is to test on trout the working hypothesis of a trigeminal involvement in the perception of magnetic intensity and inclination (Walker et al. 1997; Hellinger & Hoffmann, 2012), while another light-independent pathway is involved in the perception of horizontal magnetic field changes (Hellinger & Hoffmann, 2012). The working hypothesis was based on results obtained with electrophysiology (Walker et al. 1997) or cardiac conditioning (Hellinger & Hoffmann 2012), which invites a test with IEGs as an independent method, prompting these questions:
Do we see differential expression of IEGs in trigeminal nuclei of the trout brain when stimulated with intensity-inclination changes compared to horizontal field changes (both under dark conditions)? If so, in which other brain regions can we find neuronal correlates of horizontal-field changes?

However, before these questions can be tackled, it is necessary to adapt the IEG protocol, which is well established in mammals and birds, to a fish species (rainbow trout). Therefore, project 2 will be concerned with
a) the molecular and immunohistological techniques required to obtain magnetic activity maps, including antibody validation in vitro.
b) the design of the behavioural component, with the key question to be addressed here: How can a rainbow trout, free to move in a fish tank, be magnetically stimulated without showing unwanted behaviours likely to mask brain activity due to magnetic field perception?
After all, the animal has to be stimulated for up to an hour in order to obtain a sufficient change of IEG at the protein level. During this time, the animal should be as calm as possible to minimise noise in brain activity. To identify the optimal time of the day for the magnetic stimulation experiments, we

will determine the daily variations in activity (from video recordings) and cortisol production by the fish. We will explore if cortisol can be used as a non-invasive stress indicator for lab fish.

3. Methods & Material

3.1. Animal Subject

Juvenile rainbow trout (*Oncorhynchus mykiss*) were obtained from a commercial breeding facility in Germany and kept in a 200-liter glass aquarium 100 x 40 x 50 cm (*Marina)* at 13°C, separated by a plastic divider, which allowed water flow and visibility of the other fish. The daily light: dark cycle of 14 h:10 h was kept throughout the study. Fish were fed with commercially available fish food in the form of pellets (3,0 mm Premium Forellenfutter AG), which was also used in the food reward in the conditioning experiment. The Animal Care and Use Committees of the Lower Saxony State Office for Consumer Protection and Food Safety (LAVES, Oldenburg, Germany, Az: 3319-02502-04-17 2721) approved all animal procedures conducted in this study. All experiments were carried out in accordance with the approved guidelines.

3.2. Behavioural conditioning design

When examining magnetic-field dependent behaviour in organisms, the obvious experiment to perform would be to compare a spontaneous behaviour in a normal magnetic field and a changed one. The rainbow trout used are not wild caught in their migratory phase. Therefore, a meaningful natural behaviour in the magnetic field, such as a migration direction, is difficult to determine. In contrast, operant magnetic conditioning experiments aim at reinforcing a suitable behaviour that at first is not linked with a magnetic field, but is to become associated with it in the process of learning, where the magnetic conditioning stimulus (CS) is paired with an unconditioned stimulus (US, food reward) to reinforce the behaviour. A significant increase in the behaviour then suggests that the animal can perceive the magnetic field stimulus.

3.2.1. Experimental setup

We designed a fully automated Horner-type shuttle box, similar to what has been commonly used in avoidance task learning in fish (Horner et al., 1961; Portavella, 2004; Walker & Bitterman, 1986). The shuttle box (54 litres; 60 cm length, 20 × 30 cm height) was built from nonmagnetic materials (acrylic glass and PVC) and consists of two compartments (28,5 cm × 19 cm × 18 cm height), separated by a hurdle 3 cm wide, 14 cm long, and 15 cm high, with its upper surface 2-3 cm beneath the water level Fig. 2 for illustration).

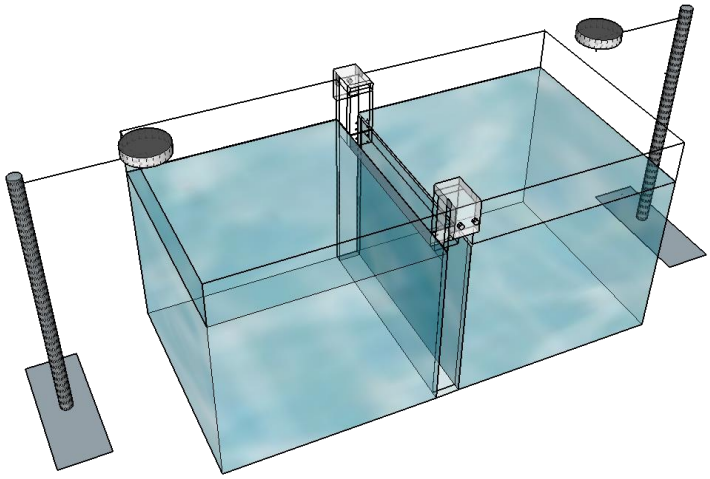

Figure 2: Shuttle box

The experimental tank (54 litres; 60 cm length, 30 × 30 cm height) consists of two compartments separated by a hurdle. An automated feeder was positioned over the far side of each compartment,and fish had to shuttle across the hurdle to obtain a food reward upon presentation of the conditioned stimulus.

The shuttle box was equipped with a custom-built infrared light barrier reaching from 0 cm to 6 cm above the hurdle to detect automatically shuttling of a fish between the two compartments. Above the compartments, an automated feeder (Grässlin Rondomatic 400) was fitted to the end side to allow the pellets to fall 3-5 cm from the aquarium wall. The shuttle box was placed in the centre of a three-axis Merritt-3-coil system consisting of 3 square coils per axis, with the number of windings being 39 in both outer coil and 20 in the inner coil, which ensures a largely homogeneous field in the coil (Merritt et al., 1983). Enamelled copper wire (1 mm conductor diameter) was wrapped on each aluminium frame (edge lengths of 180, 190, or 200 cm in X, Y, Z) in a double-wound configuration (J. L. Kirschvink, 1992). The experimental setup was positioned in the centre of the coil system such that the centre of the experimental aquarium coincided with the centre of the Merrit-coil system, see technical drawing in Fig. 3. The room housing coil and setup was shielded with aluminium plates and grounded. The coil system was energised with programmable stabilised power supply units (KEPCO Bipolar Operational Power Supply BOP 100-4, one for each magnetic field axis), placed outside the electrically shielded experimental room, and connected to the coils via shielded cables. We used a three-axis fluxgate magnetometer (Institut Dr. Foerster GmbH) placed in the centre of the setup for calibration of the magnetic field stimulus. For monitoring purposes during experimental sessions, the magnetometer was placed at the edge of the table. The shuttle box was illuminated from above with light bulbs from the ceiling. The intensity of the light was measured at the bottom of the aquarium and adjusted to 2.5 mW. We used a custom-built light table (480 nm) below the aquarium to administer the synchronised light stimulus. A camera (Abus) was mounted on top of the coil system

to overview the setup and observe the fish from the next room. The shuttle box was controlled by a microcomputer, which delivered the CS in a predefined temporal schedule and the US for positive reinforcement in case crossing was detected within 15 sec after the presentation of the CS. Furthermore, the signal acquisition, i.e., the registration of light barrier detection events, was synchronised with the stimulus administration protocol to ensure correct timing for each trial.

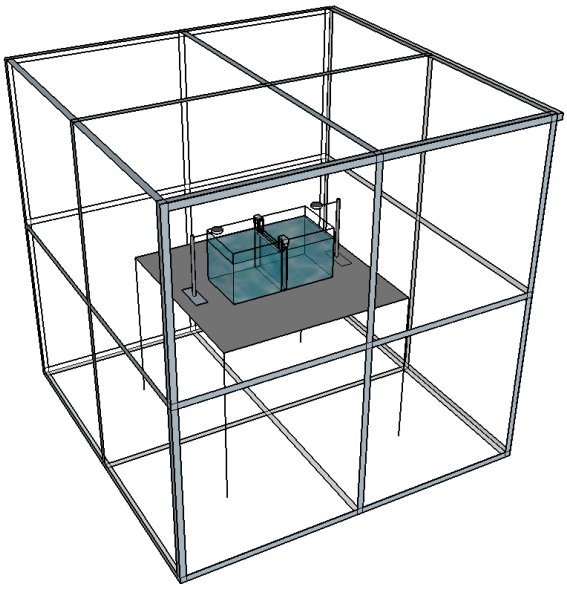

Figure 3: Three-axis square Merrit-coil system

The experimental setup is positioned in the centre of the coil system to ensure a homogeneous field throughout the aquarium.

3.2.2. Magnetic stimuli

Two different magnetic field stimuli were used as conditioned stimuli to test if rainbow trout can perceive changes both in the vertical component (stimulus 1) and in the horizontal component of the magnetic field (stimulus 2). Each magnetic field stimulus has a different information content in terms of the geomagnetic field and can, therefore, be used differently for navigation and orientation. The magnetic field stimuli were superimposed on the existing background field in Oldenburg, which has a total intensity of 48 µT with an inclination of 67°. Both stimuli oscillated at 3 Hz, thereby periodically modulating the ambient magnetic field.

An oscillating voltage (3 Hz) was generated with a signal generator (Tektronix AFG1022), amplified with the KEPCO and fed into the coil system to produce an oscillating magnetic field. As can be seen in the recordings of the field 10 cm above the base of the experimental aquarium (Fig. 4), delivery of stimulus 1 (by energising the vertical coil axis) produced an oscillatory magnetic signal along the vertical component of the magnetic field (blue trace). Fig. 5 shows the delivery of stimulus 2 (by

energising one of the horizontal coil axis X), producing an oscillatory magnetic signal along the horizontal components of the magnetic field (green and red traces). A negligible oscillation is detected in the X and Y components (green and red traces in Fig. 4) or the Z component (blue trace in Fig. 5), which is due to a minor tilt in the orientation of the magnetometer relative to the vertical / horizontal coil axis. During S- trials (non-reinforced behaviour) and inter-trial intervals, the coil system was operated in antiparallel current mode and generated no field (sham) of its own, so that only the ambient Earth's magnetic field was present.

For the first two subjects, the vertical component of B is used as a magnetic stimulus, and an oscillating magnetic field (3 Hz, ± 100 µT B_z) was presented.

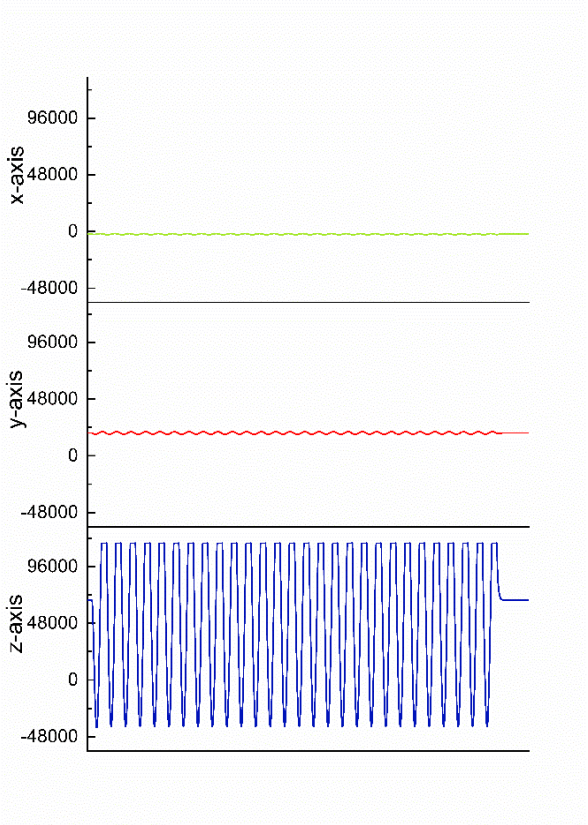

Figure 4: Stimulus 1 – periodic change in vertical component of the magnetic field

Recording of a 15-second long stimulation, with the vertical component of the magnetic field B (3 Hz, ± 100 µT z-axis) in blue. Negligible oscillations of the horizontal components (red and green traces) due to a slight tilt of the magnetometer. Visualisation of the axis can be seen in Figure 6.

For the next two individuals, an oscillating magnetic stimulus (3 Hz, ± 100 µT B_x) was presented that modulated the horizontal components of the magnetic field, but not the vertical one.

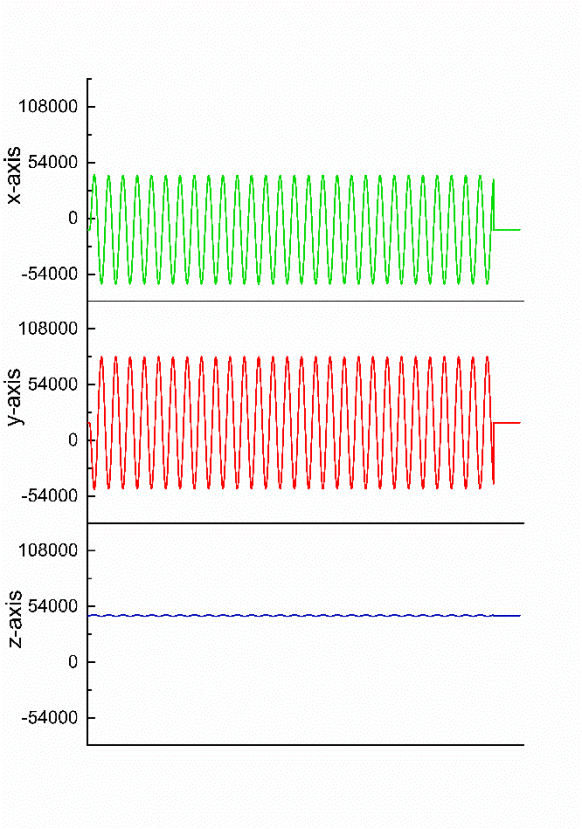

Figure 5: Stimulus 2 – periodic change in horizontal component of the magnetic field

Recording of a 15-second long stimulation, with the horizontal components of the magnetic field B (3 Hz, ± 100 µT y-axis and x-axis) in green and red. Negligible oscillations of the vertical intensity parameter due to the placement of the magnetometer in blue. Visualisation of the axis can be seen in Figure 6.

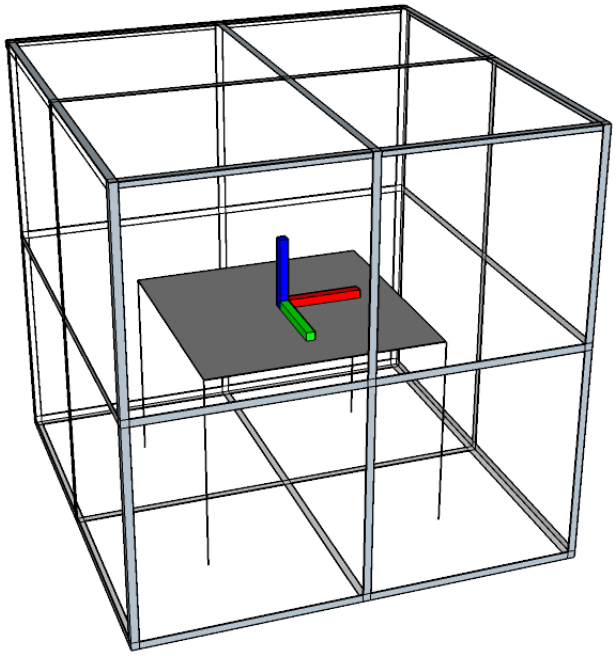

Figure 6: Definition of X, Y, Z coordination system: Z-axis (blue), the X-axis (green), and the Y-axis (red).

3.2.3. Procedure of the conditioning experiments

Experimental procedure

To minimise residual levels of odours and stress hormones and to keep the temperature (13°C) stable in the experimental setup, the water was replaced before every experiment with fresh water from the source that supplied the rainbow trout housing tanks. The water level was high enough to permit the animal to cross easily from one compartment to the other but low enough to discourage randomly crossing over the hurdle. The fish could adjust to the shuttle box for fifteen minutes before the session started.

A naïve individual was trained once per day. A training session comprises 12 trials. The conditioning stimulus (CS) was presented in a dual mode, alternating between a sinusoidally oscillating magnetic field (S+) applied simultaneously with a higher illumination of the tank and then following the next trial with only the higher illumination (S-). Every trial is defined as an interval (up to 15 sec long) during which the conditioned stimulus (CS) is presented continuously. At the moment the rainbow trout crossed the barrier within 15 sec after the onset of the CS, the trial counted as successful, and a positive reinforcement ensued, e.g. a food pellet drops from the automatic feed in the compartment the fish crossed into. The trial was discontinued if no crossing occurred during the 15-second-long presentation of the CS. Each trial was followed by a neutral inter-trial interval whose length was chosen randomly between 60 sec and 180 sec to ensure an aperiodic pattern in the sequence of trials. The animals were trained until they reached the learning criterion in not more than 25 sessions. The learning criterion was defined as three consecutive sessions, each with at least 4 correct responses (successes) out of 6 S+-trials and no false positive response (see rationale below in the section “Statistical Considerations”). If an animal had not reached the criterion in up to 25 sessions, it was excluded from the recall performance tests.

3.2.4. Data analysis and statistics

Statistical considerations for the learning criterion

As a learning criterion, we required the fish to make correct choices in three consecutive sessions to a p-value of < 0.05 in a maximum of 25 sessions. For example, we have 12 trials with 50:50 allocation (6 stimuli and 6 shams). In that case, a maximum of two false positives or two false negatives can occur and still fulfil the requirement of $p < 0.05$.

To obtain p-values, we used Fisher’s exact test for contingency tables with fixed-row sums only. Effectively, the test compares the two proportions, (CP/6) and (FP/6), with FN and CN being redundant because of fixed row sums. We used the function fisher.test from the R-package exact2x2(Fay & Hunsberger, 2021; R Core Team, 2020) using the following syntax:

Table 1: Correct positives compared with false positives in a Fisher's exact test

Trials	Stim	CP	FP	p-value	
12	6	4	0	0,030303	*
12	6	5	0	0,007576	**
12	6	5	1	0,040043	*
12	6	6	0	0,001082	***
12	6	6	1	0,007576	**
12	6	6	2	0,030303	*

3.3. Daily cycle of the stress hormone "cortisol"

In a holding tank (Solid Glass Aquarium Marina 60 x 30 x 30 cm), the same size/model as for the molecular mapping experiments, a 20 cm rainbow trout was sampled to investigate the daily cycle of the stress hormone "cortisol". The day before the sample extraction of the holding water began, the filter (External filter JBL CristalProfi e402 greenline) was cleaned, and 50% water was exchanged. All these cleaning steps ensure the best conditions for the experiment and reduce contamination-related false values.

3.3.1. Water sampling

From 07:00 to 22:00, 500 ml (a double sample size of 2 x 250 ml) of rainbow trout holding water were collected at the beginning of each hour. Every sample was coarsely filtered to remove larger particles from the water prior to the cortisol extraction. The cortisol was extracted from the water using a vacuum manifold (-50 kPa) and an SPE-column (Solid Phase Extraction CHROMABOND column HR-X). Chromabond SPE columns were dried with compressed air for one to two minutes and stored at -20°C.

3.3.2. ELISA-Test

The method by (Wedekind, H. et al., 2018) was used to determine free cortisol in rainbow trout holding water. First, all sample columns were eluted with 5 ml pure ethyl acetate via the vacuum manifold (-50kPa). The solution was collected in 8 mL snap-cap bottles and kept under constant airflow until the ethyl acetate was completely evaporated. Next, the residue in the snap-cap bottles was eluted with 200 µl distilled water. Cortisol samples were measured by using a human cortisol ELISA kit. Standard concentrations and samples were run in duplicates. All reagents and equipment came from the Cortisol-free in Salvia ELISA Kit by Demeditec; manufacturer instructions were followed. The plates were read on an Elisa Microplate Spectrophotometer set to 450 nm.

3.3.3. Analysis

Concentrations were calculated by using the 4-parameter logistic curve assay on MyAssays.com. The dilution factor was set to 0.2 as the detection was measured in ng/ml, and the samples were eluted with 200 µl distilled water. Thus, the detection limit was reduced by a factor of 5.

3.4. Design for behavioural molecular mapping

Designing a setup for behavioural, molecular mapping in fish requires a closer look at different aspects, such as activity, time of day, water quality, and temperature.

Immediate-early genes are gaining popularity as activity markers for mapping neural circuits involved in specific behaviours in many species. *In situ* methods for immediate early gene detection enable resolution at the cellular level, which is a major advantage for neural network mapping. IEG expression in neurons of resting animals is extremely low. However, any stimulation directly affects molecular mapping (Guzowski et al., 2005). A strong physical activity would mask the neuronal response induced by magnetic field stimulation.

Therefore, I analysed the behaviour of four fish (15-20cm) in two different tanks. One 55L rectangle glass aquarium (Solid Glass Aquarium Marina 60 x 30 x 30 cm) with a water volume of 25L. And a 15L round plastic bucket (radius 12,75 cm and height 30 cm) with a water volume of 10L at different times of the day. The behaviour of the fish were monitored and recorded using an infrared camera (Abus 850nm), and further analysis was done with the program BORIS (Behavioural Observation Research Interactive Software).

Another important aspect of designing a setup is to consider the time of day in which the experiments will take place. To correlate the physiological and physical activation of the animal, I created a daily cycle of cortisol hormone levels. The exact procedure is described in 3.3. *Daily cycle of the stress hormone "cortisol"*.

The experimental procedure was adapted from (Mouritsen et al., 2005)

Each animal will be exposed to a given magnetic stimulus for up to 120 min, including a period of 30 min, to adapt to the new surroundings and to ensure that any unspecific activation from handling the fish will be decreased by the time the brain tissue is collected. Following at least 60 min, in which the fish will be presented with the given stimulus (ZMF or oscillating magnetic field). Since general motor activity and mechanical stimulation can lead to brain activation independent of a given magnetic stimulus (Feenders et al., 2008), we continuously monitored the behaviour of each fish in the aquarium using infrared cameras (840 nm). A fish was only taken for brain analysis when it showed slow fin movement but showed no signs of excess motor behaviour during the last 60 min of the

experiment. If a fish showed strong activity during the first 180 min of the testing night, it was returned to its home aquarium and retested on the following evening.

3.4.1. BORIS

To better analyse the fish behaviour at different time points during the day, observational software (BORIS) was used. BORIS (Behavioural Observation Research Interactive Software) is a free, versatile, open-source event-logging software for video/audio coding and live observation. It provides a user-specific coding environment for a computer-based review of previously recorded videos. In addition, the program allows a project-based ethogram to be defined *(Friard & Gamba, 2016).*
Coding can be performed using state events (behaviour occurs for a longer time) and point events (behaviour occurs as a single time point). The coding events and the respected behaviour are listed in the following table.

Table 2: Behaviour description of the codes used for the ethogram in the observational software BORIS

Code	Event	Description
Rest	State event	Calm movement (slow fin and body movement, no contact between face and wall, best if the fish stands free in the water)
Slow	State event	Slow swimming movement (slow body movement)
Fast	State event	Normal to rapid swimming movement
Jump	State event	The head of the fish breaks through the water's surface, or the whole body breaks through the water's surface
Jagged	Point event	hectic left or right body movement (twitch)
Wall	Point event	Fish touches the wall with their face or swims directly against the wall

3.5 DiI Tracing

3.5.1. Preparation of brain tissue

Adult rainbow trout (20-25 cm) were deeply anaesthetised and killed with an overdose of MS-222 (333 mg/l), measured and decapitated just behind the gill cover. The skull was opened with a cross-section using a disposable scalpel and immersed in 4% PFA for 24 h at 4°C. After fixation, the brain was carefully removed out of the skull.

3.5.2. DiI crystal placing and Incubation

A small piece of parafilm was placed between them to separate the V brain nerve from the medulla oblongata. The DiI crystals (1,1'-Dioctadecyl-3,3,3',3'-Tetramethylindocarbocyanine Perchlorate) were applied to the V brain nerve on both sides of the brain with an insect pin, and the tissue was scratched with the tip of the pin. DiI crystals were also applied to the VII brain nerve on the left side as a reference. The locations of the DiI crystals were covered with 6% agarose. After the crystal placement, the brain was immersed in fresh fixative (4% PFA + 1% EDTA) and placed in an oven at 37°C for up to 40 days.

3.5.3. Cryosectioning

The brain was cryoprotected with a graded saccharose series 10-30% D(+)-saccharose in PBS (phosphate buffered saline) for up to 5 days at 4 °C. After embedding in Tissue-Tek® O.C.T.™ Compound, the tissue was cross-sectioned (30 µm) using a cryostat (Leica CM 1860) with polytetrafluoroethylene-coated broadband blades. The sections were mounted onto gelatin-coated SuperFrost Plus™ GOLD glass slides and stored at −20°C. Stored slides were thawed on a heating block for 45 minutes at 37°C, followed by 3 x 5-minute washes in PBS. Finally, the sections were cover-slipped with ROTI®Mount FluorCare DAPI.

3.5.4. Image analysis

Images were taken with (Zeiss Axio Scan.Z1), using a 20 × Plan-Apochromat, 0.8 NA objective. These were partially merged into projections from multiple individual images. The pixel size is 16752x20387—excitation peak at 567nm and 385nm.

3.6 Cell culture

Hek293 cells were cultivated in Dulbeccos Modified Eagle Serum (DMEM), supplemented with 10% fetal bovine serum (FBS) and 0.1% penicillin at 37°C in a humidified atmosphere containing 5% CO_2. 48 hours prior to transfection, cells were seeded in a density of $5x10^5$ cells in 6 cm dishes, coated with poly-L-lysine (PLL) in DMEM without penicillin.

3.6.1. Vector und cFos clone

The designing of the appropriate cFos-primer, the processing of the neuronal tissue as well as the following steps (RNA isolation, cDNA synthesis, amplification of cDNA, ligation of cDNA and pFLAG-CMV™-5.1 Expression Vector), to the cloning in *E.coli* bacteria was done and provided by Jasmin Fried geb. Segelken.

3.6.2. Transfection

Transfections were performed with lipofection reagent (lipofectamine 2000). One hour prior to transfection, the cultivation medium was changed. DNA and lipofectamine were applied in a 1:1 ratio (1 µg of DNA was transfected with 1 µl of lipofectamine). On a 6 cm dish with one 1 cm round coverslip, 6 µg of DNA was used for transfection. The vector DNA (cFos from rainbow trout or BAP (Bacterial Alkaline Phosphatase)) and lipofectamine were incubated separately for five minutes in 300 – 400 µl of Opti-MEM™ I, a reduced-serum medium. After a separate incubation time, the two solutions were mixed and incubated for 25 minutes. The mixture was applied to the cells and incubated for 24 hours at 37°C. After that incubation time, the medium was changed. 48 hours after transfection, cells were either fixed for immunocytochemistry or lysed for western blot analysis.

3.6.3. Specificity tests via immunocytochemistry

48 hours after transfection, cells were fixed for 10 Minutes in 4% PFA in 0.1 M PB at room temperature. Coverslips were washed for 3 x 5 minutes with PBS and incubated in PBS at 37°C overnight. Further incubation steps were performed using PBS containing 0.1 % TritonX-100 (PBS-T) for permeabilisation of cell membranes. Cells on coverslips were blocked in 10% normal goat serum (NGS) for one hour. Primary antibodies (ms@cFos (1:100) and rb@Flag (1:250)) were diluted in given concentrations with NGS and incubated for 3 days. After the incubation phase, the coverslips were washed for 3 x 5 minutes with PBS. Secondary antibodies (gt@ms Alexa 488 and gt@rb Alexa 568) in the dilution 1:600 were incubated for 2 hours. After the final incubation time, the coverslips were washed twice with PBS for 10 minutes and once for 10 minutes in distilled water, mounted with Vectashield® (mounting medium for fluorescence with DAPI) and stored until imaging at 4°C in the dark.

3.6.4. Image analysis

Fluorescence analyses for specificity test of cFos (E8) antibody in Hek293 cells were evaluated using an epifluorescence microscope (Leica DM6) using 63x (NA 1.40) Plan Apochromat oil immersion objective. These were partially merged into projections from multiple individual images. The pixel size is 2048x2048.

Fiji (Schindelin et al., 2012) (https://fiji.sc/) was used for image processing.

After splitting the channels, the in-cooperated function "*Rolling Ball Background Subtraction*" with a rolling ball radius of 150 pixels was used, to correct for unevenly illuminated background. For the composite, the modified channels were merged and overlaid to a bright field image.

3.6.5. Specificity tests via western blots

For discontinuous sodium dodecyl sulfate-polyacrylamide gel electrophoresis (SDS-PAGE), 50 µg protein of each sample was mixed with SDS sample buffer and boiled in a water bath for 3 min. Proteins were then separated in a 10% acrylamide gel for ca. 60 min at 160 V and finally transferred to a nitrocellulose membrane (Whatman PROTRAN®, pore size 0.2 µm). All reagents and equipment come from the Bio-Rad TGX Stain-Free™ FastCast™ acrylamide kits using 1.0 mm gel thickness, following manufacturer instructions.

Ponceau S membrane staining was used for visualising protein transfer and detect proteins on nitrocellulose membranes. The membrane was placed for 1 minute in the staining solution and washed afterwards with distilled water.

To detect proteins with a specific antibody, the blot was first washed with TBS-T. Then, non-specific binding sites were blocked by incubation in TBS-T containing 5% nonfat dried milk powder for one hour at 37°C. After blocking, the primary antibody (ms@cFos (1:100) or ms@Flag (1:1000)) were incubated overnight at 4°C. The excess primary antibody was removed by washing with TBS-T (3 x 10 min). Subsequently, the HRP-coupled secondary antibody (goat@ms IgG (H+L) HRP conj. (1:2000)) was applied for 2 hours at room temperature. To remove excess secondary antibody, the nitrocellulose membrane was washed twice with TBS-T for 10 minutes and once for 10 minutes in TBS.

The HRP-coupled secondary antibody was detected on the nitrocellulose membrane using the Pierce™ ECL Western Blotting-Substrat and the ChemiDoc MP Imaging System.

3.7. DAB (3,3'-Diaminobenzidine) Immunohistochemistry

3.7.1. Preparation of brain tissue

See section 3.5.1 DiI tracing – preparation of brain tissue.

3.7.2. Cryosectioning

The brain was cryoprotected with a graded saccharose series 10-30% D(+)-saccharose in PBS for up to 5 days at 4°C, embedded in Tissue-Tek® O.C.T.™ Compound and cross sectioned (30 µm) using a cryostat (Leica CM 1860) with polytetrafluoroethylene-coated broadband blades. The sections were mounted onto gelatin-coated SuperFrost Plus™ GOLD glass slides in 6 series and stored at −20°C until DAB staining occurred.

3.7.3. DAB (3,3'-Diaminobenzidine) staining

3,3' Diaminobenzidine (DAB) is a widely used chromogen for immunohistochemical staining. In the presence of the peroxidase enzyme, DAB produces a brown precipitate that is insoluble in alcohol (Mardle, 2006).

Every second series of brain slices was stained against the cFos (E8) antibody using an avidin-biotin-peroxidase complex (ABC) immunohistochemical staining procedure (Butler et al., 2019). Stored slides at -20°C were kept on a heating block for 45 minutes at 37°C, followed by a 20-minute sodium citrate buffer antigen retrieval in a hot waterbath at 96°C (10 mM sodium citrate, 0.05% Tween 20, pH 6.0). Endogenous peroxidases were inactivated with 0.5% hydrogen peroxide for 30 minutes. After every incubation or blocking step, a triple wash with TBS was performed. All further incubation steps were performed using TBS containing 0.1 % TritonX-100 (TBS-T). Unspecific binding sites were saturated by incubation in 10% normal horse serum (NHS) dissolved in TBS-T. Slices were incubated with a monoclonal mouse cFos antibody (1:100) for 3 days at 4°C horizontally in a wet chamber. After being washed, the sections were incubated for 2 hours at room temperature in the biotinylated secondary antibody (Horse anti mouse IgG biotin-conjugated (1:2000)). After additional washing, the sections were incubated for 60 minutes in avidin-biotin-peroxidase solution (Vectastain ABC-Elite Kit (1:100)). After a final washing, the peroxidase activity was detected by using a heavy-metal-intensified 3'3-diaminobenzidine (DAB) reaction substituted by β-d-glucose/glucoseoxidase (Shu et al., 1988). Stained sections were dehydrated in a graded series of alcohol (ethanol 70%, 96%, 100%), followed by Neo-Clear™ treatment and coverslipped with ROTI®Mount.

4. Results

4.1. Behavioural conditioning

While the shuttle box (Horner et a., 1961) (Behrend & Bitterman, 1964; Portavella, 2004) thus far has only been used for magnetic avoidance learning in fish (Shcherbakov et al., 2005), we have successfully adapted it to positive reinforcement conditioning to magnetic field stimuli: each of the four individually trained rainbow trout have learned to respond to an oscillatory magnetic field and thus must be able to discriminate between the static geomagnetic field and an oscillating magnetic field (3 Hz, ± 100 µT B) superimposed on it.

Specifically, individuals were trained to swim across a hurdle to obtain food when the conditioned magnetic stimulus was presented. Crossing the hurdle within 15 sec after the onset of either stimulus counted as a (positive) response. In Fig. 7, it can be seen that the response rate slowly increases with training time, both for the reinforced stimulus (S+, vertical field oscillation) and non-reinforced sham stimulus (S-).

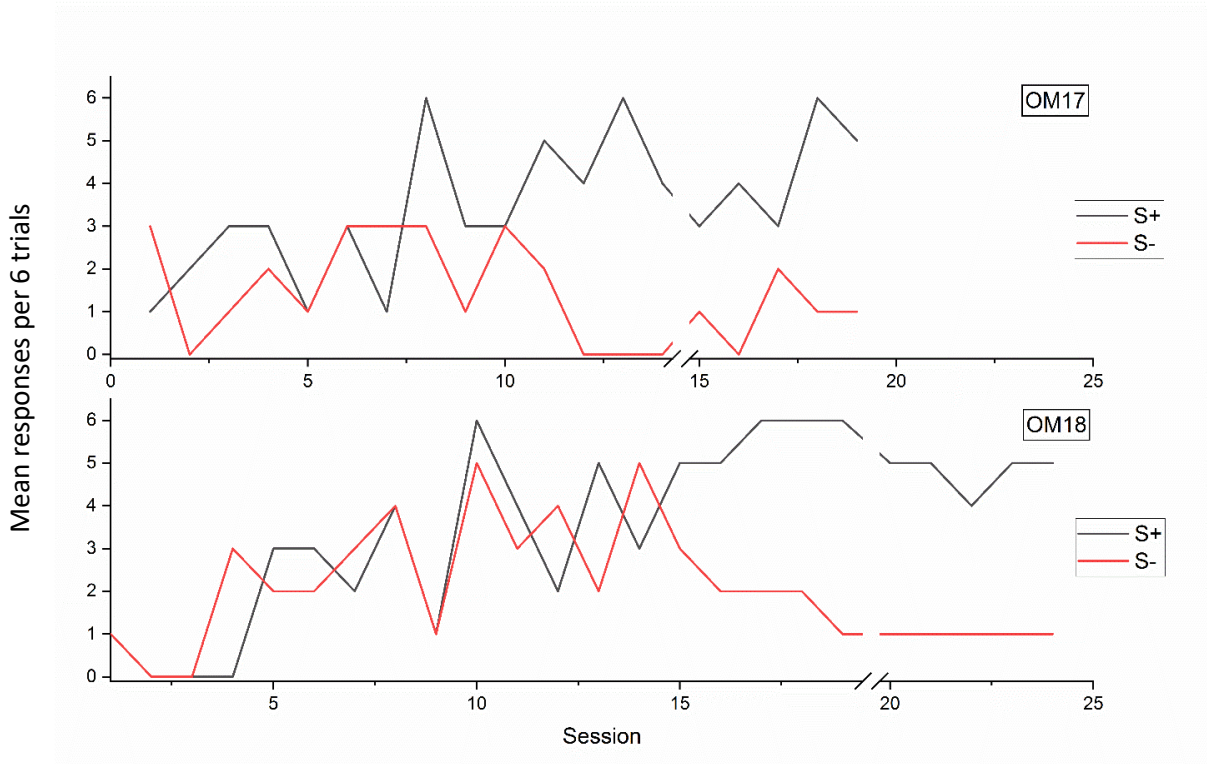

Figure 7: Individual learning and recall performance (stimulus 1, vertical field oscillation)

The response to the magnetic field stimulus is shown in black, the response to a sham stimulus is shown in red. The recall performance starts after the fish reached the set learning criterion of three consecutive sessions with a χ2 value of p<0.05. This has been marked as a break in the session axis.

A clear difference in response rates emerged after the 10th (OM 18) or 15th (OM 19) training session, with the fish responding at a consistently higher rate to the reinforced stimulus (S+) than to the non-reinforced stimulus (S−). Thus, the fish reached the pre-set learning criterion and advanced into recall tests, where the magnetic stimulus was no longer reinforced. Both fish had a very good recall performance, with the number of correct positives in five CS trials significantly exceeding the number of false positives in five sham trials (OM 17: $p = 0.03$, OM18: $p = 0.001$; $\chi 2$ – test).

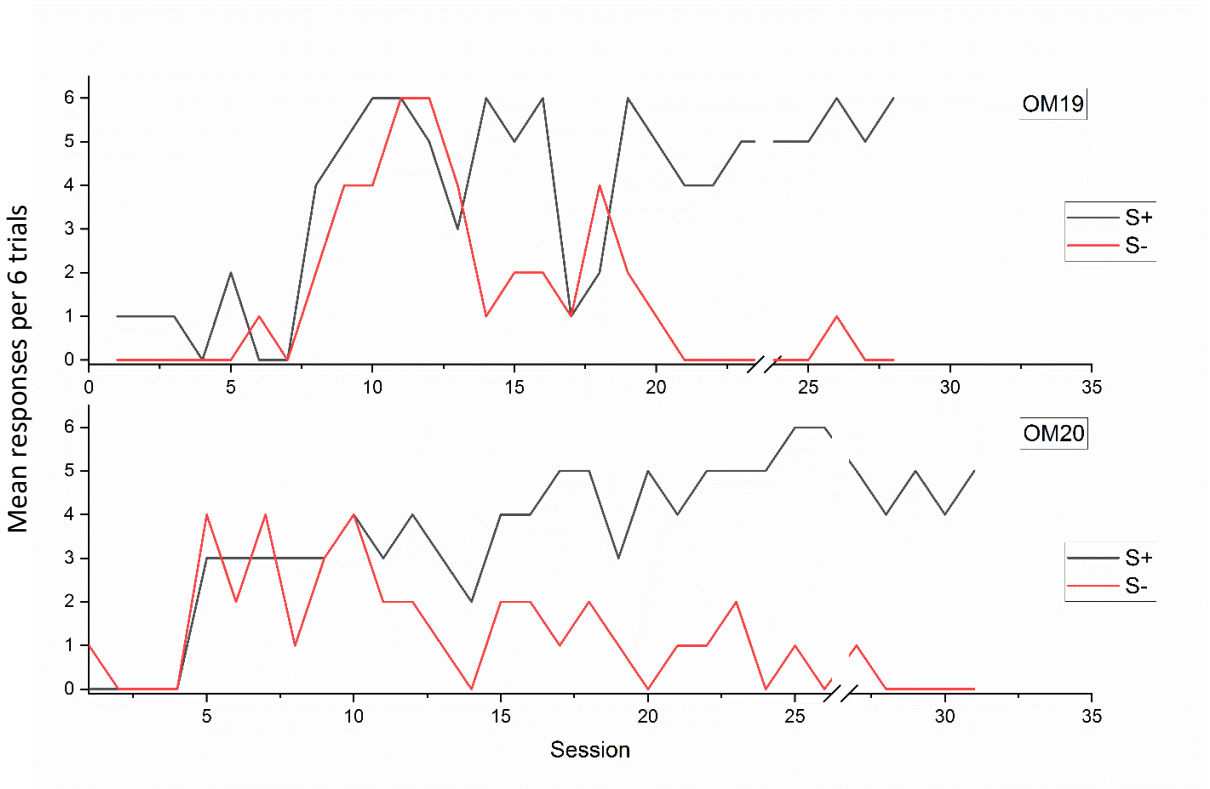

Figure 8: Individual learning and recall performance (stimulus 2, horizontal field oscillation)

The response to the magnetic field stimulus is shown in black, the response to a sham stimulus is shown in red. The recall performance starts after the fish reached the set learning criterion of three consecutive sessions with a $\chi 2$ value of $p<0.05$. This has been marked as a break in the session axis.

Fish also learned to respond to the horizontal field oscillation (Fig. 8), but on average, needed clearly more sessions (25) to reach the learning criterion compared to the vertical field oscillation (12). However, after reaching the learning criterion, both fish (OM 19 and 20) show a more robust readout in the recall performance, responding consistently more often to the CS stimulus (which was reinforced before as S+) compared to the sham stimulus ($\chi 2$ – test: $p = 0.0001$).

Figure 9 summarises each individual's correct and false positive response rates in recall tests. This shows that the 99% confidence interval (red) for the correct positive response rate to the MF stimulus is above the 50% level of guessing by chance. However, a fish may have learned to shuttle as

often as possible without taking note of the field. Therefore, for a complete statistical evaluation, we must relate the correct positives to false negatives. The respective 99% confidence intervals do not overlap for any fish (Fig. 9). Therefore, the ratios are significantly different, at least at the 1% level. Any statistical test for count data (e.g. $\chi 2$ - test) or for proportions (GLM with binomial error) gives a p-value of less than 10^{-4}. The ratio of correct to false positives is about 8 in our case.

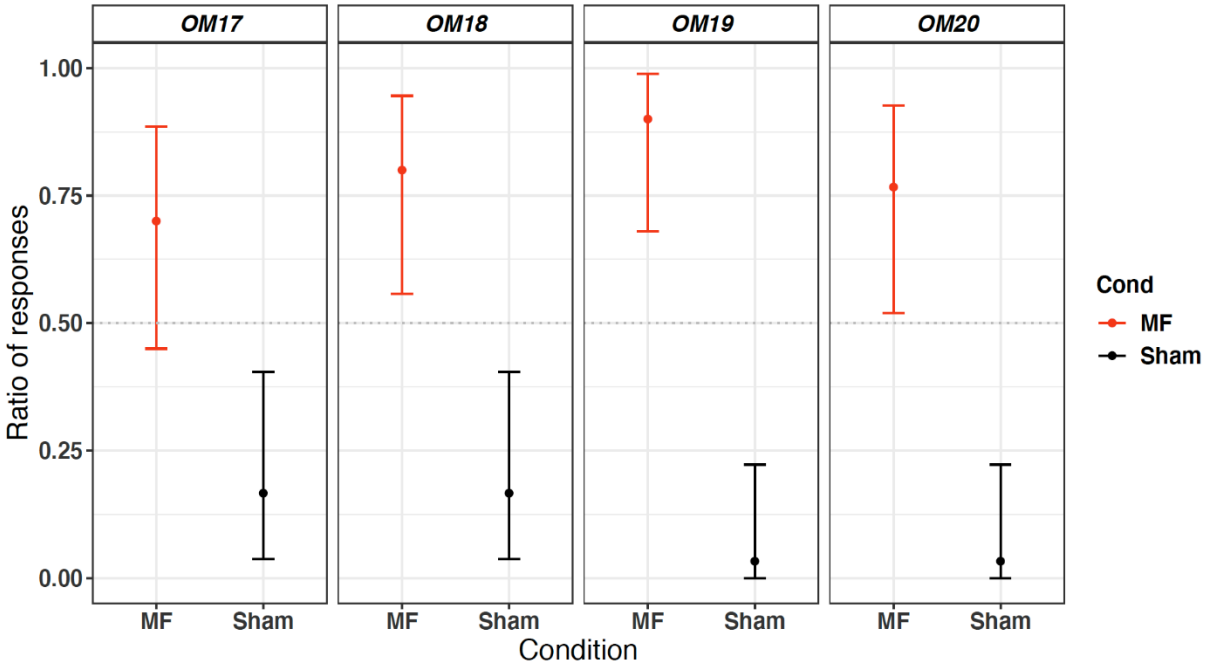

Figure 9: Recall performance

The correct positive (S+ / red) vs false positive (S- / Sham / black) response rates with a binomial confidence interval of 99%. The gray line shows 50% level of guessing by chance.

4.2. Daily cycle of the stress hormone "cortisol”

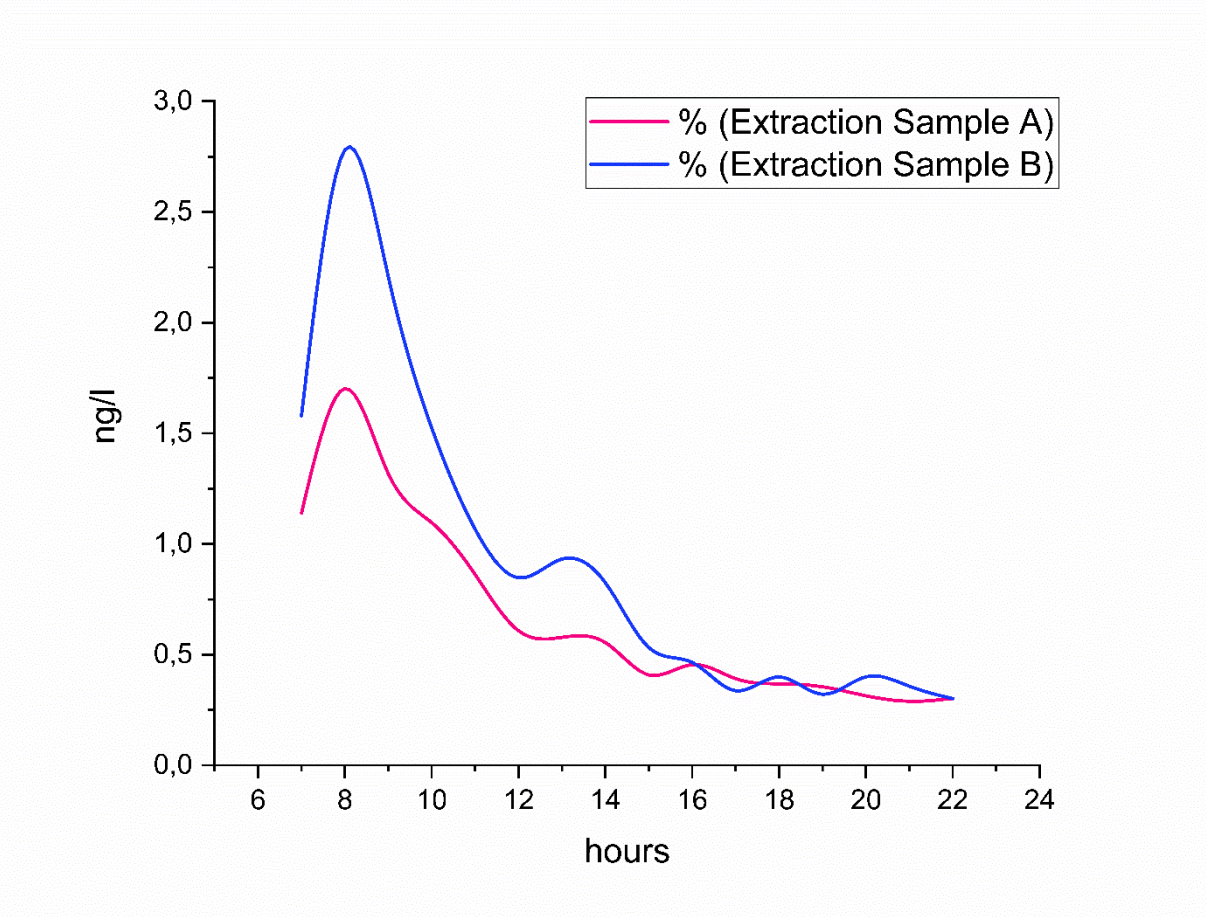

Figure 10: Diurnal variation of cortisol level in holding tank

Twofold analysis of water samples A (magenta) and B (blue) from the same time points on the 02.06.2022. Extraction samples A and B vary only in the frozen state after sample collection.

Humans produce the stress hormone cortisol, mainly in the early morning, to increase the activity of the body. To obtain the diurnal curve of cortisol production in fish, we sampled, on an hourly basis, the holding water of a single rainbow trout (20 cm) in a holding aquarium with the dimension adapted to the experimental setup for the molecular mapping behaviour study. Each point is a mean of two ELISA samples and then adjusted from ml to litre. A twofold sampling approach shows a difference in the morning hours (7:00 to 14:00). However, it appears to be only a shift in concentration, as the form of the line diagrams are very similar. In Figure 10, the highest values range from a maximum of 2.78 ng/l to a minimum of 0.37 ng/l. The highest concentration was measured at 8 am. From then on, the values decrease steadily until the afternoon at around 16 pm, when the cortisol levels are constantly low. For the Original data set, see supplement page 109.

For reproducibility, two controls were included in every run. The accepted value range for the controls can be found within the QC certificate of the *Cortisol-free in Salvia ELISA Kit (Table 3).*

Table 3: Control values for Quantification

	Mean (ng/ml)	Accepted range (ng/ml)
Control 1	0,35	0,2 – 0,5
Control 2	2,11	1,4 – 2,9

Further control experiments with a predefined amount of cortisol (30 ng) were performed in a 2 hour time range (See supplement page 113).

4.3. Behavioural time design for molecular mapping

Based on the collected data on the diurnal course of cortisol production in Figure 10, two different time intervals were selected to observe the spontaneous behaviour of two individuals, each for 1-hour, in the experimental setup for molecular mapping. One of the time intervals was from 09:30 to 10:30, i.e., after the peak of the morning cortisol levels. On the same day in the evening (starting time 19:30), inside the same setup and all conditions being the same, another individual was observed for one hour. With the Software BORIS, the video footage of the fish from the different time points was analysed. Anticipated behaviour for molecular mapping is a relaxed state, with little to no movement of the animals. As molecular mapping is a neuronal activity marking, every disturbance might mask the activity based on magnetic field changes.

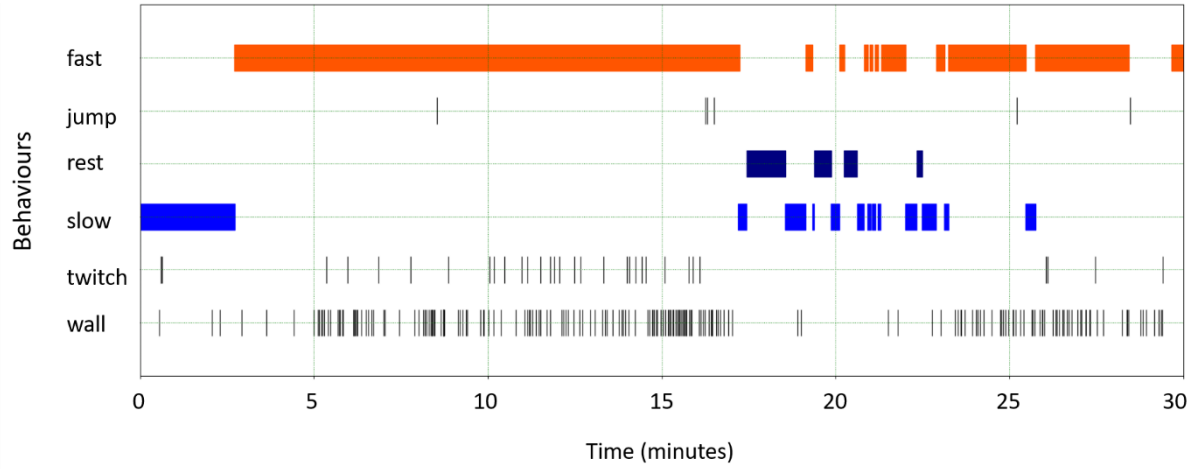

Figure 11: 30 minute sections of the observed hour in the morning from 09:30 to 10:30

Behaviour was coded with single events like twitching, touching the wall and jumping. As well as longer occurring events like slow and fast swimming. For a full description of the seen behaviour see table 2. The full analysis of the video can be found in the supplement (Sup-fig. 24).

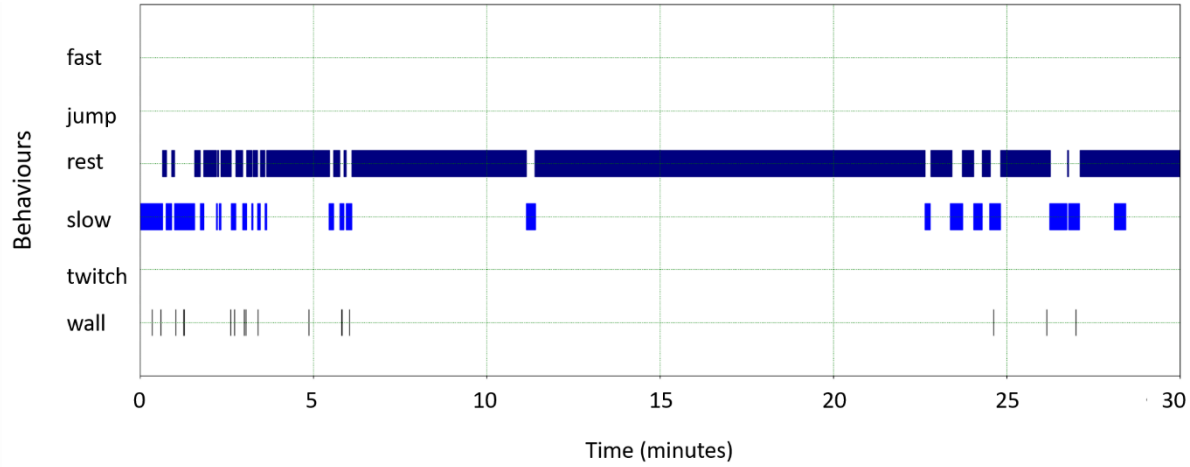

Figure 12: 30 minute sections of the observed hour in the evening from 19:30 to 20:30.

Behaviour was coded with single events like touching the wall, as well as longer occurring events like slow and resting phases. For a full description of the seen behaviour, see table 2. The full analysis of the video can be found in the supplement (Sub-fig. 25).

As the two ethograms clearly show, there is a stunning difference in the behaviour between the morning hours to the evening. The fish in the morning hours (Fig. 11) shows normal to rapid swimming movement during more than 80% of the whole observed hour. As well as having multiple single events of touching the wall with their face or swimming directly against the wall. The activity shown in the morning resembles exploratory behaviour and foraging.

During the evening hours (19:30 to 20:30), the second fish naïve to the experimental apparatus showed much calmer behaviour. In the beginning, slow swimming movements are apparent. However, the most frequently seen behaviour in Fig. 12 is rest, classified as calm movement (slow fin and body movement, no contact between face and wall, best if the fish stands free in the water). During the slow swimming movements, the chances of touching the walls increased only slightly, with up to 8 hits during the presented 30 min ethogram (Fig. 12). Table 4 shows, in comparison, all events for the 60 minutes the fish were observed during the morning and the evening. When speaking of the hit rate, during the morning, the fish touched the wall with a body part, but most of the time with his head 351 times. During the evening, the fish touched the wall only 45 times over a duration of 60 minutes, which can clearly reduce (albeit not totally abolish) unwanted trigeminal activation. Furthermore, it is remarkable that most of the time (40 minutes) was spent on fast swimming in the morning but on the resting phase in the evening. As rainbow trout align themselves along a current flow or an object, the previously described behaviour is most normal in a calm individual.

Table 4: Time budget of numbers and durations of occurrences for one hour of observed video analysis

	morning		evening	
Behaviour	Total number of occurrences	Total duration (min)	Total number of occurrences	Total duration (min)
rest	4	2.164	48	40.951
slow	34	12.439	49	19.518
fast	30	44.507	0	0
jump	7	NA	0	NA
twitch	64	NA	0	NA
wall	351	NA	45	NA

4.4. DiI Tracing Study

As mentioned in the introduction, the rosV branch of the trigeminal nerve was suggested to be involved in magnetoreception (Walker et al., 1997). While it can be assumed that the axons of rosV project to a trigeminal nucleus in the hindbrain, such a connection has not been published for trout. For this purpose, a fluorescent carbocyanine tracer, DiI, was used to trace retrogradely from the nervus trigeminus V to motor nuclei and sensory processing centres. In want of a brain atlas for trout, we assign the regions identified with tracing to neuroanatomical regions known from zebrafish (Wullimann et al., 1996) or goldfish (Puzdrowski, 1988).

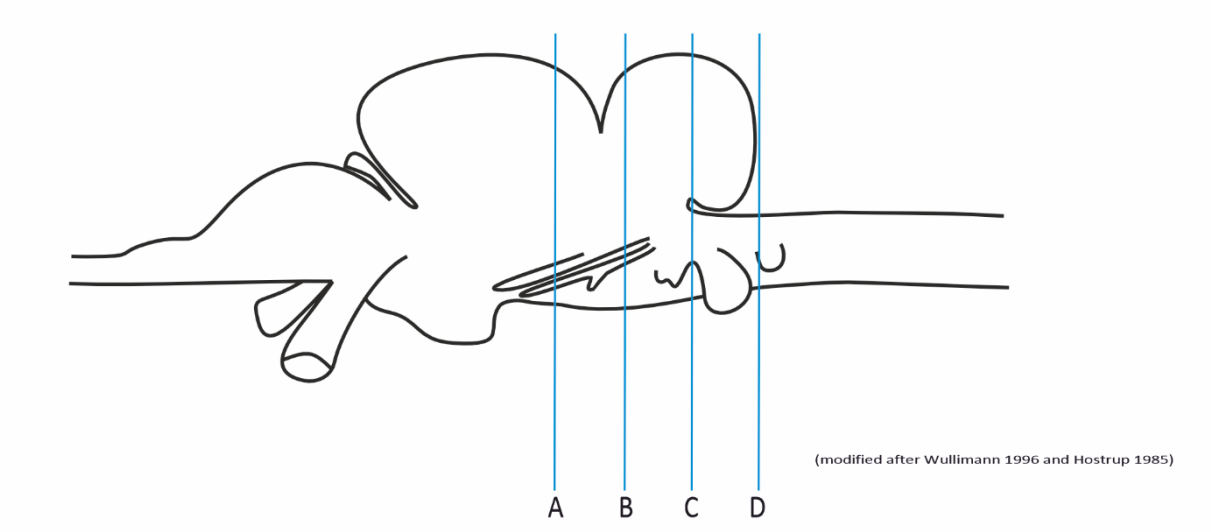

Figure 13: Lateral view of the adult rainbow trout brain

Lines indicate the position of tissue sections illustrated in the following series of cross sections. Individual displayed sections were taken at equal intervals of 360 µm. The brainstem, which harbours most cranial nerve roots except for the optical and olfactory nerves, is covered rostrally by the cerebellum. The medulla oblongata grades into the spinal cord.

The medulla oblongata (MO) contains the sensory and motor nuclei of the trigeminal nerve V, as well as abducens VI, facial VII, octaval VIII, glossopharyngeal IX and vagal nerves X.

There are two distinct trigeminal motor neurons. One is located dorsally to the lateral longitudinal fascicle (NVmd). The other is located at the ventral edge (NVmv) of the fascicle. Both of these neurons extend more into the caudal region, where the lateral longitudinal fascicles run more medially. Trigeminal sensory nuclei are to be classified as follows: The most rostral is the isthmic primary sensory trigeminal nucleus (NVs). It is located more caudally at the media-dorsum of the descending root of the trigeminal nerve (DV). Less clearly defined is the sensory nucleus (NDV) of the descending root (DG). It can best be identified at the caudal octavelateralis level (Puzdrowski, 1988; Wullimann et al., 1996).

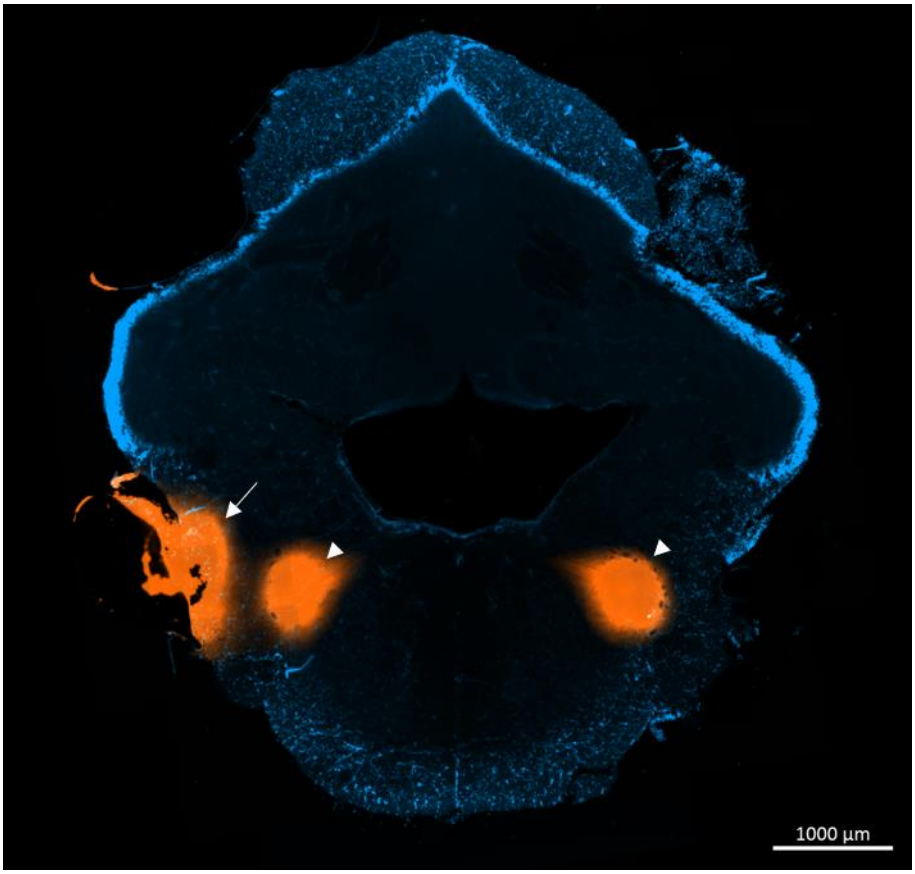

Figure 14: Cross section A

The white arrow indicates the last fluorescent radiance from the trigeminal nerve V, and the white arrowhead indicates the descending trigeminal root DV and the Isthmic primary trigeminal nucleus (NV).

As the trigeminal nerve enters the brain stem, it divides into two trigeminal roots. The sensory nerve V not only sends fibres to the Isthmic primary trigeminal nucleus (NV) but also turns into the descending trigeminal root (DV) as it descends to the caudal tip of the medulla oblongata. Seen in Figure 14, the radiance of the fluorescent dye makes the descending trigeminal root and the isthmic primary trigeminal nucleus indistinguishable from one another.

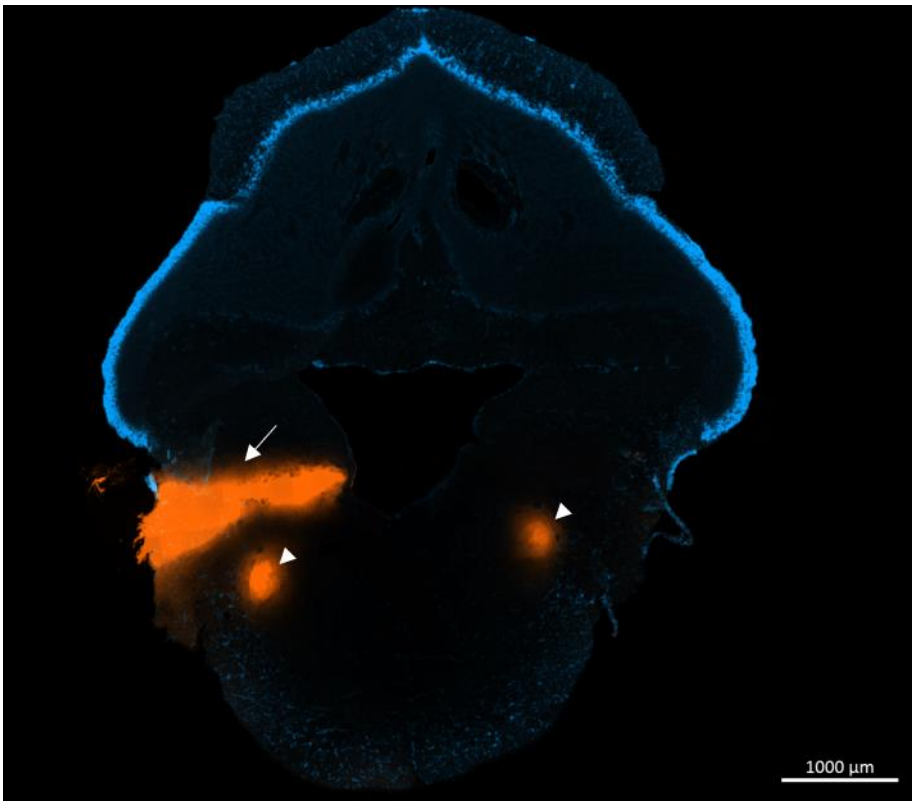

Figure 15: Cross section B

White arrow indicates the sensory root of the facial nerve (VII), and the white arrowhead indicates the descending trigeminal root (DV).

The tracing of the facial VII nerve was selected as a controlled marker, as the sensory root of the facial nerve provides a very specific structure (Fig. 15).

The sensory root of the trigeminal verve V divides into rostral bundle and the descending trigeminal root (DV), which descends in the medulla oblongata (Fig. 15, 16 and 17). The DV provides somatosensory input to the nucleus of the descending trigeminal root (NDV) and, further, caudally to the medial funicular nucleus (MFN).

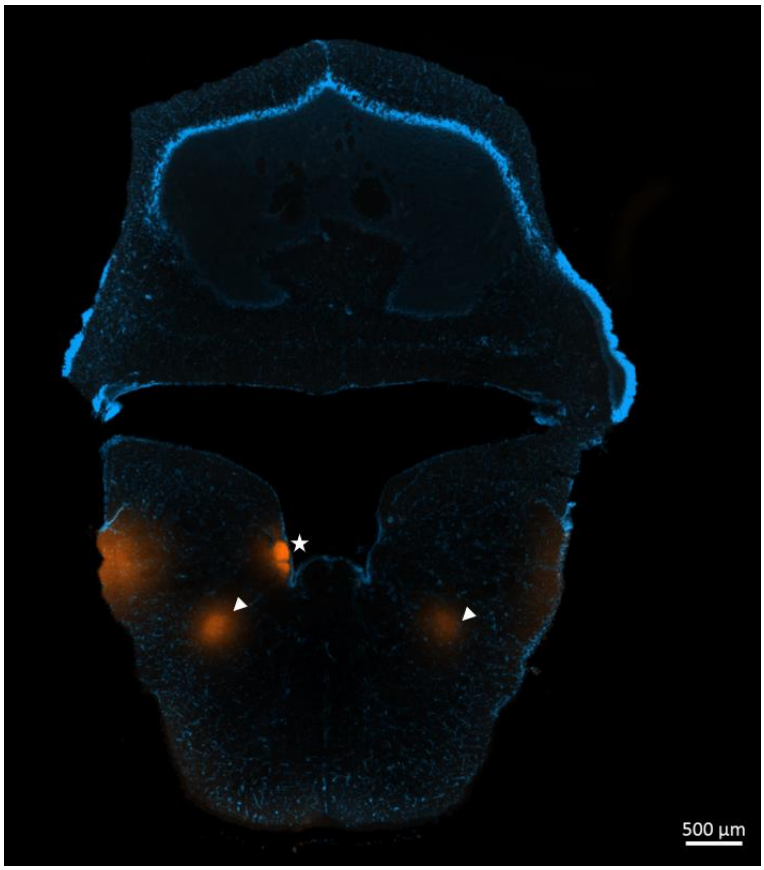

Figure 16: Cross section C

Lateral view of the rainbow trout brain. White arrowhead indicates the descending trigeminal root (DV), white star indicates the lobus facialis (LVII)

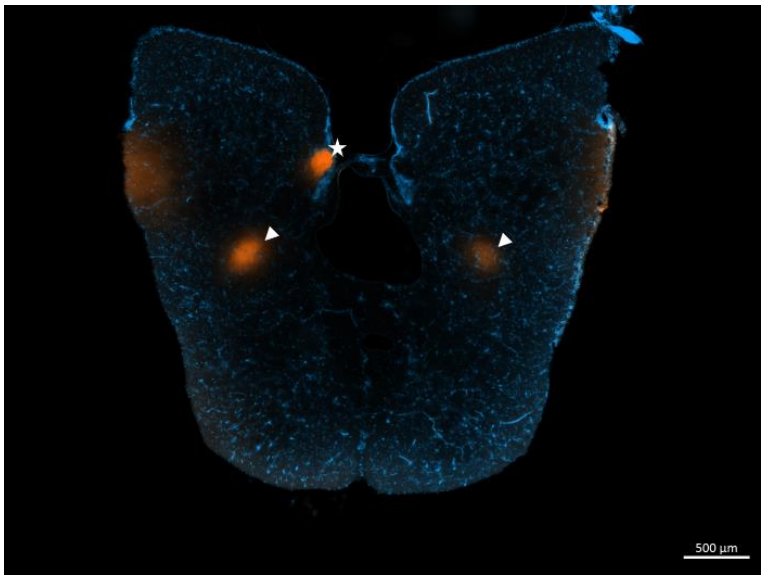

Figure 17: Cross section D

Lateral view of the rainbow trout brain. White arrow head indicates the descending trigeminal root (DV), white star indicates the lobus facialis (LVII).

4.5. Antibody cFos Validation

As part of the long-term research project on magnetic field perception in the fish brain, using behavioural molecular mapping, the monoclonal antibody E8 against cFos, which was used in earlier IEG studies on rodents and birds, had to be validated, first against cFos of rainbow trout to rule out false negatives, and then on brain tissue of trout to assess the chances of obtaining false positives due to cross-reactivity, i.e. binding to unspecific epitopes which may be present in trout.

4.5.1. Immunocytochemistry

First, it was necessary to test the immunoreactivity of the antibody with cFos of rainbow trout. For this purpose, trout cFos was expressed with a pFLAG-CMV™-5.1 expression vector in a human embryonic kidney (Hek293) cells, which as non-neuronal cells have no significant expression of human cFos. cFos detected by the specific E8 antibody was found to be colocalised with the pFlag peptide sequence detected with a specific pFlag antibody (merged fluorescence image, see Fig. 18), which confirms that the anti-cFos antibody recognises the trout variant of the antigen. Most cells in the bright field image (Fig. 18) were negative for both cFos and pFlag, with the transfection being slightly below 30%, as calculated from an overview image (Sup-fig. 26) for one of the transfection experiments. Secondary antibody controls (Sup-fig. 27) show a lower fluorescence and no co-localisations, which confirms that the signals observed with primary and secondary antibody combined are due to cFos. Taken together, this shows indeed that the cFos antibody E8 can detect cFos from rainbow trout expressed in HEK cells.

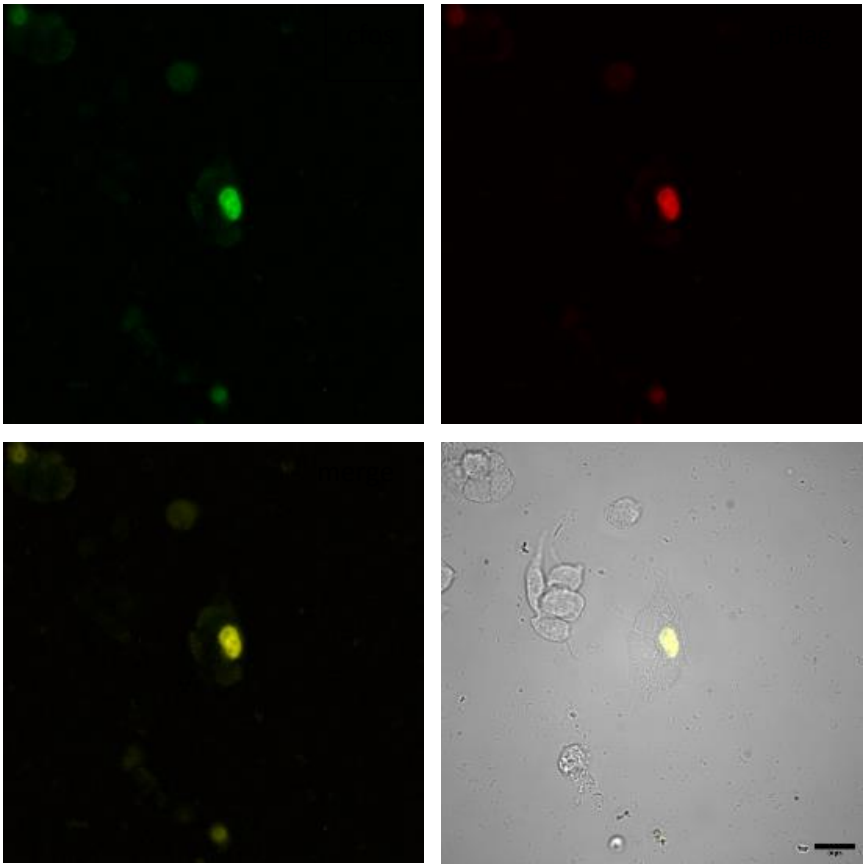

Figure 18: Specificity test of cFos (E8) antibody in Hek293 cells

Hek293 cells were transfected with vectorDNA (cFos sequence rainbow trout) and analysed based on the co-localization of vector induced pFlag with vectorDNA in the cell nuclei. Bars = 20 µm

4.5.2. Western blots

cFos immunoreactivity was quantified by Western blot using total homogenates of HEK cells transfected with cFos in a pFLAG-CMV™-5.1 Expression Vector, in relation to a negative control, i.e., HEK cells transfected with an N-terminal FLAG® fusion protein of *E. coli* bacterial alkaline phosphatase (BAP) with a calculated molecular mass of 49.3 kDa, i.e. similar to cFos. Fig. 19 shows anti-cFos immunoreactivity only for the cFos transfected HEK cells, but not for the negative control. The cFos (E8) antibody binds to cFos protein sequences with a calculated molecular weight between 39kD to 62 kDa.

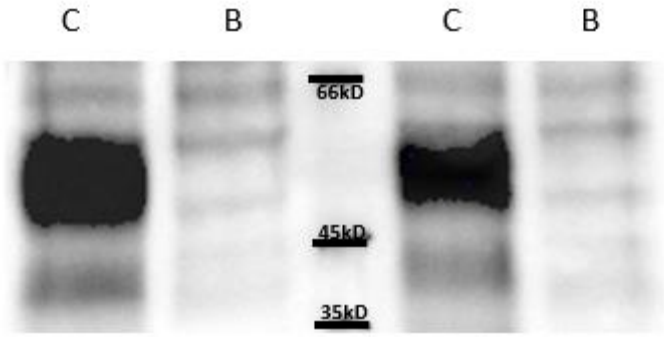

Figure 19: Cutout of the double Western blot with a cFos immunoreactivity in transfected Hek293 cells.

Original in supplement page 147. In the protein line titled "C", the Hek cells were transfected with the cFos sequence of a rainbow trout. Moreover, in the lines titled "B", the Hek cells were transfected with an Amino-terminal FLAG-BAP fusion protein.

For further controls, the transfected HEK cells were tested on their immunoreactivity with an antibody binding to the FLAG fusion protein. As shown in Fig. 20, the monoclonal antibody ANTI-FLAG® M2 binds to fusion proteins containing a FLAG- peptide sequence in both transfected HEK cell cases (cFos and BAP). The FLAG- peptide sequence has a calculated molecular weight of 1,01kD, and even with the multiple cloning sites of the vector, the overall molecular weight of an empty vector would not show up on a western blot.

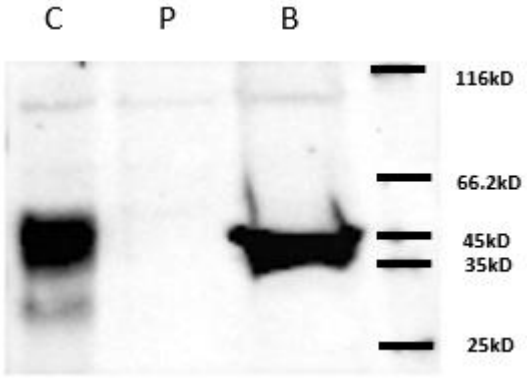

Figure 20: Cutout of Western blot with pFlag immunoreactivity in transfected Hek293 cells.

Original in supplement page 147. Lane "C" is derived from HEK cells transfected with pFLAG-CMV™-5.1 containing the cFos- sequence of rainbow trout, lane "P" from HEK cells transfected with empty pFLAG-CMV™-5.1 (negative control), lane "B" from HEK cells transfected with an Amino-terminal FLAG-BAP Fusion Protein.

4.6. The Avidin–Biotin Complex (ABC) Method

The avidin-biotin complex (ABC) method has been used to conjugate both the secondary antibody and the amplifier (the DAB precipitation enzyme, horseradish peroxidase, HRP) with biotin to be linked irreversibly with avidin. Avidin, with its four biotin-binding sites, would ideally bind three biotinylated amplifier molecules and one biotinylated secondary antibody, producing a base amplification of 3:1, with other finite ratios being less effective and 0:4 or 4:0, resulting in negative results. It is clear that a number of controls are needed to ensure that dark staining (due to precipitated DAB) indicates the desired immunoreactivity, where the secondary antibody attached to the ABC complex is bound to the primary antibody which in turn has bound to its cognate antigen (Fig. 21 ABC DAB process).

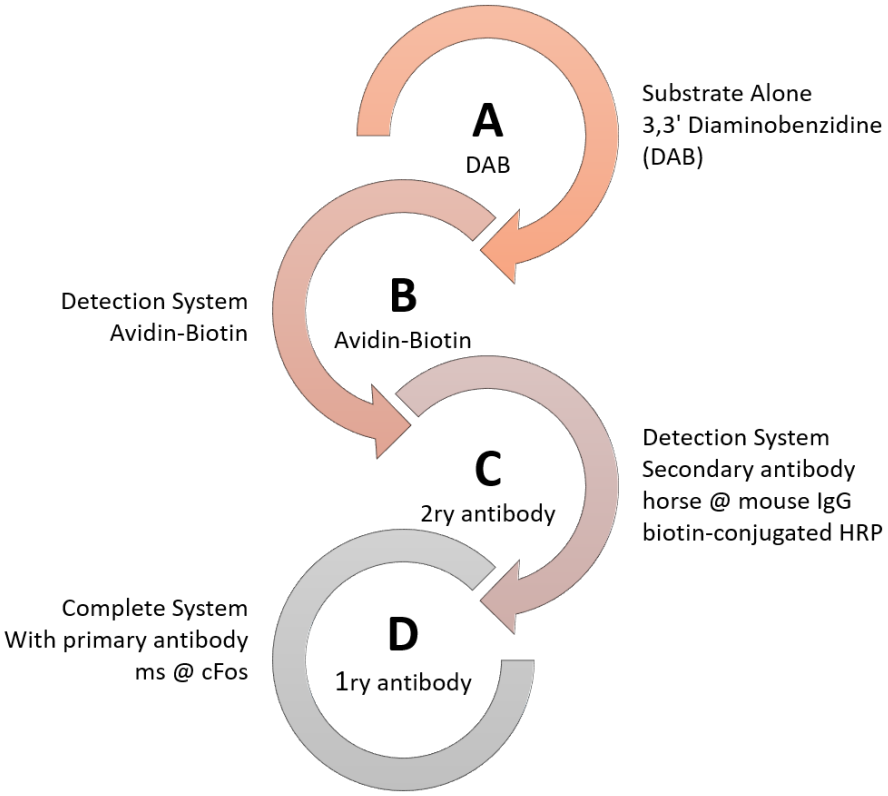

Figure 21: Visual sequence of the previously described ABC–DAB process

Deletion controls were performed to evaluate primary, secondary, and background staining.
The substrate solution (DAB) can lead to endogenous enzyme reaction and develop a visible product in the cells, making the background indistinguishable from the target protein, which was not the case (Fig. 22 A). Further, if not all biotin binding sites of the avidin-biotin complex are saturated, the complex may label endogenous protein-bound biotin or lectins, which would obviously lead to false conclusions. Again, this was not the case here (Fig. 22 B). A simarly wrong conclusion would result from cross-reactivity between secondary antibody and proteins with similar amino acid sequences to

the primary antibody, which was not observed either (Fig. 22 C). Thus, the brain tissue passed the series of delection controls, showing no reactivity. At last, the complete avidin-biotin complex - DAB enhancement with primary antibody results in DAB staining (Fig 22 D), which in the light of absence of staining in negative controls, suggests a specific immunoreactivity due to the primary antibody ms@cFos E8, with no broken links in the reaction chain depicted in Fig. 21.

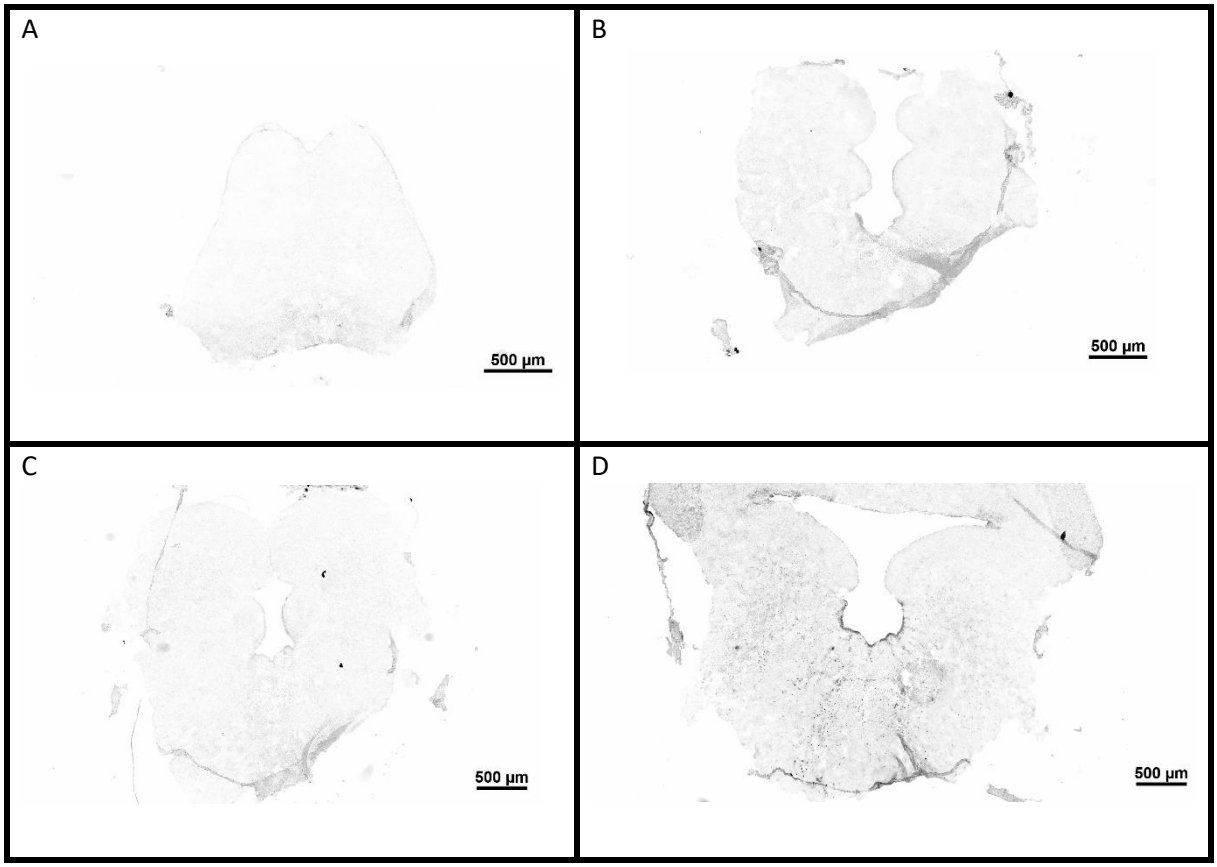

Figure 22: Comparison of staining after ABC–DAB procedure with deletion controls

Trout brain tissue with (A) only 3,3'-Diaminobenzidine (DAB) added, (B) with avidin-biotin complex added, (C) with secondary antibody horse@mouse IgG biotin-conjugated HRP added, (D) with primary antibody mouse@cFos E8 added; all steps were performed on one series of cross sectioned rainbow trout brain.

After successfully testing the staining procedure, a number of ABC-DAB stained tissue sections were analysed in terms of cFos abundance in specific brain areas. The example shown in Fig. 23 (cross section through hindbrain) had a particularly strong cFos expression in the cerebellum, specifically in the granular layer of the corpus cerebelli with corpopetal connections to the rhombencephalon (Wullimann & Northcutt, 1988). Cerebellar activity is no surprise given that the fish were mostly swimming in the tank before they were sacrificed for the study. Zooming onto the medulla oblongata, a clear immunoreaction is visible in some regions, with little activity in the descending

trigeminal root (DV) and in the nucleus of the descending trigeminal root, the identification of which would not have been possible without the knowledge gained from the DiI tracing (see Section 4.4)

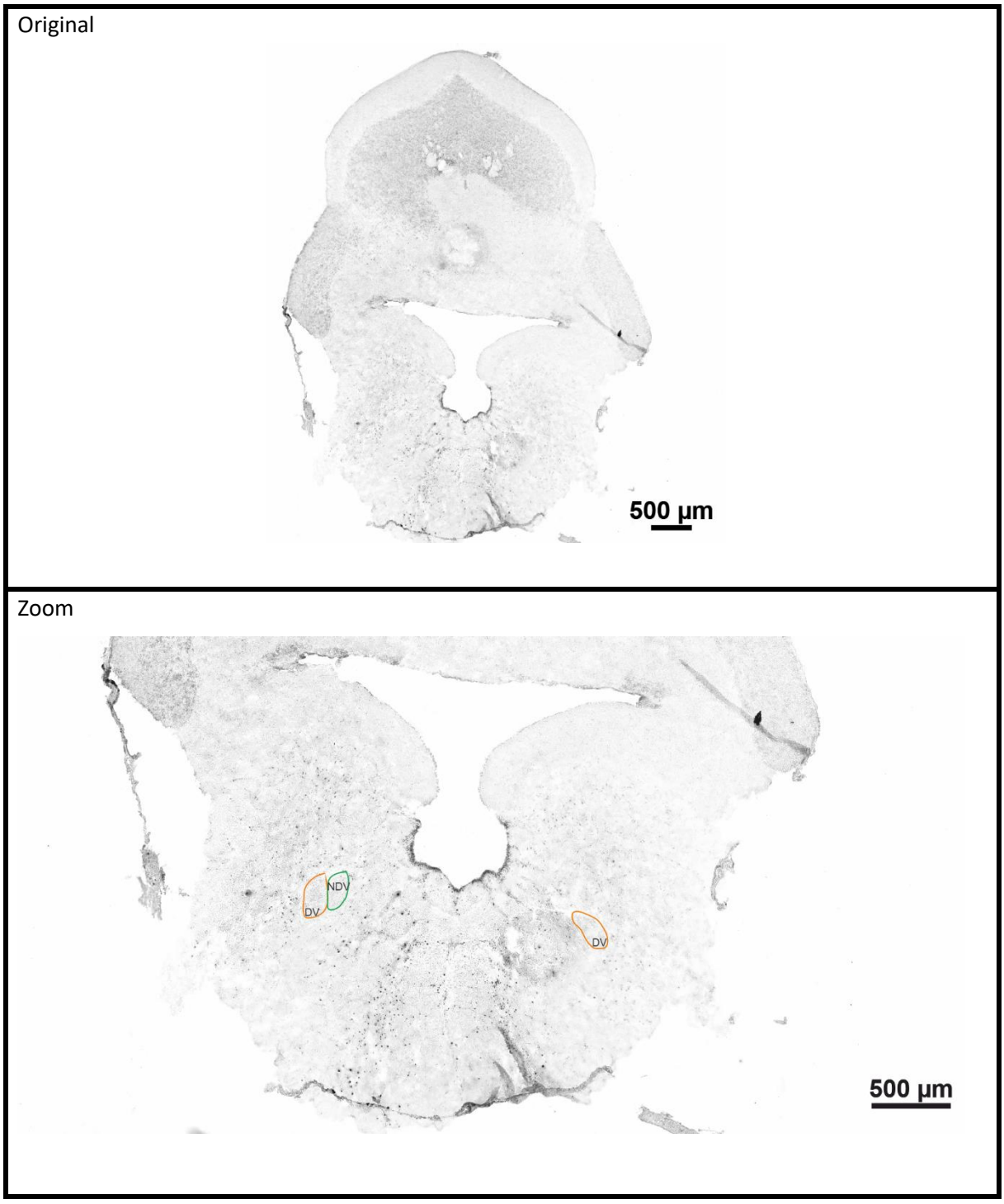

Figure 23:Original and zoom from the complete ABC - DAB process

Orange encircled areas indicates the descending trigeminal root (DV), green encircled area indicates the nucleus of the descending trigeminal root.

5. Discussion

5.1 Behavioural conditioning

Our results clearly show that rainbow trout (*Oncorhynchus mykiss*) can be trained in our Horner-type shuttle box paradigm to respond to an oscillating magnetic field as positively reinforced stimulus (S+), and did so significantly more often compared to a non-reinforced sham stimulus (S-). Although the learning rate differed among the four animals studied, they all reached a predefined learning criterion and showed robust conditioned responses in subsequent recall performance tests (without reinforcement), with the correct positive rate being, on average, eight times higher than the false positive rate ($p<0.01$). In comparison, other magnetic conditioning experiments on rainbow trout (Haugh & Walker, 1998; Shcherbakov et al., 2005; Walker et al., 1997) or yellowfin tuna (Walker, 1984) reported a ca. 20% difference between S+ and S- responses, both measuring the striking rate at the same feeder. The small effect size obtained in previous studies can be attributed to a high rate of feeder use during S- trials, because fish were not discouraged from waiting around the singular feeder and therefore did not have to invest energy to get to the feeder. In contrast, fish had to shuttle to approach the feeder with food in our paradigm. Therefore, our results suggest that shuttling is a much clearer operant response and readout compared to striking rate at a singular feeder. This can be seen in Fig. 9, showing the correct positive (CP, MF stimulus) and false positive (FP, sham) response rates per individual. The 99% confidence interval for the CP rate is above the 50% level of guessing by chance. However, fish may have learned to shuttle as often as possible without taking note of the field. Therefore, for a complete statistical evaluation, we need to put the CP rate in relation to FP rate, which differs highly significantly ($\chi 2$ – test $p < 10^{-4}$). In previous work, feeder usage has been treated as a continuous variable, using ANOVA or t-test, but in essence is a count variable too, so that the previously reported p-values (< 0.05) may not be precise.

It was found earlier that the requirements for successful magnetic conditioning are a conditioned movement response and a conditioned stimulus that is spatially distinctive from the non-reinforced one, for example, a gradient field vs a homogeneous field (Haugh & Walker, 1998). However, Shcherbakov et al. (2005), as well as Hellinger and Hoffmann (2009, 2012), reported that trout could be conditioned to a sudden, but spatially homogenous change in magnetic field, and we here demonstrated the same for a sinusoidally oscillating, but again spatially homogenous field. One may argue that these conditioned magnetic stimuli are highly artificial since such dramatic changes do not occur in the natural geomagnetic field, making it unlikely that animals have a default behavioural program to respond to rapid field changes (R. Wiltschko & Wiltschko, 1996). In contrast, rapid changes in chemical, visual, mechanical (acoustic, tactile), or thermal sensory modalities often

indicate new environmental situations that necessitate a behavioural response. On the other hand, fish often make body turns, implying fast changes of the magnetic field in the body-fixed reference of the fish, so it would be beneficial for fish to update the field reading at a high rate.

When it comes to detecting the magnetic signal, there are three possible magnetoreceptor mechanisms based on magnetic particles, radical pairs, and electromagnetic induction. Magnetoreception by magnetic particles is currently considered the most plausible possibility for teleost fish, even though there is no conclusive evidence yet for the structural correlate of the magnetoreceptor. Walker et al. (1997) identified magnetically responsive nerve fibres in the ramus ophthalmicus superficialis trigemini (rosV) of rainbow trout and traced them with a lipophilic dye into the sensory periphery, with some traced processes terminating in the lamina propria of the olfactory rosette. A putative magnetoreceptor containing intracellular reflective particles, presumably magnetite crystals (Diebel et al., 2000), was identified near the terminals (Walker et al., 1997). Although the presence of intracellular reflective particles has been confirmed recently (Bellinger et al., 2022), the very nature of the magnetoreceptor remains enigmatic. A key challenge in identifying magnetic particle-based magnetoreceptor structures is the need for a robust histological protocol excluding tissue contamination with externally incorporated particles, particularly in the olfactory rosettes (Curdt et al., 2022).

Teleost fish express cryptochromes in various cell types of the retina (Haug et al., 2015), notably Cry4, which is a hot candidate for the light-dependent radical-pair mechanism of magnetoreception in birds (Xu et al., 2021). Based on our study, a light-dependent radical-pair mechanism cannot be ruled out in rainbow trout, as all experiments were performed under white light conditions to keep the feeders visible. However, (Hellinger & Hoffmann, 2009, 2012) have shown that rainbow trout can detect changes in intensity/inclination and direction in total darkness.

Last, magnetoreception by electromagnetic induction with inner-ear semicircular canals as an accessory organ (Jungerman & Rosenblum, 1980) has long been considered impossible in animals that are not equipped with highly sensitive electroreceptors (Winklhofer, 2019) but have recently been suggested as a feasible possibility for homing pigeons (Nimpf et al., 2019). The sensitivity for voltage gated ion channel in rainbow trout have yet to be investigated. However, in the case of zebrafish, it is suggested that they do not have the crucial amino-acid motif in the sequence data of the voltage-sensitive calcium channel $Ca_V1.3$ (Bellono, Leitch, et al., 2017; Nimpf et al., 2019).

As opposed to radical pair and magnetic-particle based mechanisms, the induction mechanism is not directly sensitive to the magnetic field, but to its derivative with respect to time. To test for electromagnetic induction, we can lower the oscillation frequency of the conditioned stimulus in recall experiments to the point where the rate of magnetic field change falls below the detection threshold of a semicircular canal. Should conditioned responses sustain, one could reject the induction mechanism.

5.2 Retrograded tracing of the trigeminal nerve V

Neuroanatomy has been concerned with tracing neural connections since the early days of Golgi and Caajal, which has had a significant impact on the study of neural functions and the development and maturation of the nervous system. Axonal transport has resulted in the development of a long list of markers, referred to as "anterograde" or "retrograde" tracers, based on the axon's preferred path of transport (Vercelli et al., 2000).

DiI (*1,1'-Dioctadecyl-3,3,3',3'-Tetramethylindocarbocyanine Perchlorate*) is a lipophilic membrane dye that spreads by lateral diffusion to cover the whole cell. It is weakly fluorescent until it enters membranes. The tracer and implementation method has pros and cons regarding cost, time and distance, specificity, single-cell labelling, multi-cell labelling, and user-friendliness. In this study, DiI performed well in labelling the descending trigeminal root (DV) retrogradely into the medulla oblongata (Fig. 14-17). However, as mentioned in other studies, DiI's major disadvantage is its slow diffusion, which can take anywhere from weeks to months to analyse, as well as the radiation of the stain (Heilingoetter & Jensen, 2016).

Using the anatomical references from (Wullimann et al., 1996), the marked areas of the DiI could be further identified and categorised. Due to the closeness of the nuclei to the root areas of the descending trigeminal nerve V, it is difficult to differentiate between them using only the fluorescent stain. To further investigate and identify the processing brain areas, it is recommended to consider a series of sections, with each parallel section of cFos staining as an overview stain (for example, Nissl). This will enable a more accurate identification of the brain areas.

5.3 Immediate early gene cFos as a neuronal marker

In songbirds, a number of candidate brain areas have been identified in magnetic field perception, such as Cluster N for the light-dependent inclination compass (Zapka et al., 2009) or trigeminal nuclei for map information (Heyers et al., 2010). Key experiments by (Hellinger & Hoffmann, 2012) on rainbow trout also point to the trigeminal system as a site for magnetic intensity and inclination

perception. Further, they found that conditioned responses to a 90° direction change persist in darkness, suggesting that compass information in fish – unlike birds – is conveyed through a light-independent pathway. Recent experiments on juvenile medaka (Myklatun et al., 2018) point to an involvement of the lateral hindbrain, from where all cranial sensory nerves emerge, except for the I. (olfactory) and II. (optical) nerve. There are few hints toward the location and internal structure of candidate magnetoreceptor cells, their afferent nerves, and central projections in the brain. Earlier reports of candidate receptor cells in trigeminally innervated, lateral parts of the olfactory organ (Walker et al., 1997) have not stood up to the acid test of independent replication.

A brain atlas for rainbow trout is not available, which would otherwise facilitate studies of brain activity under magnetic stimulation. To identify the key brain areas connected to the trigeminal system, I applied DiI stain crystals on the trigeminal nerve and traced its projections into the brain. These results can now be used to verify the brain areas which, under magnetic stimulation, have differential expression of immediate early genes (IEGs) as a proxy for neuronal activity.
While IEG expression studies have been immensely useful in studying magnetic activation patterns in bird brains (Elbers et al., 2017; Heyers et al., 2010; Kobylkov et al., 2020; Zapka et al., 2009), the protocols cannot be transferred to fish brains without first testing if available IEG antibodies against cfos or ZENK also recognise the fish-specific IEG homologues.

For *in vitro* validation of the cFos antibody, I have expressed the cFos homolog from rainbow trout in HEK cells and quantified antibody binding in western blots. In addition, I established a histochemical staining protocol (DAB) to label primary antibodies against IEGs (cFos) for rainbow trout and used it for visualising neuronal activity in stimulus-specific processing regions. When it comes to molecular mapping of behaviour with IEGs, the animal has to be stimulated for up to an hour. During this time, the animal should be as calm as possible to minimise noise in brain activity.
The stress hormone "cortisol" study confirmed the release of free corticosteroids, both cortisol and cortisone, into the water by rainbow trout, being able to modify and evaluate a daily cycle. The procedure, therefore, provides a good basis for a non-invasive stress assay for fish. Water cortisol concentrations (ng / l^{-1}) can be used directly as a relative measure of stress status in experimental tank systems.

Although the amount of free cortisol released through the gills appears to be less than the amount of plasma derived cortisol compared to the metabolites in bile, there are many benefits to measuring the free cortisol in water. Since cortisol in water comes directly from the gill (as opposed to metabolites in faeces, which may have been stored for several hours or even days), the

concentration of cortisol in water is likely to provide a better understanding of what is happening to the fish. There will always be a time difference between plasma and water concentrations (Ellis et al., 2004). Furthermore, the daily variation in cortisol production of (unstimulated) trout was used to find a suitable time of day for the stimulation experiments. The endocrinological proxy for physiological activity was in turn validated by analysis of video-recorded behaviour at different times of the day, confirming the correlation between low motional activity and low cortisol levels.

6. Conclusions

The results obtained in this work, using a conditioning experiment, a tracing study and a basic preparation of a molecular mapping experiment, provide further information for the stimulus perception of magnetic field information for rainbow trout.

1. Regarding behavioural responses to operant magnetic conditioning, we have presented a successful conditioning approach to train individual rainbow trout to respond to a magnetic signal. Our paradigm uses a strict learning criterion and provides recall performance tests as readouts.

2. DiI tracing performed well in labelling the descending trigeminal root (DV) retrogradely into the medulla oblongata. Using the anatomical references from (Wullimann et al., 1996), the marked areas of the DiI could be further identified and categorised. However, due to the closeness of the nuclei to the root areas of the descending trigeminal nerve V, the tracing study can only be used as a guideline for the region of interest in the hindbrain.

3. Water cortisol concentrations (ng / l^{-1}) can be used directly as a relative measure of stress status in experimental tank systems. The endocrinological proxy for physiological activity was in turn, validated by analysis of video-recorded behaviour at different times of the day, confirming the correlation between low motional activity and low cortisol levels.

4. Antibodies are commonly used to visualise specific antigens, enabling the elucidation of expression patterns or localisation of a particular protein. To prevent false interpretations based on cross-reactivity, we needed to confirm the specificity of antibodies before their use. The specificity test of the mouse@cFos E8 antibody was performed with a rainbow trout cFos cDNA sequence in a pFLAG-CMV™-5.1 Expression Vector, transfected into Hek cells and further analysed with western blots and immunocytochemistry.

7. Publications

Participation in other projects that are not the subject of this dissertation:

Curdt, F., Haase, K., **Ziegenbalg, L.**, Greb, H., Heyers, D., & Winklhofer, M. (2022). Prussian blue technique is prone to yield false negative results in magnetoreception research. *Scientific Reports*, *12*(1), 8803.

Attached below is the manuscript for "Multisensory avoidance conditioning in individual zebrafish combining visual and magnetic modality." by Laura Ziegenbalg[1], Susanne Schwarze[1], Michael Winklhofer[1,2]

8. References

Ahmad, M., & Cashmore, A. R. (1993). HY4 gene of A. thaliana encodes a protein with characteristics of a blue-light photoreceptor. *Nature*, *366*(6451), 162–166. https://doi.org/10.1038/366162a0

Akoev, G. N., Ilyinsky, O. B., & Zadan, P. M. (1976). Responses of electroreceptors (ampullae of lorenzini) of Skates to electric and magnetic fields. *Journal of Comparative Physiology A*, *106*(2), 127–136. https://doi.org/10.1007/BF00620494

Andrianov, G. N., Brown, H. R., & Ilyinsky, O. B. (1974). Responses of central neurons to electrical and magnetic stimuli of the ampullae of lorenzini in the Black Sea skate. *Journal of Comparative Physiology A*, *93*(4), 287–299. https://doi.org/10.1007/BF00606798

Balay, S. D., Widen, S. A., & Waskiewicz, A. J. (2020). Analysis of zebrafish cryptochrome 2 and 4 expression in UV cone photoreceptors. *Gene Expression Patterns*, *35*, 119100. https://doi.org/10.1016/j.gep.2020.119100

Bassetto, M., Reichl, T., Kobylkov, D., Kattnig, D. R., Winklhofer, M., Hore, P. J., & Mouritsen, H. (2023). No evidence for magnetic field effects on the behaviour of Drosophila. *Nature*, *620*(7974), 595–599. https://doi.org/10.1038/s41586-023-06397-7

Bates, D., Mächler, M., Bolker, B., & Walker, S. (2015). Fitting linear mixed-effects models using **lme4**. *Journal of Statistical Software*, *67*(1). https://doi.org/10.18637/jss.v067.i01

Beason, R., & Semm, P. (1996). Does the avian ophthalmic nerve carry magnetic navigational information? *Journal of Experimental Biology*, *199*(5), 1241–1244. https://doi.org/10.1242/jeb.199.5.1241

Behrend, E. R., & Bitterman, M. E. (1964). Avoidance-Conditioning in the Fish: Further Studies of the CS-US Interval. *The American Journal of Psychology*, *77*(1), 15. https://doi.org/10.2307/1419268

Bellinger, M. R., Wei, J., Hartmann, U., Cadiou, H., Winklhofer, M., & Banks, M. A. (2022). Conservation of magnetite biomineralization genes in all domains of life and implications for

magnetic sensing. *Proceedings of the National Academy of Sciences*, *119*(3), e2108655119. https://doi.org/10.1073/pnas.2108655119

Bellono, N. W., Bayrer, J. R., Leitch, D. B., Castro, J., Zhang, C., O'Donnell, T. A., Brierley, S. M., Ingraham, H. A., & Julius, D. (2017). Enterochromaffin Cells Are Gut Chemosensors that Couple to Sensory Neural Pathways. *Cell*, *170*(1), 185-198.e16. https://doi.org/10.1016/j.cell.2017.05.034

Bellono, N. W., Leitch, D. B., & Julius, D. (2017). Molecular basis of ancestral vertebrate electroreception. *Nature*, *543*(7645), 391–396. https://doi.org/10.1038/nature21401

Blakemore, R. (1975). Magnetotactic Bacteria. *Science*, *190*(4212), 377–379. https://doi.org/10.1126/science.170679

Blakemore, R. P. (1982). Magnetotactic Bacteria. *Annual Review of Microbiology*, *36*(1), 217–238. https://doi.org/10.1146/annurev.mi.36.100182.001245

Butler, J. L., Barham, B. J., & Heidenreich, B. A. (2019). Comparison of indirect peroxidase and avidin-biotin-peroxidase complex (ABC) immunohistochemical staining procedures for c-fos in rat brain. *Journal of Anatomy*, *234*(6), 936–942. https://doi.org/10.1111/joa.12967

Chew, G. L., & Brown, G. E. (1989). Orientation of rainbow trout (Salmo gairdneri) in normal and null magnetic fields. *Canadian Journal of Zoology*, *67*(3), 641–643. https://doi.org/10.1139/z89-092

Cresci, A., De Rosa, R., & Agnisola, C. (2019). Assessing the influence of personality on sensitivity to magnetic fields in zebrafish. *Journal of Visualized Experiments*, *145*, 59229. https://doi.org/10.3791/59229

Curdt, F., Haase, K., Ziegenbalg, L., Greb, H., Heyers, D., & Winklhofer, M. (2022). *Prussian Blue Technique is Prone To Yield False Negative Results In Magnetoreception Research* [Preprint]. In Review. https://doi.org/10.21203/rs.3.rs-1324083/v1

Dahlbom, S. J., Lagman, D., Lundstedt-Enkel, K., Sundström, L. F., & Winberg, S. (2011). Boldness predicts social status in zebrafish (*Danio rerio*). *PLoS ONE*, *6*(8), e23565. https://doi.org/10.1371/journal.pone.0023565

Diebel, C. E., Proksch, R., Green, C. R., Neilson, P., & Walker, M. M. (2000). Magnetite defines a vertebrate magnetoreceptor. *Nature*, *406*(6793), 299–302. https://doi.org/10.1038/35018561

Dunlop, R., Millsopp, S., & Laming, P. (2006). Avoidance learning in goldfish (*Carassius auratus*) and trout (*Oncorhynchus mykiss*) and implications for pain perception. *Applied Animal Behaviour Science*, *97*(2–4), Article 2–4. https://doi.org/10.1016/j.applanim.2005.06.018socially

Durif, C. M. F., Browman, H. I., Phillips, J. B., Skiftesvik, A. B., Vøllestad, L. A., & Stockhausen, H. H. (2013). Magnetic Compass Orientation in the European Eel. *PLoS ONE*, *8*(3), e59212. https://doi.org/10.1371/journal.pone.0059212

Elbers, D., Bulte, M., Bairlein, F., Mouritsen, H., & Heyers, D. (2017). Magnetic activation in the brain of the migratory northern wheatear (Oenanthe oenanthe). *Journal of Comparative Physiology A*, *203*(8), 591–600. https://doi.org/10.1007/s00359-017-1167-7

Ellis, T., James, J. D., Stewart, C., & Scott, A. P. (2004). A non-invasive stress assay based upon measurement of free cortisol released into the water by rainbow trout. *Journal of Fish Biology*, *65*(5), 1233–1252. https://doi.org/10.1111/j.0022-1112.2004.00499.x

Fay, M. P., & Hunsberger, S. A. (2021). Practical valid inferences for the two-sample binomial problem. *Statistics Surveys*, *15*(none). https://doi.org/10.1214/21-SS131

Feenders, G., Liedvogel, M., Rivas, M., Zapka, M., Horita, H., Hara, E., Wada, K., Mouritsen, H., & Jarvis, E. D. (2008). Molecular Mapping of Movement-Associated Areas in the Avian Brain: A Motor Theory for Vocal Learning Origin. *PLoS ONE*, *3*(3), e1768. https://doi.org/10.1371/journal.pone.0001768

Fleissner, G., Stahl, B., Thalau, P., Falkenberg, G., & Fleissner, G. (2007). A novel concept of Fe-mineral-based magnetoreception: Histological and physicochemical data from the upper

beak of homing pigeons. *Naturwissenschaften*, *94*(8), 631–642. https://doi.org/10.1007/s00114-007-0236-0

Frankel, R. B., Blakemore, R. P., & Wolfe, R. S. (1979). Magnetite in Freshwater Magnetotactic Bacteria. *Science*, *203*(4387), 1355–1356. https://doi.org/10.1126/science.203.4387.1355

Friard, O., & Gamba, M. (2016). BORIS: A free, versatile open-source event-logging software for video/audio coding and live observations. *Methods in Ecology and Evolution*, *7*(11), 1325–1330. https://doi.org/10.1111/2041-210X.12584

Gallistel, C. R., Fairhurst, S., & Balsam, P. (2004). The learning curve: Implications of a quantitative analysis. *Proceedings of the National Academy of Sciences*, *101*(36), 13124–13131. https://doi.org/10.1073/pnas.0404965101

Gegear, R. J., Casselman, A., Waddell, S., & Reppert, S. M. (2008). Cryptochrome mediates light-dependent magnetosensitivity in Drosophila. *Nature*, *454*(7207), Article 7207. https://doi.org/10.1038/nature07183

Giovani, B., Byrdin, M., Ahmad, M., & Brettel, K. (2003). Light-induced electron transfer in a cryptochrome blue-light photoreceptor. *Nature Structural & Molecular Biology*, *10*(6), 489–490. https://doi.org/10.1038/nsb933

Gottfried, J. A., & Dolan, R. J. (2003). The nose smells what the eye sees. *Neuron*, *39*(2), 375–386. https://doi.org/10.1016/S0896-6273(03)00392-1

Günther, A., Einwich, A., Sjulstok, E., Feederle, R., Bolte, P., Koch, K.-W., Solov'yov, I. A., & Mouritsen, H. (2018). Double-Cone Localization and Seasonal Expression Pattern Suggest a Role in Magnetoreception for European Robin Cryptochrome 4. *Current Biology*, *28*(2), 211-223.e4. https://doi.org/10.1016/j.cub.2017.12.003

Guo, J., & Guo, A. (2005). Crossmodal interactions between olfactory and visual learning in Drosophila. *Science (New York, N.Y.)*, *309*(5732), 307–310. https://doi.org/10.1126/science.1111280

Guzowski, J. F., Timlin, J. A., Roysam, B., McNaughton, B. L., Worley, P. F., & Barnes, C. A. (2005). Mapping behaviorally relevant neural circuits with immediate-early gene expression. *Current Opinion in Neurobiology*, *15*(5), 599–606. https://doi.org/10.1016/j.conb.2005.08.018

Hartmann, S., Vogt, R., Kunze, J., Rauschert, A., Kuhnert, K.-D., Wanzenböck, J., Lamatsch, D. K., & Witte, K. (2018). Zebrafish larvae show negative phototaxis to near-infrared light. *PLOS ONE*, *13*(11), e0207264. https://doi.org/10.1371/journal.pone.0207264

Haug, M. F., Gesemann, M., Lazović, V., & Neuhauss, S. C. F. (2015). Eumetazoan Cryptochrome Phylogeny and Evolution. *Genome Biology and Evolution*, *7*(2), 601–619. https://doi.org/10.1093/gbe/evv010

Haugh, C. V., & Walker, M. M. (1998). Magnetic Discrimination Learning in Rainbow Trout (Oncorhynchus mykiss). *Journal of Navigation*, *51*(1), 35–45. https://doi.org/10.1017/s0373463397007595

Heilingoetter, C. L., & Jensen, M. B. (2016). Histological methods for *ex vivo* axon tracing: A systematic review. *Neurological Research*, *38*(7), 561–569. https://doi.org/10.1080/01616412.2016.1153820

Helfman, G. S., Collette, B. B., Facey, D. E., & Bowen, B. W. (2009). *The diversity of fishes: Biology, evolution, and ecology.* John Wiley & Sons.

Hellinger, J., & Hoffmann, K.-P. (2009). Magnetic field perception in the Rainbow Trout, Oncorhynchus mykiss. *Journal of Comparative Physiology A*, *195*(9), 873–879. https://doi.org/10.1007/s00359-009-0466-z

Hellinger, J., & Hoffmann, K.-P. (2012). Magnetic field perception in the rainbow trout Oncorynchus mykiss: Magnetite mediated, light dependent or both? *Journal of Comparative Physiology A*, *198*(8), 593–605. https://doi.org/10.1007/s00359-012-0732-3

Heyers, D., Zapka, M., Hoffmeister, M., Wild, J. M., & Mouritsen, H. (2010). Magnetic field changes activate the trigeminal brainstem complex in a migratory bird. *Proceedings of the National Academy of Sciences*, *107*(20), 9394–9399. https://doi.org/10.1073/pnas.0907068107

Horner, J. L., Longo, N., & Bitterman, M. E. (1961). A Shuttle Box for Fish and a Control Circuit of General Applicability. *The American Journal of Psychology*, *74*(1), 114. https://doi.org/10.2307/1419835

Johnsen, S., & Lohmann, K. J. (2005). The physics and neurobiology of magnetoreception. *Nature Reviews Neuroscience*, *6*(9), 703–712. https://doi.org/10.1038/nrn1745

Jungerman, R. L., & Rosenblum, B. (1980). Magnetic induction for the sensing of magnetic fields by animals—An analysis. *Journal of Theoretical Biology*, *87*(1), 25–32. https://doi.org/10.1016/0022-5193(80)90217-9

Kalmijn, Ad. J. (1971). The Electric Sense of Sharks and Rays. *Journal of Experimental Biology*, *55*(2), 371–383. https://doi.org/10.1242/jeb.55.2.371

Kalmijn, Ad. J. (1982). Electric and Magnetic Field Detection in Elasmobranch Fishes. *Science*, *218*(4575), 916–918. https://doi.org/10.1126/science.7134985

Keeton, W. T. (1971). Magnets Interfere with Pigeon Homing. *Proceedings of the National Academy of Sciences*, *68*(1), 102–106. https://doi.org/10.1073/pnas.68.1.102

Kirschvink, J. (2001). Magnetite-based magnetoreception. *Current Opinion in Neurobiology*, *11*(4), 462–467. https://doi.org/10.1016/s0959-4388(00)00235-x

Kirschvink, J. L. (1992). Uniform magnetic fields and double-wrapped coil systems: Improved techniques for the design of bioelectromagnetic experiments. *Bioelectromagnetics*, *13*(5), 401–411. https://doi.org/10.1002/bem.2250130507

Kirschvink, J. L., Winklhofer, M., & Walker, M. M. (2010). Biophysics of magnetic orientation: Strengthening the interface between theory and experimental design. *Journal of The Royal Society Interface*, *7*(suppl_2). https://doi.org/10.1098/rsif.2009.0491.focus

Kishkinev, D., Mouritsen, H., & Mora, C. V. (2012). An attempt to develop an operant conditioning paradigm to test for magnetic discrimination behavior in a migratory songbird. *Journal of Ornithology*, *153*(4), 1165–1177. https://doi.org/10.1007/s10336-012-0847-x

Kishkinev, D., Chernetsov, N., Heyers, D., & Mouritsen, H. (2013). Migratory Reed Warblers Need Intact Trigeminal Nerves to Correct for a 1,000 km Eastward Displacement. *PLoS ONE*, *8*(6), e65847. https://doi.org/10.1371/journal.pone.0065847

Kobylkov, D., Schwarze, S., Michalik, B., Winklhofer, M., Mouritsen, H., & Heyers, D. (2020). A newly identified trigeminal brain pathway in a night-migratory bird could be dedicated to transmitting magnetic map information. *Proceedings of the Royal Society B: Biological Sciences*, *287*(1919), 20192788. https://doi.org/10.1098/rspb.2019.2788

Krylov, V. V., Osipova, E. A., Pavlova, V. V., & Batrakova, A. A. (2016). Influence of magnetic field on the spatial orientation in zebrafish (*Danio rerio*) (Cyprinidae) and Roach (*Rutilus rutilus*) (Cyprinidae). *Journal of Ichthyology*, *56*(3), Article 3. https://doi.org/10.1134/s0032945216030073

Leberecht, B., Wong, S. Y., Satish, B., Döge, S., Hindman, J., Venkatraman, L., Apte, S., Haase, K., Musielak, I., Dautaj, G., Solov'yov, I. A., Winklhofer, M., Mouritsen, H., & Hore, P. J. (2023). Upper bound for broadband radiofrequency field disruption of magnetic compass orientation in night-migratory songbirds. *Proceedings of the National Academy of Sciences*, *120*(28), e2301153120. https://doi.org/10.1073/pnas.2301153120

Liedvogel, M., Maeda, K., Henbest, K., Schleicher, E., Simon, T., Timmel, C. R., Hore, P. J., & Mouritsen, H. (2007). Chemical Magnetoreception: Bird Cryptochrome 1a Is Excited by Blue Light and Forms Long-Lived Radical-Pairs. *PLoS ONE*, *2*(10), e1106. https://doi.org/10.1371/journal.pone.0001106

Lindauer, M., & Martin, H. (1968). Die Schwereorientierung der Bienen unter dem Einfluß des Erdmagnetfeldes. *Zeitschrift für Vergleichende Physiologie*, *60*(3), 219–243. https://doi.org/10.1007/BF00298600

Maeda, K., Henbest, K. B., Cintolesi, F., Kuprov, I., Rodgers, C. T., Liddell, P. A., Gust, D., Timmel, C. R., & Hore, P. J. (2008). Chemical compass model of avian magnetoreception. *Nature*, *453*(7193), 387–390. https://doi.org/10.1038/nature06834

Mardle, S. (2006). The selection of reporter labels. In *Immunohistochemistry: Methods Express*.

Merkel, Fredrick Wilhelm & Wiltschko, Wolfgang. (1965). Magnetismus und richtungsfinden zugunruhiger Rotkehlchen (Erithacus rubecula). *Vogelwarte*, *23 (1)*, 71–77.

Merritt, R., Purcell, C., & Stroink, G. (1983). Uniform magnetic field produced by three, four, and five square coils. *Review of Scientific Instruments*, *54*(7), 879–882. https://doi.org/10.1063/1.1137480

Meyer, C. G., Holland, K. N., & Papastamatiou, Y. P. (2005). Sharks can detect changes in the geomagnetic field. *Journal of The Royal Society Interface*, *2*(2), 129–130. https://doi.org/10.1098/rsif.2004.0021

Miller, J. (1982). Divided attention: Evidence for coactivation with redundant signals. *Cognitive Psychology*, *14*(2), 247–279. https://doi.org/10.1016/0010-0285(82)90010-X

Mora, C. V., Davison, M., & Walker, M. M. (2009). Conditioning as a Technique for Studying the Sensory Systems Involved in Animal Orientation, Homing and Navigation – a Review. *Journal of Navigation*, *62*(4), Article 4. https://doi.org/10.1017/s0373463309990063

Mouritsen, H. (2018). Long-distance navigation and magnetoreception in migratory animals. *Nature*, *558*(7708), 50–59. https://doi.org/10.1038/s41586-018-0176-1

Mouritsen, H. (2022). Magnetoreception in birds and its use for long-distance migration. In *Sturkie's Avian Physiology* (S. 233–256). Elsevier. https://doi.org/10.1016/B978-0-12-819770-7.00040-2

Mouritsen, H., Feenders, G., Liedvogel, M., & Kropp, W. (2004). Migratory Birds Use Head Scans to Detect the Direction of the Earth's Magnetic Field. *Current Biology*, *14*(21), 1946–1949. https://doi.org/10.1016/j.cub.2004.10.025

Mouritsen, H., Feenders, G., Liedvogel, M., Wada, K., & Jarvis, E. D. (2005). Night-vision brain area in migratory songbirds. *Proceedings of the National Academy of Sciences*, *102*(23), 8339–8344. https://doi.org/10.1073/pnas.0409575102

Murray, R. W. (1960). Electrical Sensitivity of the Ampullæ of Lorenzini. *Nature*, *187*(4741), 957–957. https://doi.org/10.1038/187957a0

Myklatun, A., Lauri, A., Eder, S. H. K., Cappetta, M., Shcherbakov, D., Wurst, W., Winklhofer, M., & Westmeyer, G. G. (2018). Zebrafish and medaka offer insights into the neurobehavioral correlates of vertebrate magnetoreception. *Nature Communications*, *9*(1), 802. https://doi.org/10.1038/s41467-018-03090-6

Nießner, C., Denzau, S., Gross, J. C., Peichl, L., Bischof, H.-J., Fleissner, G., Wiltschko, W., & Wiltschko, R. (2011). Avian Ultraviolet/Violet Cones Identified as Probable Magnetoreceptors. *PLoS ONE*, *6*(5), e20091. https://doi.org/10.1371/journal.pone.0020091

Nimpf, S., Nordmann, G. C., Kagerbauer, D., Malkemper, E. P., Landler, L., Papadaki-Anastasopoulou, A., Ushakova, L., Wenninger-Weinzierl, A., Novatchkova, M., Vincent, P., Lendl, T., Colombini, M., Mason, M. J., & Keays, D. A. (2019). A putative mechanism for magnetoreception by electromagnetic induction in the pigeon inner ear. *Current Biology*, *29*(23), 4052-4059.e4. https://doi.org/10.1016/j.cub.2019.09.048

Nishi, T., Kawamura, G., & Matsumoto, K. (2004). Magnetic sense in the Japanese eel, *Anguilla japonica* , as determined by conditioning and electrocardiography. *Journal of Experimental Biology*, *207*(17), 2965–2970. https://doi.org/10.1242/jeb.01131

Nordmann, G. C., Hochstoeger, T., & Keays, D. A. (2017). Magnetoreception—A sense without a receptor. *PLOS Biology*, *15*(10), e2003234. https://doi.org/10.1371/journal.pbio.2003234

Osipova, E. A., Pavlova, V. V., Nepomnyashchikh, V. A., & Krylov, V. V. (2016). Influence of magnetic field on zebrafish activity and orientation in a plus maze. *Behavioural Processes*, *122*, 80–86. https://doi.org/10.1016/j.beproc.2015.11.009

Overmier, J. B., & Papini, M. R. (1986). Factors modulating the effects of teleost telencephalon ablation on retention, relearning, and extinction of instrumental avoidance behavior. *Behavioral Neuroscience*, *100*(2), 190–199, 289. https://doi.org/10.1037/0735-7044.100.2.190

Ozturk, N., Selby, C. P., Song, S.-H., Ye, R., Tan, C., Kao, Y.-T., Zhong, D., & Sancar, A. (2009). Comparative Photochemistry of Animal Type 1 and Type 4 Cryptochromes. *Biochemistry*, *48*(36), 8585–8593. https://doi.org/10.1021/bi901043s

Paulin, M. G. (1995). Electroreception and the compass sense of sharks. *Journal of Theoretical Biology*, *174*(3), 325–339. https://doi.org/10.1006/jtbi.1995.0102

Phillips, J. B., & Borland, S. C. (1992). Behavioural evidence for use of a light-dependent magnetoreception mechanism by a vertebrate. *Nature*, *359*(6391), 142–144. https://doi.org/10.1038/359142a0

Portavella, M. (2004). Avoidance Response in Goldfish: Emotional and Temporal Involvement of Medial and Lateral Telencephalic Pallium. *Journal of Neuroscience*, *24*(9), 2335–2342. https://doi.org/10.1523/jneurosci.4930-03.2004

Putman, N. F., Jenkins, E. S., Michielsens, C. G. J., & Noakes, D. L. G. (2014). Geomagnetic imprinting predicts spatio-temporal variation in homing migration of pink and sockeye salmon. *Journal of The Royal Society Interface*, *11*(99), 20140542. https://doi.org/10.1098/rsif.2014.0542

Putman, N. F., Meinke, A. M., & Noakes, D. L. G. (2014). Rearing in a distorted magnetic field disrupts the 'map sense' of juvenile steelhead trout. *Biology Letters*, *10*(6), 20140169. https://doi.org/10.1098/rsbl.2014.0169

Putman, N. F., Scanlan, M. M., Billman, E. J., O'Neil, J. P., Couture, R. B., Quinn, T. P., Lohmann, K. J., & Noakes, D. L. G. (2014). An Inherited Magnetic Map Guides Ocean Navigation in Juvenile Pacific Salmon. *Current Biology*, *24*(4), 446–450. https://doi.org/10.1016/j.cub.2014.01.017

Putman, N. F., Williams, C. R., Gallagher, E. P., & Dittman, A. H. (2020). A sense of place: Pink salmon use a magnetic map for orientation. *Journal of Experimental Biology*, jeb.218735. https://doi.org/10.1242/jeb.218735

Puzdrowski, R. L. (1988). Afferent projections of the trigeminal nerve in the goldfish, Carassius auratus. *Journal of Morphology*, *198*(2), 131–147. https://doi.org/10.1002/jmor.1051980202

Quinn, T. P. (1980). Evidence for celestial and magnetic compass orientation in lake migrating sockeye salmon fry. *Journal of Comparative Physiology ? A*, *137*(3), 243–248. https://doi.org/10.1007/bf00657119

Quinn, T. P., & Brannon, E. L. (1982). The use of celestial and magnetic cues by orienting sockeye salmon smolts. *Journal of Comparative Physiology ? A*, *147*(4), 547–552. https://doi.org/10.1007/BF00612020

Quinn, T. P., & Groot, C. (1983). Orientation of Chum Salmon (*Oncorhynchus keta*) After Internal and External Magnetic Field Alteration. *Canadian Journal of Fisheries and Aquatic Sciences*, *40*(10), 1598–1606. https://doi.org/10.1139/f83-185

Quinn, T. P., Merrill, R. T., & Brannon, E. L. (1981). Magnetic field detection in sockeye salmon. *Journal of Experimental Zoology*, *217*(1), 137–142. https://doi.org/10.1002/jez.1402170114

R Core Team. (2020). *R: A language and environment for statistical computing. R Foundation for Statistical Computing.* Vienna, Austria. https://www.R-project.org/

Raposo, D., Sheppard, J. P., Schrater, P. R., & Churchland, A. K. (2012). Multisensory decision-making in rats and humans. *Journal of Neuroscience*, *32*(11), 3726–3735. https://doi.org/10.1523/JNEUROSCI.4998-11.2012

Rowe, C. (2002). Sound improves visual discrimination learning in avian predators. *Proceedings of the Royal Society of London. Series B: Biological Sciences*, *269*(1498), 1353–1357. https://doi.org/10.1098/rspb.2002.2012

Ritz, T., Adem, S., & Schulten, K. (2000). A Model for Photoreceptor-Based Magnetoreception in Birds. *Biophysical Journal*, *78*(2), 707–718. https://doi.org/10.1016/S0006-3495(00)76629-X

Sancar, A. (2004). Regulation of the Mammalian Circadian Clock by Cryptochrome. *Journal of Biological Chemistry*, *279*(33), 34079–34082. https://doi.org/10.1074/jbc.R400016200

Sancar, A., & Sancar, G. B. (1988). DNA REPAIR ENZYMES. *Annual Review of Biochemistry*, *57*(1), 29–67. https://doi.org/10.1146/annurev.bi.57.070188.000333

Schindelin, J., Arganda-Carreras, I., Frise, E., Kaynig, V., Longair, M., Pietzsch, T., Preibisch, S., Rueden, C., Saalfeld, S., Schmid, B., Tinevez, J.-Y., White, D. J., Hartenstein, V., Eliceiri, K., Tomancak, P., & Cardona, A. (2012). Fiji: An open-source platform for biological-image analysis. *Nature Methods*, *9*(7), 676–682. https://doi.org/10.1038/nmeth.2019

Schulten, K., Swenberg, C. E., & Weller, A. (1978). A Biomagnetic Sensory Mechanism Based on Magnetic Field Modulated Coherent Electron Spin Motion. *Zeitschrift Für Physikalische Chemie*, *111*(1), 1–5. https://doi.org/10.1524/zpch.1978.111.1.001

Shcherbakov, D., Winklhofer, M., Petersen, N., Steidle, J., Hilbig, R., & Blum, M. (2005). Magnetosensation in zebrafish. *Current Biology*, *15*(5), R161–R162. https://doi.org/10.1016/j.cub.2005.02.039

Shcherbakov, D., Knörzer, A., Espenhahn, S., Hilbig, R., Haas, U., & Blum, M. (2013). Sensitivity differences in fish offer near-Infrared vision as an adaptable evolutionary trait. *PLoS ONE*, *8*(5), e64429. https://doi.org/10.1371/journal.pone.0064429

Shu, S., Ju, G., & Fan, L. (1988). The glucose oxidase-DAB-nickel method in peroxidase histochemistry of the nervous system. *Neuroscience Letters*, *85*(2), 169–171. https://doi.org/10.1016/0304-3940(88)90346-1

Skiles, D. D. (1985). The Geomagnetic Field Its Nature, History, and Biological Relevance. In J. L. Kirschvink, D. S. Jones, & B. J. MacFadden (Hrsg.), *Magnetite Biomineralization and Magnetoreception in Organisms* (Bd. 5, S. 43–102). Springer US. https://doi.org/10.1007/978-1-4613-0313-8_3

Takahashi, J. S. (2017). Transcriptional architecture of the mammalian circadian clock. *Nature Reviews Genetics*, *18*(3), 164–179. https://doi.org/10.1038/nrg.2016.150

Takebe, A., Furutani, T., Wada, T., Koinuma, M., Kubo, Y., Okano, K., & Okano, T. (2012). Zebrafish respond to the geomagnetic field by bimodal and group-dependent orientation. *Scientific Reports*, *2*(1). https://doi.org/10.1038/srep00727

Taylor, P. B. (1986). Experimental evidence for geomagnetic orientation in juvenile salmon, Oncorhynchus tschawytscha Walbaum. *Journal of Fish Biology*, *28*(5), 607–623. https://doi.org/10.1111/j.1095-8649.1986.tb05196.x

Tesch, F.-W. (1974). Influence of geomagnetism and salinity on the directional choice of eels. *Helgoländer Wissenschaftliche Meeresuntersuchungen*, *26*(3–4), 382–395. https://doi.org/10.1007/BF01627623

Tran, S., & Gerlai, R. (2013). Individual differences in activity levels in zebrafish (*Danio rerio*). *Behavioural Brain Research*, *257*, 224–229. https://doi.org/10.1016/j.bbr.2013.09.040

Van Gelder, R. N., Wee, R., Lee, J. A., & Tu, D. C. (2003). Reduced Pupillary Light Responses in Mice Lacking Cryptochromes. *Science*, *299*(5604), 222–222. https://doi.org/10.1126/science.1079536

Vercelli, A., Repici, M., Garbossa, D., & Grimaldi, A. (2000). Recent techniques for tracing pathways in the central nervous system of developing and adult mammals. *Brain Research Bulletin*, *51*(1), 11–28. https://doi.org/10.1016/S0361-9230(99)00229-4

Viguier, C. (1882). Le sens d'orientation et ses organs chez les animaux etchez l'homme. *Revue Philosophique de la France et de l'Étranger*, 1–36.

Vital, C., & Martins, E. P. (2013). Socially-central zebrafish influence group behavior more than those on the social periphery. *PLoS ONE*, *8*(1), e55503. https://doi.org/10.1371/journal.pone.0055503

Walcott, C., & Green, R. P. (1974). Orientation of Homing Pigeons Altered by a Change in the Direction of an Applied Magnetic Field. *Science*, *184*(4133), 180–182. https://doi.org/10.1126/science.184.4133.180

Walker, M. M. (1984). Learned magnetic field discrimination in yellowfin tuna,Thunnus albacares. *Journal of Comparative Physiology A*, *155*(5), 673–679. https://doi.org/10.1007/bf00610853

Walker, M. M. (1988). Production of single-domain magnetite throughout life by sockeye salmon. *J Exp Biol.*, *140*, 51–63.

Walker, M. M., & Bitterman, M. E. (1986). Attempts to train goldfish to respond to magnetic field stimuli. *Naturwissenschaften*, *73*(1), 12–16. https://doi.org/10.1007/bf01168800

Walker, M. M., Dennis, T. E., & Kirschvink, J. L. (2002). The magnetic sense and its use in long-distance navigation by animals. *Current Opinion in Neurobiology*, *12*(6), 735–744. https://doi.org/10.1016/s0959-4388(02)00389-6

Walker, M. M., Diebel, C. E., Haugh, C. V., Pankhurst, P. M., Montgomery, J. C., & Green, C. R. (1997). Structure and function of the vertebrate magnetic sense. *Nature*, *390*(6658), 371–376. https://doi.org/10.1038/37057

Walker, M. M., Kirschvink, J. L., Chang, S.-B. R., & Dizon, A. E. (1984). A Candidate Magnetic Sense Organ in the Yellowfin Tuna, *Thunnus albacares*. *Science*, *224*(4650), 751–753. https://doi.org/10.1126/science.224.4650.751

Ward, B. K., Tan, G. X.-J., Roberts, D. C., Della Santina, C. C., Zee, D. S., & Carey, J. P. (2014). Strong Static Magnetic Fields Elicit Swimming Behaviors Consistent with Direct Vestibular Stimulation in Adult Zebrafish. *PLoS ONE*, *9*(3), e92109. https://doi.org/10.1371/journal.pone.0092109

Wedekind, H., Meriac, A., Lübke, K., & Rieder, J. (2018). Freies Cortisol im Wasser als Marker zur Stressbestimmung in der Aquakultur. *Tagungsband der XVII. Gemeinschaftstagung der Deutschen, Österreichischen und Schweizer Sektionen der European Association of Fish Pathologists EAFP*.

Wiltschko, R., & Wiltschko, W. (1995). *Magnetic Orientation in Animals* (Bd. 33). Springer Berlin Heidelberg. https://doi.org/10.1007/978-3-642-79749-1

Wiltschko, R., & Wiltschko, W. (1996). Magnetoreception: Why Is Conditioning So Seldom Successful? *Naturwissenschaften*, *83*(6), 241–247. https://doi.org/10.1007/s001140050281

Wiltschko, W., & Wiltschko, R. (1972). Magnetic Compass of European Robins. *Science*, *176*(4030), 62–64. https://doi.org/10.1126/science.176.4030.62

Winklhofer, M. (2010). Magnetoreception. *Journal of The Royal Society Interface*, *7*(suppl_2). https://doi.org/10.1098/rsif.2010.0010.focus

Winklhofer, M. (2019). Magnetoreception: A dynamo in the inner ear of pigeons. *Current Biology*, *29*(23), R1224–R1226. https://doi.org/10.1016/j.cub.2019.10.022

Winklhofer, M., & Kirschvink, J. L. (2010). A quantitative assessment of torque-transducer models for magnetoreception. *Journal of The Royal Society Interface*, *7*(suppl_2), S273–S289. https://doi.org/10.1098/rsif.2009.0435.focus

Woodard, W. T., & Bitterman, M. E. (1971). Classical conditioning of goldfish in the shuttlebox. *Behavior Research Methods & Instrumentation*, *3*(4), Article 4. https://doi.org/10.3758/bf03208132

Wu, L.-Q., & Dickman, J. D. (2011). Magnetoreception in an Avian Brain in Part Mediated by Inner Ear Lagena. *Current Biology*, *21*(5), 418–423. https://doi.org/10.1016/j.cub.2011.01.058

Wullimann, M. F., & Northcutt, R. G. (1988). Connections of the Corpus Cerebelli in the Green Sunfish and the Common Goldfish: A Comparison of Perciform and Cypriniform Teleosts (Part 2 of 2). *Brain, Behavior and Evolution*, *32*(5), 305–316. https://doi.org/10.1159/000316057

Wullimann, M. F., Rupp, B., & Reichert, H. (1996). *Neuroanatomy of the zebrafish brain: A topological atlas* (Softcover reprint of the hardcover 1st edition). Birkhäuser Verlag.

Xu, J., Jarocha, L. E., Zollitsch, T., Konowalczyk, M., Henbest, K. B., Richert, S., Golesworthy, M. J., Schmidt, J., Déjean, V., Sowood, D. J. C., Bassetto, M., Luo, J., Walton, J. R., Fleming, J., Wei, Y., Pitcher, T. L., Moise, G., Herrmann, M., Yin, H., … Hore, P. J. (2021). Magnetic sensitivity of cryptochrome 4 from a migratory songbird. *Nature*, *594*(7864), 535–540. https://doi.org/10.1038/s41586-021-03618-9

Zapka, M., Heyers, D., Hein, C. M., Engels, S., Schneider, N.-L., Hans, J., Weiler, S., Dreyer, D., Kishkinev, D., Wild, J. M., & Mouritsen, H. (2009). Visual but not trigeminal mediation of magnetic compass information in a migratory bird. *Nature*, *461*(7268), 1274–1277. https://doi.org/10.1038/nature08528

Supplement

Original read out data from the Horner-type shuttle box.

Consisting of the session number, date, if a stimulation was given, on which side of the aquarium the fish was when the stimulus was given, if there was a reaction, the reaction time, and the time interval between two trials.

Data was categorised into correct positive and false positive trials. And further analysed in “Origin 2020” and represented in graphical form.

Sup-table 5: Original behaviour read out data from rainbow trout coded OM17 tested in the vertical field (B)

Session	Datum	Reiz	0->links 1->rechts	Reaktion	Reaktionszeit(ms)	Wartezeit(ms)
Session 1	23.10.2020	1	0	0	20992	102000
		0	0	1	4768	106000
		1	1	0	20992	150000
		0	0	0	20992	136992
		1	0	0	20992	102000
		0	1	0	20992	76000
		1	1	0	20992	172992
		0	1	1	14480	102992
		1	1	1	1488	72992
		0	1	0	20992	140000
		1	1	0	20992	108992
		0	1	1	16080	106000
Session2	24.10.2020	1	0	1	3184	166000
		0	1	0	16000	126992
		1	1	0	16000	56992
		0	1	0	16000	68992
		1	1	0	16000	126000
		0	1	0	16000	108992
		1	1	0	16000	92000
		0	1	0	16000	108992
		1	0	1	15504	80000
		0	0	0	16000	134000
		1	1	0	16000	58992
		0	1	0	16000	108000
Session 3	26.10.2020	1	1	0	16000	68000
		0	1	0	16000	128992
		1	1	0	16000	154000
		0	0	0	16000	152000
		1	1	1	1584	116000

		0	0	0	16000	142992
		1	0	1	4512	134000
		0	1	0	16000	96992
		1	1	1	3856	150000
		0	0	1	11856	106000
		1	1	0	16000	138000
		0	1	0	16000	74000
Session 4	27.10.2020	1	1	0	16000	124000
		0	1	0	16000	84992
		1	1	0	16000	126992
		0	1	0	16000	66000
		1	1	1	9952	142992
		0	1	0	16000	160992
		1	1	1	12784	166992
		0	0	1	8624	124992
		1	0	1	9696	168000
		0	0	0	16000	138000
		1	1	0	16000	50992
		0	1	1	928	88992
Session 5	28.10.2020	1	1	1	14496	116992
		0	0	0	16000	172000
		1	0	0	16000	114992
		0	1	0	16000	60000
		1	1	0	16000	180000
		0	0	0	16000	172992
		1	0	0	16000	128000
		0	0	0	16000	120000
		1	1	0	16000	170000
		0	1	1	13520	164000
		1	0	0	16000	68992
		0	0	0	16000	50992
Session 6	29.10.2020	1	1	0	16000	50992
		0	0	1	14976	68000
		1	1	1	7600	96000
		0	0	1	2320	106992
		1	0	1	12256	158992
		0	0	0	16000	66992
		1	1	0	16000	112992
		0	1	0	16000	162992
		1	0	1	12704	126992
		0	0	1	6640	138992
		1	0	0	16000	94000
		0	0	0	16000	94992

Session 7	30.10.2020	1	1	0	16000	162992
		0	1	0	16000	156000
		1	1	0	16000	62992
		0	0	0	16000	128000
		1	1	0	16000	164992
		0	1	1	3520	172992
		1	0	0	16000	76992
		0	0	0	16000	118992
		1	0	0	16000	156000
		0	0	1	6800	58992
		1	0	1	14096	82000
		0	1	1	15264	156992
Session 8	31.10.2020	1	0	1	5232	78992
		0	1	1	14608	90000
		1	1	1	10320	52992
		0	0	0	16000	72992
		1	0	1	6800	106000
		0	1	0	16000	50000
		1	1	1	4816	70000
		0	1	1	944	154992
		1	0	1	12128	68000
		0	0	1	2400	158000
		1	1	1	2720	142000
		0	0	0	16000	78992
Session 9	02.11.2020	1	1	1	6544	56000
		0	0	0	16000	102000
		1	1	1	6160	120992
		0	0	0	16000	56992
		1	1	0	15168	60000
		0	1	0	16000	132992
		1	1	1	14999	78000
		0	0	1	698	124000
		1	1	0	16000	138000
		0	0	0	16000	170000
		1	1	0	16000	90000
		0	0	0	16000	172992
Session 10	03.11.2020	1	0	0	15648	166000
		0	1	0	16000	180000
		1	0	1	9728	66000
		0	0	1	13712	166992

		1	1	1	13504	136000
		0	0	0	15248	142992
		1	1	0	15808	72992
		0	1	1	14880	112992
		1	1	0	16000	152992
		0	0	1	576	116000
		1	0	1	6768	92992
		0	1	0	15536	104000
Session11	04.11.2020	1	1	0	16000	138000
		1	0	1	7440	138992
		0	1	1	8768	116992
		1	0	1	8784	172000
		0	0	0	4144	144000
		1	0	1	1824	136992
		0	0	0	16000	122992
		1	1	1	11040	56000
		0	1	1	5248	66000
		1	1	0	16000	134992
		0	0	0	16000	122000
		1	1	1	11360	68992
Session 12	05.11.2020	1	0	1	9792	168000
		0	1	0	16000	156992
		1	1	1	13504	76000
		0	0	0	16000	130000
		1	0	0	16000	98000
		0	0	0	16000	138992
		1	0	1	10960	102000
		0	0	1	16000	164992
		1	1	0	16000	112992
		0	1	0	16000	160000
		1	1	1	12176	176000
		0	0	0	16000	144992
Session 13	06.11.2020	1	0	1	4800	76000
		0	1	0	16000	134000
		1	1	1	9040	164000
		0	1	0	16000	108992
		1	0	1	13424	110992
		0	1	0	16000	126992
		1	0	1	176	96992
		0	0	0	16000	52992
		1	1	1	14096	78000
		0	1	0	16000	80992

			1	1	1	7104	154000
			0	1	0	16000	88992
Session 14	07.11.2020		1	1	1	7360	160992
			0	0	0	16000	176000
			1	0	1	13312	60000
			0	1	0	16000	120000
			1	1	1	13056	76992
			0	1	0	16000	88992
			1	0	0	16000	166992
			0	1	0	16000	130992
			1	0	1	9984	166992
			0	1	0	16000	158000
			1	1	0	15824	158992
			0	0	0	1232	166000
Recall 1	10.11.2020		1	1	1	12998	94992
			0	0	0	1264	84000
		MF		1	0	10653	70000
			0	0	0	16000	148000
			1	0	1	16000	140000
		Sham		1	0	16000	132992
			1	0	1	16000	114000
			0	0	0	16000	176000
			1	1	1	14152	60992
		Sham		1	0	16000	118992
			1	1	0	13648	94000
			0	1	0	16000	50992
			1	1	0	16000	146992
			0	1	0	16000	84000
		MF		1	0	784	138000
			0	1	0	16000	152992
Recall 2	11.11.2020		1	0	0	7904	80000
			0	1	1	16000	82000
		MF		1	0	16000	62000
			0	1	0	16000	156992
			1	0	0	11504	114992
			0	0	0	16000	74992
			1	0	1	10272	142000
		Sham		1	1	16000	80000
			1	1	0	8976	70000
			0	1	1	16000	130992
			1	0	0	16000	126992
		Sham		0	0	16000	148992

			1	1	1	16000	54000
			0	0	0	16000	136992
		MF		0	0	16000	144992
			0	0	1	16000	104000
Recall 3	12.11.2020		1	0	1	16000	130000
		MF		1	0	320	64000
			1	0	1	16000	170000
			0	1	0	16000	158992
			1	1	1	16000	66000
			1	1	0	16000	76000
			1	1	1	8240	96000
			0	1	0	11216	64000
			0	0	1	16000	144992
			1	1	0	11600	82000
			0	1	1	16000	132000
			0	1	0	16000	144992
			1	1	1	13008	150992
			0	1	0	16000	104000
		MF		1	1	16000	112000
			0	0	1	7008	88992
Recall 4	13.11.2020		1	0	1	10448	168992
			0	0	0	16000	62992
			1	0	1	8704	84000
		Sham		1	0	16000	130992
			1	1	1	10384	82000
			0	1	1	16000	74000
		MF		1	0	13104	70992
			0	1	0	2128	124000
			1	0	1	7504	102992
		Sham		0	0	16000	88000
			1	1	1	6208	108000
			0	0	0	16000	166000
			1	1	0	2464	132992
			0	1	0	16000	64000
		MF		1	1	6496	118992
			0	0	0	16000	138992
Recall 5	17.11.2020		1	0	1	6992	175992
			0	1	0	16000	60000
			1	1	0	7504	70000
		Sham		1	0	16000	146992
			1	0	0	13472	102992
			0	0	1	64	62992
		MF		1	1	13620	76992
			0	1	0	16000	108000

1	1	1	12000	80000
Sham	1	0	16000	102992
1	0	1	9120	86000
0	0	0	16000	68992
0	1	1	16000	100000
1	1	0	16000	50000
0	1	0	10320	150992
MF	0	1	16000	138992

Sup-table 6: Original behaviour read out data from rainbow trout coded OM18 tested in the vertical field (B)

Session	Datum	Reiz	Reiz 0->links 1->rechts	Reaktion	Reaktionszeit(ms)	Wartezeit(ms)
Session 1	23.10.2020	1	1	0	20992	58000
		0	1	0	20992	126992
		1	1	1	9072	50000
		0	0	0	20992	50000
		1	0	0	20992	76000
		0	1	1	5968	94000
		1	0	0	20992	92000
		0	1	0	20992	76992
		1	1	0	20992	180000
		0	0	0	20992	116000
		1	1	0	20992	68992
		0	0	0	20992	82992
Session2	13.08.2020	1	1	0	16000	58000
		0	1	0	16000	148000
		1	1	0	16000	76992
		0	0	0	12272	158000
		1	1	0	16000	144000
		0	1	0	16000	126992
		1	1	0	16000	96992
		0	1	0	16000	142992
		1	0	0	16000	68992
		0	1	0	16000	90000
		1	0	0	16000	132000
		0	1	0	16000	146992
Session 3	26.10.2020	1	0	0	16000	148992
		0	0	0	16000	58992
		1	1	0	16000	170000
		0	1	0	16000	58000

		1	1	0	16000	144992
		0	1	0	16000	80992
		1	1	0	16000	80992
		0	1	0	16000	70992
		1	1	0	16000	172992
		0	1	0	16000	94992
		1	0	0	16000	112992
		0	0	0	16000	72000
Session 4	27.10.2020	1	1	0	16000	138000
		0	1	0	16000	114992
		1	1	0	16000	102992
		0	1	0	16000	132992
		1	0	0	16000	120000
		0	0	1	2864	106992
		1	1	0	16000	134000
		0	1	0	16000	50992
		1	0	0	16000	70992
		0	0	1	9600	128992
		1	1	0	16000	162000
		0	1	1	7744	100992
Session 5	28.10.2020	1	0	1	14352	124992
		0	1	0	16000	102000
		1	0	0	16000	154992
		0	1	0	16000	66992
		1	1	0	16000	62992
		0	0	0	16000	134992
		1	1	0	16000	104000
		0	0	1	6960	168000
		1	0	1	1408	86992
		0	1	1	4352	132992
		1	0	1	4416	178992
		0	1	0	16000	104992
Session 6	29.10.2020	1	1	1	4288	54000
		0	0	0	16000	82000
		1	0	0	16000	124992
		0	1	0	16000	84992
		1	1	0	16000	106992
		0	0	1	8912	142000
		1	0	1	1072	126000
		0	1	0	16000	54992
		1	1	0	12944	104000
		0	0	0	9184	90992
		1	1	1	14704	180000
		0	0	1	12576	168992

Session 7	30.10.2020	1	1	0	15392	156000
		0	0	1	10352	162000
		1	1	0	16000	114992
		0	1	0	16000	72992
		1	0	1	13168	106000
		0	1	1	9120	98000
		1	1	0	16000	160000
		0	0	1	7856	126000
		1	1	0	16000	166000
		0	0	0	16000	64000
		1	0	1	2240	156000
		0	1	0	16000	124000
Session 8	31.10.2020	1	0	1	2064	166000
		0	1	0	16000	148000
		1	0	0	16000	76000
		0	0	1	8432	104992
		1	1	1	9584	100992
		0	0	1	9792	164992
		1	0	1	6752	168000
		0	0	1	672	134000
		1	1	0	16000	102000
		0	0	0	16000	84992
		1	0	1	4016	172992
		0	1	1	12992	76992
Session 9	02.11.2020	1	1	0	16000	72992
		0	1	0	16000	106992
		1	1	0	16000	104992
		0	0	0	16000	158000
		1	0	1	11520	138000
		0	0	0	16000	106000
		1	0	0	16000	90992
		0	1	1	7888	130992
		1	0	0	16000	128992
		0	0	0	16000	154000
		1	1	0	16000	124000
		0	1	0	16000	176992
Session 10	03.11.2020	1	1	1	6848	94992
		0	0	1	5520	132000
		1	0	1	3440	102000
		0	0	1	1808	168000
		1	0	1	4000	160000
		0	1	1	1344	94992
		1	0	1	7008	96000

		0	0	1	11040	162992
		1	0	1	7760	82992
		0	0	0	16000	124000
		1	0	1	2144	64992
		0	0	1	5872	172000
Session 11	04.11.2020	1	1	1	5120	56000
		0	1	1	12032	86992
		1	1	0	16000	164992
		0	1	1	16	82992
		1	1	1	6704	156992
		0	1	1	10464	62000
		1	0	0	16000	168000
		0	0	1	8432	56000
		1	1	1	5072	80992
		0	1	0	16000	92992
		1	0	1	4528	132992
		0	1	0	16000	92992
Session 12	05.11.2020	1	0	1	5856	142992
		0	1	1	12128	126992
		1	1	0	16000	110992
		0	1	0	16000	100992
		1	1	0	16000	148992
		0	0	1	5616	152992
		1	0	1	4720	70000
		0	0	1	7376	118992
		1	1	0	16000	140000
		0	1	1	9456	58000
		1	1	0	16000	126992
		0	1	0	16000	76000
Session 13	06.11.2020	1	1	1	12864	74992
		0	1	0	16000	50000
		1	1	1	880	66992
		0	1	0	16000	170992
		1	1	0	16000	82000
		0	1	1	12432	134992
		1	0	1	4416	136000
		0	0	0	0	146000
		1	0	1	2528	164992
		0	0	1	7408	120000
		1	0	1	1664	108992
		0	0	0	16000	126992
Session 14	07.11.2020	1	1	0	16000	92992

		0	1	1	8304	54992
		1	0	0	16000	146000
		0	1	1	11376	52000
		1	1	0	16000	76000
		0	0	1	9808	134992
		1	0	1	944	130000
		0	1	1	9136	78992
		1	0	1	3056	130992
		0	0	1	8592	104000
		1	1	1	4960	156992
		0	0	0	16000	78000
Session 15	09.11.2020	1	0	1	4544	104992
		0	0	0	16000	120000
		1	0	1	2992	180000
		0	1	0	0	128000
		1	1	0	32	152992
		1	1	1	2048	178992
		1	0	1	192	142992
		1	0	1	2128	104000
		1	1	1	6768	74000
		1	0	1	3872	110000
		1	1	0	16000	118992
		1	1	0	16000	174000
Session 16	10.11.2020	1	1	1	3744	118000
		0	1	0	16000	86000
		1	1	1	4016	64000
		0	1	0	16000	108992
		1	0	1	2208	172992
		0	1	0	16000	124992
		1	1	1	4864	122992
		0	1	0	16000	156992
		1	1	1	320	112992
		0	0	1	13648	78000
		1	1	0	16000	58000
		0	0	0	16000	132992
Session 17	11.11.2020	1	0	1	13648	146000
		0	0	0	16000	182992
		1	1	1	3264	138000
		0	1	0	16000	136992
		1	1	1	8160	172992
		0	0	1	10400	116992
		1	1	1	9216	90992
		0	0	0	16000	112000
		1	0	1	3712	90992

			0	1	1	11120	104992
			1	1	1	7696	150000
			0	0	0	16000	52992
Session 18	12.11.2020		1	0	1	2496	174000
			0	1	1	13120	150000
			1	1	1	10720	174992
			0	0	0	16000	84992
			1	1	1	864	178000
			0	1	0	16000	54000
			1	1	1	3920	94992
			0	1	0	16000	114992
			1	1	1	2256	140000
			0	0	1	9168	114000
			1	0	1	13264	164000
			0	0	0	16000	70992
Session 19	13.11.2020		1	0	1	2288	68000
			0	0	1	12416	98000
			1	1	1	3488	152992
			0	0	0	16000	142000
			1	0	1	704	72992
			0	0	0	16000	60000
			1	0	1	5408	178000
			0	1	0	16000	84992
			1	1	1	1904	140000
			0	0	0	16000	140000
			1	1	1	7360	114000
			0	0	0	16000	166000
Recall 1	14.11.2020		1	1	1	7744	148000
		Sham		0	0	16000	114000
			1	0	1	4192	172992
			0	0	0	16000	74992
			1	0	1	7664	94992
			0	1	0	16000	88992
		MF		1	0	16000	124992
			0	1	0	16000	64992
			1	0	1	2208	140000
		Sham		0	0	16000	114992
			1	0	1	7664	94992
			0	0	0	16000	88992
			0	1	0	16000	124992
			0	0	0	16000	64992
			0	0	1	2208	140000
			0	1	0	16000	114992

Recall 2	16.11.2020		1	0	1	2448	122992
			0	0	1	8944	96000
			1	1	1	10752	180000
		Sham		1	0	16000	122992
			1	1	1	9184	110000
			0	0	0	16000	56992
		MF		0	0	16000	142000
			0	1	0	16000	112992
			1	1	1	2816	74000
		Sham		1	0	16000	112000
			1	0	0	16000	122992
			0	0	0	16000	90992
		MF		1	1	1936	166000
			0	0	0	0	140992
			1	1	1	3168	122992
			0	1	0	16000	150992
Recall 3	17.11.2020		1	1	1	1792	84000
			0	1	0	16000	116000
		Sham		0	0	16000	136000
			0	1	1	448	82992
			1	1	1	6640	98992
			0	0	0	16000	90992
		?		1	1	7568	110992
			0	0	0	16000	170000
		MF		1	1	1200	144000
			0	1	0	16000	156000
			1	0	1	7664	116000
			0	0	0	16000	132992
		?		1	1	11808	94000
		Sham		1	0	16000	124992
			1	0	1	12832	156000
			0	0	0	16000	74000
Recall 4	18.11.2020		1	1	1	2992	128992
			0	0	0	16000	122000
			1	0	1	11552	76000
		Sham		0	0	16000	66000
			1	1	1	7568	128992
			0	0	0	16000	134992
		MF		0	1	2592	176000
			0	0	0	16000	150992
			1	1	0	16000	110992
		Sham		1	0	16000	160992
			1	1	1	656	82992
			0	0	1	9920	68000

			1	1	1	12032	158992
			0	1	0	16000	132992
		MF		0	1	128	88000
			0	1	0	16000	112992
Recall 5	20.11.2020		1	0	1	2752	160000
			0	1	0	16000	174000
			1	0	1	5168	74000
		sham		0	0	16000	162992
			1	0	0	16000	74992
			0	0	0	16000	106000
		MF		0	1	4656	116000
			0	0	0	16000	136000
			1	1	1	208	60992
		sham		1	0	16000	84992
			1	0	1	7312	136992
			0	0	0	16000	86000
		MF		1	0	16000	158000
			0	1	1	12864	84992
			1	1	1	12000	86000
			0	1	0	16000	174992

Sup-table 7: Original behaviour read out data from rainbow trout coded OM19 tested in the horizontal field (B)

Session	Datum	Reiz	Reiz 0->links 1->rechts	Reaktion	Reaktionszeit(ms)	Wartezeit(ms)
Session 1	28.01.2021	1	1	0	16000	106000
		2	1	0	16000	158000
		1	1	0	6016	68992
		2	0	0	16000	132000
		1	1	0	16000	170992
		2	1	0	16000	168992
		2	0	0	16000	58992
		1	0	0	16000	102000
		2	0	0	16000	104000
		1	1	0	16000	180000
		2	1	0	16000	126000
		1	0	0	16000	72000
Session2	29.01.2021	1	1	1	1696	80992
		2	0	0	16000	78000
		1	0	0	16000	56000
		2	1	0	16000	54000

		1	0	0	16000	130992
		2	0	0	16000	72992
		1	0	0	16000	176000
		2	0	0	16000	162000
		1	1	0	16000	160992
		2	1	0	16000	142992
		1	1	0	16000	162992
		2	1	0	16000	104000
Session 3	30.01.2021	1	1	0	16000	140992
		2	1	0	16000	174992
		1	0	0	16000	112000
		2	1	0	16000	74992
		1	0	0	16000	90992
		2	1	0	16000	172000
		1	1	1	12912	162992
		2	1	0	16000	154000
		2	1	0	16000	102000
		1	1	0	16000	90992
		1	1	0	16000	96000
		2	1	0	16000	74992
Session 4	01.02.2021	1	1	0	16000	112992
		2	1	0	16000	64000
		1	1	0	16000	104992
		2	1	0	16000	154000
		1	0	0	16000	142000
		2	0	0	16000	168992
		1	0	0	16000	56992
		2	0	0	16000	90000
		1	0	0	16000	132000
		2	0	0	16000	142000
		1	0	0	16000	102992
		2	0	0	16000	104000
Session 5	02.02.2021	1	0	1	12704	158000
		2	1	0	16000	102000
		1	1	1	11632	156992
		2	1	0	16000	176000
		1	0	0	16000	112992
		2	0	0	16000	126000
		1	0	0	16000	126992
		2	0	0	16000	130000
		1	0	0	16000	142992
		2	0	0	16000	52000
		1	0	0	16000	60992
		2	0	0	16000	88000

Session 6	03.02.2021	1	0	0	16000	66992
		2	1	0	16000	160000
		1	1	0	16000	66992
		2	1	0	16000	122992
		1	1	0	16000	78000
		2	1	0	16000	172992
		1	1	0	16000	116000
		2	1	1	14096	120000
		1	0	0	16000	148992
		2	1	0	16000	78992
		1	1	0	16000	132000
		2	0	0	16000	54000
Session 7	04.02.2021	1	0	0	16000	176992
		2	1	0	16000	132992
		1	0	0	16000	154000
		2	1	0	16000	158000
		1	1	0	16000	92000
		2	1	0	16000	132992
		1	0	0	16000	116000
		2	0	0	16000	154000
		1	0	0	16000	166000
		2	0	0	16000	170992
		1	0	0	16000	164000
		2	0	0	16000	166992
Session 8	05.02.2021	1	1	1	6592	82000
		2	0	0	16000	104000
		1	0	0	16000	164992
		2	0	1	12176	142992
		1	0	1	11680	154992
		2	1	0	16000	86992
		1	1	1	4384	70000
		2	0	0	16000	122992
		1	0	0	16000	152992
		2	0	0	16000	140992
		1	1	1	448	52000
		2	1	1	4720	80992
Session 9	06.02.2021	1	1	1	8240	152000
		2	1	0	16000	160992
		1	1	1	10544	142992
		2	1	1	10528	138000
		1	0	1	3360	142992
		2	1	1	768	164000
		1	1	1	2144	50000

		2	1	1	6960	78992
		1	0	0	16000	166992
		2	1	1	6512	122992
		1	0	1	5712	70992
		2	0	0	16000	132992
Session 10	08.02.2021	1	0	1	9600	64992
		2	1	0	16000	68000
		1	1	1	7168	130000
		2	1	1	2048	106000
		1	0	1	848	52000
		2	1	1	9872	110000
		1	0	1	544	106992
		2	1	0	16000	158000
		1	1	1	112	106000
		2	1	1	3296	78992
		1	1	1	7264	56992
		2	0	1	6816	84000
Session 11	09.02.2021	1	0	1	848	176000
		2	1	1	2096	116992
		1	0	1	6912	136992
		2	0	1	11920	122992
		1	1	1	960	102000
		2	1	1	6400	70000
		1	1	1	3776	72000
		2	1	1	7232	90992
		1	1	1	960	126992
		2	0	1	11664	168000
		1	1	1	3616	138000
		2	0	1	7680	166000
Session 12	10.02.2021	1	0	1	10304	88000
		2	0	1	13568	152992
		1	0	1	2016	122000
		2	1	1	4944	110992
		1	1	0	16000	144000
		2	0	1	5920	58000
		1	1	1	10320	114992
		2	0	1	10848	168992
		1	1	1	9056	116000
		2	0	1	1648	68000
		1	0	1	7728	154000
		2	1	1	12832	66000
Session 13	11.02.2021	1	0	0	16000	56000
		2	0	0	16000	52992

		1	0	1	6064	128000
		2	1	1	6112	160000
		1	1	1	6400	58992
		2	0	1	6272	172000
		1	1	1	5712	60992
		2	1	1	8720	128992
		1	0	1	2144	156992
		2	1	0	16000	90992
		1	1	1	5520	138000
		2	1	0	16000	158992
Session 14	12.02.2021	1	0	1	13808	114992
		2	0	0	16000	86992
		1	0	1	1200	64992
		2	1	0	16000	124992
		1	1	1	12912	86992
		2	1	0	16000	166992
		1	1	1	2464	112992
		2	0	1	9104	70992
		1	0	1	2528	58000
		2	1	0	16000	68992
		1	1	1	11456	86992
		2	0	0	16000	68000
Session 15	13.02.2021	1	0	1	2144	92992
		2	1	0	16000	82000
		1	1	0	16000	160000
		2	1	0	16000	168000
		1	1	1	5392	110992
		2	0	1	9408	68000
		1	1	1	6672	62000
		2	1	1	7168	72000
		1	1	1	2064	80992
		2	1	0	16000	96992
		1	0	1	6912	166000
		2	0	0	16000	130000
Session16	15.02.2021	1	0	1	3696	84992
		2	1	1	3808	64000
		1	1	1	1424	58992
		2	0	0	16000	124000
		1	1	1	2336	120992
		2	1	0	16000	158000
		1	1	1	2112	160000
		2	0	1	10896	122000
		1	1	1	1904	74000
		2	1	0	16000	160992

		1	1	1	3024	56992
		2	0	0	16000	62992
Session 17	16.02.2021	1	0	1	8848	78000
		2	0	0	16000	150992
		1	1	0	16000	94000
		2	0	1	8448	82992
		1	0	0	16000	124992
		2	1	0	16000	86992
		1	0	0	16000	154992
		2	0	0	16000	98000
		1	0	0	16000	178992
		2	1	0	16000	144000
		1	0	0	16000	74000
		2	1	0	16000	170000
Session 18	17.02.2021	1	0	0	16000	110992
		2	0	1	9520	62992
		1	0	1	6128	50992
		2	1	0	16000	54000
		1	1	0	16000	90992
		2	0	0	16000	92992
		1	1	1	13184	168992
		2	0	1	10752	138000
		1	0	0	16000	134000
		2	1	1	7696	52000
		1	1	0	16000	168992
		2	0	1	9216	156000
Session 19	18.02.2021	1	1	1	14144	96000
		2	0	1	12256	126000
		1	1	1	6800	96000
		2	1	0	16000	66992
		1	1	1	12416	78000
		2	0	0	16000	132992
		1	1	1	3776	76000
		2	0	0	16000	76992
		1	0	1	10384	122000
		2	1	1	5104	138000
		1	1	1	10368	70000
		2	1	0	16000	74000
Session 20	19.02.2021	1	0	0	16000	180000
		2	0	0	16000	114992
		1	0	1	7584	50000

		2	1	0	16000	144000
		1	0	1	4816	162992
		2	1	1	12256	70992
		1	1	1	5824	64000
		2	1	0	16000	66992
		1	0	1	3968	126000
		2	1	0	16000	78000
		1	0	1	11472	94000
		2	1	0	16000	172992
Session 21	20.02.2021	1	0	0	16000	168992
		2	1	0	16000	120000
		1	0	1	8240	118000
		2	0	0	16000	86992
		1	1	1	11824	118000
		2	1	0	16000	176992
		1	1	1	7968	76000
		2	1	0	16000	102000
		1	0	1	14288	120000
		2	1	0	16000	160000
		1	1	0	16000	64992
		2	0	0	16000	88000
Session 22	22.02.2021	1	1	0	16000	70992
		2	1	0	16000	158992
		1	1	1	6560	156992
		2	1	0	16000	114000
		1	1	1	5920	96992
		2	0	0	16000	58000
		1	1	1	464	126000
		2	0	0	16000	86000
		1	1	0	16000	138000
		2	0	0	16000	160992
		1	1	1	13424	170992
		2	1	0	16000	172992
Session 23	23.02.2021	1	0	0	16000	84992
		2	1	0	16000	126992
		1	0	1	7744	154992
		2	0	0	16000	106992
		1	1	1	656	160992
		2	1	0	16000	152992
		1	1	1	11920	114992
		2	1	0	16000	138992

		1	1	1	4800	150992
		2	1	0	16000	84992
		1	0	1	7648	82992
		2	0	0	16000	114992
Recall 1	24.02.2021					
MF	1	0	1	0	3440	64992
	2	1	0	1	16000	82992
MF	1	0	1	0	5280	156000
	0	0	0	1	16000	142992
	2	0	0	1	16000	128992
L	0	0	0	1	16000	70992
MF	1	0	1	0	4416	154000
	0	0	0	1	16000	176992
	2	1	0	1	16000	58992
L	0	1	1	0	8096	96992
MF	1	1	0	1	16000	60000
	2	1	0	1	16000	102992
MF	1	1	1	0	10768	80992
	2	0	0	1	16000	68000
MF	1	1	1	0	10064	124000
	2	1	0	1	16000	116992
Recall 2	25.02.2021					
MF	1	1	1	0	4896	92992
	2	0	0	1	16000	98992
MF	1	0	0	1	16000	80000
	0	0	1	0	7360	90992
	2	0	0	1	16000	162992
MF	1	0	1	0	9856	64000
	2	1	0	1	16000	96000
L	0	1	0	1	16000	128992
MF	1	0	1	0	11536	168000
	0	0	0	1	16000	166992
	2	0	0	1	16000	78000
L	0	0	0	1	16000	74000
MF	1	0	1	0	5808	140992
	2	1	0	1	16000	90000
MF	1	0	1	0	12880	148000
	2	0	0	1	16000	160000
Recall 3	27.02.2021					
MF	1	0	1	0	6848	86000
	2	1	0	1	16000	118992
MF	1	1	1	0	1728	150992
L	0	1	0	1	16000	118992
	2	1	1	0	12512	76000

MF		1	0	1	0	3120	94000
		0	0	0	1	16000	164992
		2	0	0	1	16000	80000
		0	0	0	1	16000	166000
MF		1	0	1	0	3248	52000
		2	0	0	1	16000	156992
L		0	0	0	1	16000	126992
		2	1	0	1	16000	132992
MF		1	0	1	0	4080	112992
		2	0	0	1	16000	64992
MF		1	1	1	0	4208	100000
Recall 4	28.02.2021						
MF		1	1	1	0	4464	50000
		2	0	0	1	16000	168992
MF		1	0	1	0	4624	154000
L		0	0	0	1	16000	158000
		2	1	0	1	16000	114992
L		0	1	0	1	16000	98992
MF		1	1	0	1	16000	108992
		0	1	0	1	16000	104000
		2	0	0	1	16000	114992
MF		1	0	1	0	11072	98992
		2	1	0	1	16000	140000
		0	1	0	1	16000	132992
MF		1	1	1	0	12640	124992
		2	1	0	1	16000	148000
MF		1	1	1	0	4656	140992
		2	1	0	1	16000	166992
Recall 5	01.03.2021						
MF		1	0	1	0	7888	74992
		2	0	0	1	16000	50992
MF		1	1	1	0	13616	92000
		0	1	0	1	16000	112000
		2	1	0	1	16000	142000
MF		1	1	1	0	9072	108992
L		0	1	1	0	6544	136000
		2	0	0	1	16000	114992
MF		1	0	1	0	5488	122992
		0	0	0	1	16000	152000
		2	1	0	1	16000	172000
L		0	1	0	1	16000	156000
MF		1	1	1	0	7904	160992
		2	0	0	1	16000	144992
MF		1	1	1	0	2352	108000
		2	0	0	1	16000	160000

Sup-table 8: Original behaviour read out data from rainbow trout coded OM20 tested in the horizontal field (B)

Session	Datum	Reiz	0->links 1->rechts	Reaktion	Reaktionszeit(ms)	Wartezeit(ms)
Session 1	25.01.2021	1	0	0	16000	68000
		2	0	0	16000	50000
		1	0	0	16000	166000
		2	1	0	5680	56992
		1	1	0	16000	64992
		2	0	0	16000	78992
		1	0	0	16000	156000
		2	0	0	16000	52992
		1	0	0	16000	66992
		2	0	0	16000	64992
		1	0	0	16000	58000
		2	0	0	16000	148992
Session2	26.01.2021	1	0	0	16000	118000
		2	0	0	16000	114992
		1	0	0	16000	106992
		2	0	0	16000	56000
		1	0	0	16000	116000
		2	0	0	16000	56000
		1	0	0	16000	50000
		2	0	0	16000	80992
		1	0	0	16000	122000
		2	0	0	16000	66000
		1	0	0	16000	78992
		2	0	0	16000	152992
Session 3	27.01.2021	1	1	0	16000	122000
		2	0	0	16000	156992
		1	0	0	16000	152000
		2	0	0	16000	88000
		1	1	0	16000	66992
		2	1	0	16000	62992
		1	0	0	16000	178992
		2	0	0	16000	52992
		1	0	0	16000	166992
		2	0	0	16000	88000
		1	0	0	16000	84992
		2	0	0	16000	166992
Session 4	28.01.2021	1	1	0	16000	176992
		2	1	0	16000	76000
		1	1	0	16000	64992
		2	1	0	16000	98000

		1	1	0	16000	90992
		2	1	0	16000	94992
		1	1	0	16000	114000
		2	1	0	16000	160000
		1	1	0	16000	84992
		2	1	0	16000	110000
		1	1	0	16000	128992
		2	1	0	16000	100000
Session 5	29.01.2021	1	1	1	14448	168000
		2	0	1	2112	146992
		1	0	0	16000	80992
		2	0	0	16000	66992
		1	0	0	16000	66992
		2	0	1	1248	64000
		1	1	1	7968	54000
		2	0	0	16000	144000
		1	0	0	16000	110000
		2	1	1	13616	62000
		1	1	1	3200	130992
		2	1	1	6464	168000
Session 6	30.01.2021	1	0	0	16000	168992
		2	1	0	16000	116000
		1	0	0	16000	174000
		2	0	0	16000	158992
		1	0	1	7328	68992
		2	1	0	320	164000
		1	0	1	8992	128992
		2	0	0	14912	70000
		1	0	1	1600	94000
		2	1	0	16000	100000
		1	1	0	16000	108000
		2	1	0	16000	130992
Session 7	01.02.2021	1	0	0	16000	118000
		2	0	0	16000	98000
		1	0	0	16000	150992
		2	0	0	16000	136992
		1	1	0	16000	140992
		2	0	0	13232	80000
		1	0	1	3504	66992
		2	0	1	1968	102000
		1	1	1	1808	50000
		2	0	0	2528	78992
		1	0	1	3888	98000
		2	1	0	3952	50992

Session 8	02.02.2021	1	0	1	12992	126000
		2	1	0	16000	102992
		1	1	1	5888	114992
		2	0	0	16000	66000
		1	0	0	16000	134000
		2	0	0	16000	92000
		1	0	0	16000	96992
		2	0	0	16000	148000
		1	0	0	16000	64992
		2	1	1	9952	150992
		1	1	1	11632	54992
		2	0	0	16000	168000
Session 9	03.02.2021	1	0	0	16000	70000
		2	0	1	4752	92000
		1	1	0	16000	122000
		2	1	0	16000	90000
		1	1	0	16000	114000
		2	1	1	3664	122992
		1	1	1	2544	136000
		2	1	1	3824	134000
		1	1	1	816	74992
		2	0	0	16000	58992
		1	1	1	1152	100000
		2	0	0	16000	164000
Session 10	04.02.2021	1	0	1	2336	124992
		2	1	1	10416	52000
		1	1	1	7312	172992
		2	0	0	16000	58992
		1	1	1	7264	142992
		2	1	1	6528	114992
		1	0	0	16000	74992
		2	0	0	16000	160992
		1	1	1	2064	100992
		2	1	1	11600	120992
		1	1	0	16000	150992
		2	0	1	10864	144000
Session 11	05.02.2021	1	0	0	16000	74992
		2	0	0	16000	86992
		1	1	1	3152	102992
		2	0	0	16000	174000
		1	0	0	16000	96000
		2	1	0	16000	82992
		1	1	1	3712	114992

		2	1	1	10352	80000
		1	0	0	16000	112992
		2	0	0	16000	156000
		1	0	1	2288	170000
		2	0	1	3104	162992
Session 12	06.02.2021	1	0	1	5344	140000
		2	1	0	16000	146992
		1	1	0	16000	108992
		2	1	1	7552	104000
		1	1	1	6896	146000
		2	0	1	9824	170000
		1	0	1	6208	76992
		2	1	0	16000	146992
		1	1	0	16000	154000
		2	1	0	16000	164000
		1	1	1	13952	68992
		2	0	0	16000	162000
Session 13	08.02.2021	1	1	0	16000	56000
		2	1	0	16000	70992
		1	1	1	9744	100000
		2	0	0	16000	144000
		1	0	0	16000	76000
		2	0	1	9760	52000
		1	1	0	16000	78000
		2	0	0	16000	52992
		1	0	1	10368	174992
		2	1	0	16000	146992
		1	0	1	4208	72992
		2	0	0	16000	118992
Session 14	09.02.2021	1	1	1	3488	76992
		2	0	0	16000	132000
		1	0	0	16000	100000
		2	1	0	16000	174992
		1	1	0	16000	146992
		2	1	0	16000	136992
		1	1	0	16000	160992
		2	0	0	16000	124000
		1	0	1	8368	94992
		2	0	0	16000	160992
		1	1	0	16000	178992
		2	1	0	16000	154000

Session 15	10.02.2021	1	0	1	5248	170992
		2	1	1	4416	120992
		1	1	1	6704	106000
		2	0	0	16000	52000
		1	1	0	16000	100000
		2	0	0	16000	152000
		1	1	0	16000	54000
		2	1	0	16000	172000
		1	0	1	11264	92000
		2	0	0	16000	58992
		1	0	1	12864	126992
		2	1	1	9248	76992
Session16	13.02.2021	1	1	1	8944	140000
		2	0	0	16000	100000
		1	0	1	5840	50992
		2	1	0	16000	84992
		1	1	0	16000	116992
		2	1	0	16000	108000
		1	1	0	16000	146992
		2	1	1	8912	70992
		1	0	1	4000	66000
		2	1	0	16000	134000
		1	1	1	6160	104992
		2	1	1	6816	70992
Session 17	15.02.2021	1	1	1	3888	144992
		2	0	1	6464	174000
		1	1	1	1696	86992
		2	0	0	16000	164000
		1	1	1	8672	50000
		2	0	0	16000	68992
		1	1	1	5872	156000
		2	0	0	16000	142992
		1	0	1	464	64000
		2	1	0	16000	64000
		1	0	0	16000	98992
		2	1	0	16000	102000
Session 18	16.02.2021	1	1	1	4048	64000
		2	0	1	9872	120992
		1	0	1	11664	50992

		2	1	0	16000	170992
		1	1	0	16000	168992
		2	1	1	9072	62992
		1	1	1	2624	120000
		2	1	0	16000	96992
		1	1	1	10016	136992
		2	0	0	16000	144000
		1	0	1	7760	100000
		2	1	0	16000	56992
Session 19	17.02.2021	1	0	1	7104	84000
		2	1	0	16000	142000
		1	1	0	16000	56992
		2	0	0	16000	118000
		1	1	1	1008	60992
		2	0	0	16000	62992
		1	0	1	2352	132992
		2	1	0	16000	74992
		1	0	0	16000	164992
		2	0	0	16000	86992
		1	0	0	16000	84992
		2	0	1	10672	154000
Session 20	18.02.2021	1	1	1	13856	60992
		2	1	0	16000	144000
		1	1	1	11712	172992
		2	0	0	16000	94992
		1	1	1	13872	128992
		2	0	0	16000	54000
		1	0	1	6256	164000
		2	0	0	16000	60992
		1	0	0	16000	86992
		2	0	0	16000	136992
		1	0	1	13664	106000
		2	1	0	16000	170992
Session 21	19.02.2021	1	1	1	4144	128000
		2	1	0	16000	178992
		1	1	1	7520	162000
		2	0	0	16000	84992
		1	0	0	16000	86000
		2	0	0	16000	158992
		1	0	1	13760	68992
		2	0	1	8128	88000

		1	1	0	16000	54992
		2	0	0	16000	110000
		1	0	1	10016	166992
		2	1	0	16000	174000
Session 22	20.02.2021	1	0	1	9600	64000
		2	0	1	9424	126992
		1	0	1	9072	148000
		2	1	0	16000	70000
		1	1	1	13360	122000
		2	1	0	16000	74000
		1	1	0	16000	134992
		2	1	0	16000	118000
		1	0	1	12672	94000
		2	1	0	16000	126992
		1	1	1	12560	56000
		2	1	0	16000	120000
Session 23	22.02.2021	1	1	0	16000	146000
		2	1	1	10352	148000
		1	0	1	11632	150992
		2	0	0	16000	68000
		1	1	1	12576	160000
		2	0	1	8192	76000
		1	1	1	7424	84000
		2	1	0	16000	134000
		1	0	1	3440	76992
		2	1	0	16000	80000
		1	1	1	8512	88992
		2	0	0	16000	108992
Session 24	23.02.2021	1	1	1	8944	174000
		2	0	0	16000	162992
		1	0	1	11792	74992
		2	0	0	16000	92992
		1	1	1	3200	126000
		2	0	0	16000	128992
		1	0	0	16000	146000
		2	1	0	16000	66992
		1	0	1	5904	80000
		2	1	0	16000	142000
		1	1	1	12112	56992
		2	0	0	16000	160000

Session 25	24.02.2021	1	0	1	5440	84000
		2	1	1	7008	58000
		2	0	1	528	166000
		1	1	0	16000	142000
		2	1	1	3552	156000
		1	1	0	16000	130000
		2	1	1	9840	104992
		1	1	0	16000	106992
		2	0	1	5920	146992
		1	0	0	16000	116992
		2	1	1	8000	110992
		2	0	0	16000	158000
Session 26	25.02.2021	1	0	1	10240	62992
		2	1	0	16000	140000
		2	0	0	16000	152000
		1	0	1	11408	54992
		2	1	0	16000	76000
		1	1	1	6752	138992
		2	0	0	16000	122000
		1	1	1	5600	112992
		2	0	0	16000	122992
		1	1	1	5424	166000
		2	1	0	16000	170992
		1	1	1	9968	130000
Recall 1	26.02.2021					
MF	1	1	1	0	8288	146992
L	0	1	0	1	16000	60000
	2	0	0	1	16000	82000
MF	1	1	0	1	16000	74992
	2	1	0	1	16000	148000
	0	1	0	1	16000	100992
MF	1	0	1	0	8560	152000
	2	0	1	0	12784	138000
L	0	0	0	1	16000	78000
MF	1	0	1	0	13184	154992
	0	0	0	1	16000	172000
	2	1	0	1	16000	78992
MF	1	0	1	0	8816	108000
	2	1	0	1	16000	170000
	2	0	0	1	16000	72000
MF	1	1	1	0	12256	52992

Recall 2	28.02.2021					
MF	1	0	0	1	16000	64000
	2	1	0	1	16000	56000
MF	1	0	1	1	15024	98992
	0	0	0	1	16000	134000
	2	0	0	1	16000	60000
MF	1	1	1	0	6560	98000
L	0	1	0	1	16000	110000
	2	1	0	1	16000	140000
MF	1	0	1	0	6064	160000
	2	0	0	1	16000	72992
MF	1	1	1	0	11968	72000
	0	1	0	1	16000	148000
	2	1	0	1	16000	86992
L	0	1	0	1	16000	106992
MF	1	1	1	0	12880	80000
	2	0	0	1	16000	72000
Recall 3	01.03.2021					
MF	1	0	1	0	10960	174992
	2	1	0	1	16000	120992
	0	1	1	0	9776	112992
?	1	1	0	1	16000	54000
?	1	1	0	1	16000	76000
MF	1	1	1	0	12544	112992
L	0	1	0	1	16000	74992
	2	1	0	1	16000	174000
	0	1	1	0	6560	80000
?	1	0	0	1	16000	74000
?	1	1	0	1	16000	138000
L	0	1	0	1	16000	106992
MF	1	0	1	0	11344	150992
	2	1	0	1	16000	142000
MF	1	1	0	1	16000	68000
	2	0	0	1	16000	114000
Recall 4	02.03.2021					
MF	1	1	1	0	9904	78992
	0	1	0	1	16000	80992
	2	1	0	1	16000	138992
MF	1	0	0	1	16000	116992
	2	0	0	1	16000	136000
MF	1	0	1	0	11792	102992
	2	1	0	1	16000	168000
MF	1	1	1	0	10304	142992

L	0	1	0	1	16000	118992
	2	0	0	1	16000	126000
	0	0	0	1	16000	88992
MF	1	0	1	0	13520	96000
L	0	0	0	1	16000	66000
	2	1	0	1	16000	116000
MF	1	1	0	1	16000	52992
	2	1	0	1	16000	166992
Recall 5	03.03.2021					
MF	1	1	1	0	9552	124000
L	0	1	0	1	16000	52000
	2	1	0	1	16000	110992
L	0	1	0	1	16000	116992
MF	1	0	1	0	3696	166000
	0	0	0	1	16000	100992
MF	1	0	1	0	11824	144000
	2	1	0	1	16000	112000
MF	1	1	0	1	16000	54992
	0	1	0	1	16000	90992
	2	0	0	1	16000	76992
MF	1	0	1	0	12064	86992
	2	1	0	1	16000	62000
MF	1	0	1	0	9056	174992
	2	0	0	1	16000	84992
MF	1	0	1	0	11920	60992

ELISA Test: original data Extraction Sample A

Daily cortisol levels from 02.06.2022. Elisa test was performed on 08.06.22. Samples were five days in a frozen state.

Sample	Dilution	Wells	Raw	Conc.	Conc. (Average)	%CV	SD	SEM
Control1		G1	1,69	0,4071	0,387	7,36	0,0285	0,0201
		G2	1,75	0,3668				
Control2		H1	0,765	2,161	2,042	8,24	0,168	0,119
		H2	0,819	1,923				
7	0,2	A3	0,985	0,277	0,277	-	-	0
7	0,2	B3	0,956	0,2926	0,2926	-	-	0
8	0,2	C3	0,771	0,4265	0,4265	-	-	0
8	0,2	D3	0,773	0,4247	0,4247	-	-	0
9	0,2	E3	0,879	0,3401	0,3401	-	-	0
9	0,2	F3	0,911	0,3192	0,3192	-	-	0
10	0,2	G3	0,982	0,2786	0,2786	-	-	0
10	0,2	H3	0,999	0,2699	0,2699	-	-	0
11	0,2	A4	1,11	0,2196	0,2196	-	-	0
11	0,2	B4	1,13	0,2117	0,2117	-	-	0
12	0,2	C4	1,31	0,1561	0,1561	-	-	0
12	0,2	D4	1,35	0,1476	0,1476	-	-	0
13	0,2	E4	1,35	0,1471	0,1471	-	-	0
13	0,2	F4	1,37	0,142	0,142	-	-	0
14	0,2	G4	1,37	0,1418	0,1418	-	-	0
14	0,2	H4	1,4	0,1355	0,1355	-	-	0
15	0,2	A5	1,59	0,09727	0,09727	-	-	0
15	0,2	B5	1,54	0,1067	0,1067	-	-	0
16	0,2	C5	1,55	0,1051	0,1051	-	-	0
16	0,2	D5	1,46	0,1223	0,1223	-	-	0
17	0,2	E5	1,59	0,09761	0,09761	-	-	0
17	0,2	F5	1,59	0,09794	0,09794	-	-	0
18	0,2	G5	1,57	0,1007	0,1007	-	-	0
18	0,2	H5	1,68	0,08361	0,08361	-	-	0
19	0,2	A6	1,64	0,08937	0,08937	-	-	0

19	0,2	B6	1,65	0,08798	0,08798	-	-	0
20	0,2	C6	1,67	0,0848	0,0848	-	-	0
20	0,2	D6	1,76	0,07243	0,07243	-	-	0
21	0,2	E6	1,77	0,07099	0,07099	-	-	0
21	0,2	F6	1,75	0,07363	0,07363	-	-	0
22	0,2	G6	1,76	0,07217	0,07217	-	-	0
22	0,2	H6	1,71	0,07913	0,07913	-	-	0

ELISA Test: original data Extraction Sample B

Daily cortisol levels from 02.06.2022. Elisa test was performed on 14.06.22; samples were eleven days in a frozen state.

Sample	Dilution	Wells	Raw	Conc.	Conc. (Average)	%CV	SD	SEM
Control1		G1	1,67	0,3832	0,3532	12	0,0425	0,03
		G2	1,74	0,3231				
Control2		H1	0,756	2,467	2,401	3,89	0,0934	0,066
		H2	0,78	2,335				
7	0,2	A3	0,838	0,4104	0,4104	-	-	0
7	0,2	B3	0,875	0,3789	0,3789	-	-	0
8	0,2	C3	0,549	0,8382	0,8382	-	-	0
8	0,2	D3	0,708	0,5525	0,5525	-	-	0
9	0,2	E3	0,78	0,467	0,467	-	-	0
9	0,2	F3	0,65	0,6379	0,6379	-	-	0
10	0,2	G3	0,883	0,3725	0,3725	-	-	0
10	0,2	H3	0,862	0,3896	0,3896	-	-	0
11	0,2	A4	0,988	0,2995	0,2995	-	-	0
11	0,2	B4	1,11	0,2339	0,2339	-	-	0
12	0,2	C4	1,17	0,2088	0,2088	-	-	0
12	0,2	D4	1,16	0,2146	0,2146	-	-	0
13	0,2	E4	1,24	0,1818	0,1818	-	-	0
13	0,2	F4	1,01	0,2841	0,2841	-	-	0
14	0,2	G4	1,18	0,2047	0,2047	-	-	0
14	0,2	H4	1,17	0,2076	0,2076	-	-	0
15	0,2	A5	1,41	0,1312	0,1312	-	-	0
15	0,2	B5	1,39	0,1349	0,1349	-	-	0
16	0,2	C5	1,5	0,1087	0,1087	-	-	0
16	0,2	D5	1,44	0,1239	0,1239	-	-	0
17	0,2	E5	1,61	0,08639	0,08639	-	-	0
17	0,2	F5	1,64	0,08203	0,08203	-	-	0
18	0,2	G5	1,57	0,09502	0,09502	-	-	0
18	0,2	H5	1,52	0,1045	0,1045	-	-	0

19	0,2	A6	1,66	0,0787	0,0787	-	-	0
19	0,2	B6	1,64	0,08168	0,08168	-	-	0
20	0,2	C6	1,61	0,08657	0,08657	-	-	0
20	0,2	D6	1,48	0,1132	0,1132	-	-	0
21	0,2	E6	1,75	0,06387	0,06387	-	-	0
21	0,2	F6	1,47	0,115	0,115	-	-	0
22	0,2	G6	1,7	0,07199	0,07199	-	-	0
22	0,2	H6	1,66	0,0787	0,0787	-	-	0

ELISA Test: Control experiment with a predefined amount of cortisol (30ng)

Sample	Wells	Raw	Conc.	Conc. (Average)	%CV	SD	SEM
Control1	G1	2,2	0,3618	0,3424	7,99	0,0274	0,0194
	G2	2,26	0,3231				
Control2	H1	0,94	2,513	2,314	12,2	0,282	0,199
	H2	1,05	2,114				
T0D	A3	0,17	30,28	30,28	-	-	0
T0D	B3	0,172	29,71	29,71	-	-	0
T30D	C3	0,171	29,99	29,99	-	-	0
T30D	D3	0,172	29,71	29,71	-	-	0
T60D	E3	0,175	28,88	28,88	-	-	0
T60D	F3	0,174	29,15	29,15	-	-	0
T90D	G3	0,175	28,88	28,88	-	-	0
T90D	H3	0,17	30,28	30,28	-	-	0
T120D	A4	0,177	28,35	28,35	-	-	0
T120D	B4	0,172	29,71	29,71	-	-	0

Control experiments with a predefined amount of cortisol (30 ng) were performed in a 2 hour time range, sampling times from starting point every 30 minutes. The obtained results were used to calculate the recovery and degradation rate of cortisol.

Specificity (Cross Reactivity)

The following materials have been evaluated for cross reactivity by the manufacturer.

Steroids	% Cross reactivity
Testosterone	< 0.1
Corticosterone	6.2
Cortisone	0.8
11-Deoxycorticosterone	2.6
11-Deoxycortisol	50
Dexamethasone	< 0.1
Estriol	< 0.1
Estrone	< 0.1
Prednisolone	100
Prednisone	0.9
Progesterone	< 0.1
17-Hydroxyprogesterone	1.3
Danazole	< 0.1
Pregnenolone	< 0.1
Estradiol	< 0.1
Androstenedione	< 0.1

Behavioural time design for molecular mapping

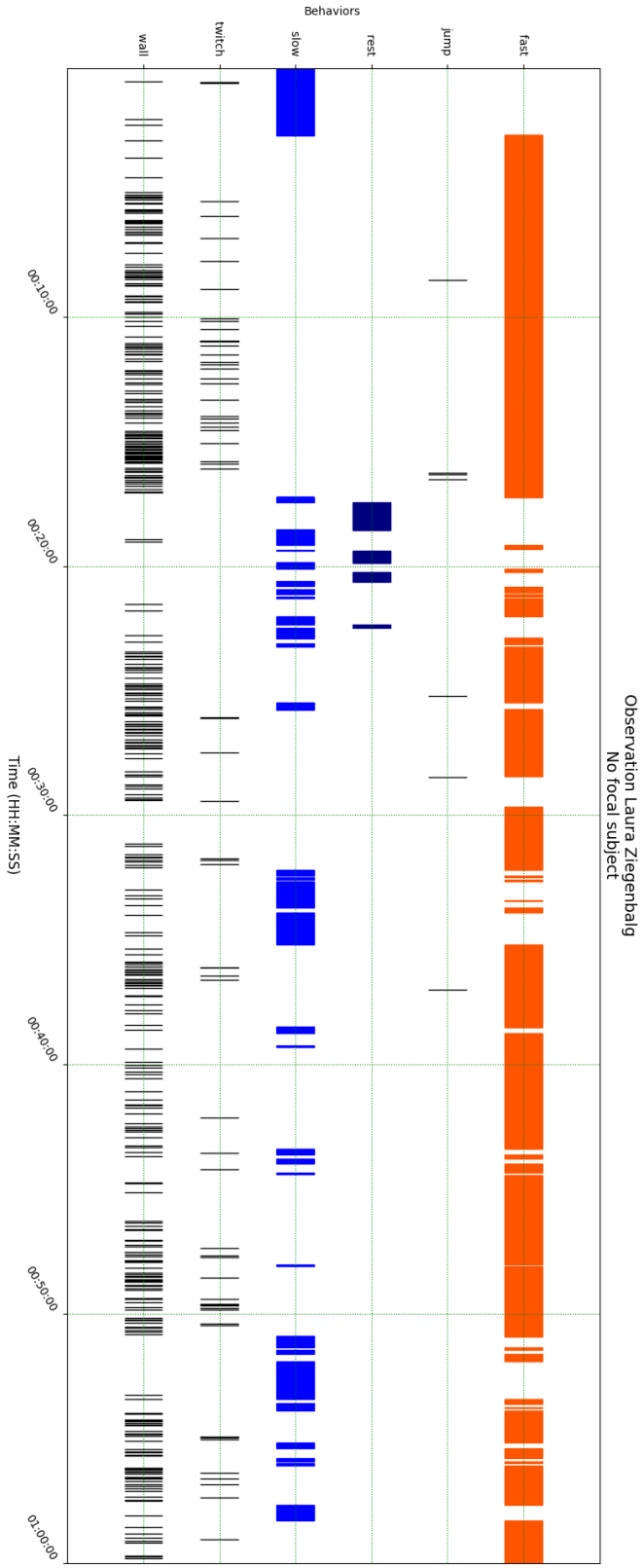

Sup-figure 24: Ethogram of the morning experimental phase

Ethogram of 60 minutes in the morning from 09:30 to 10:30. Behaviour was coded with single events like twitching, touching the wall and jumping, as well as longer occurring events like slow and fast swimming. For a full description of the seen behaviour, see Table 2. Occurring events in numbers, see table 4.

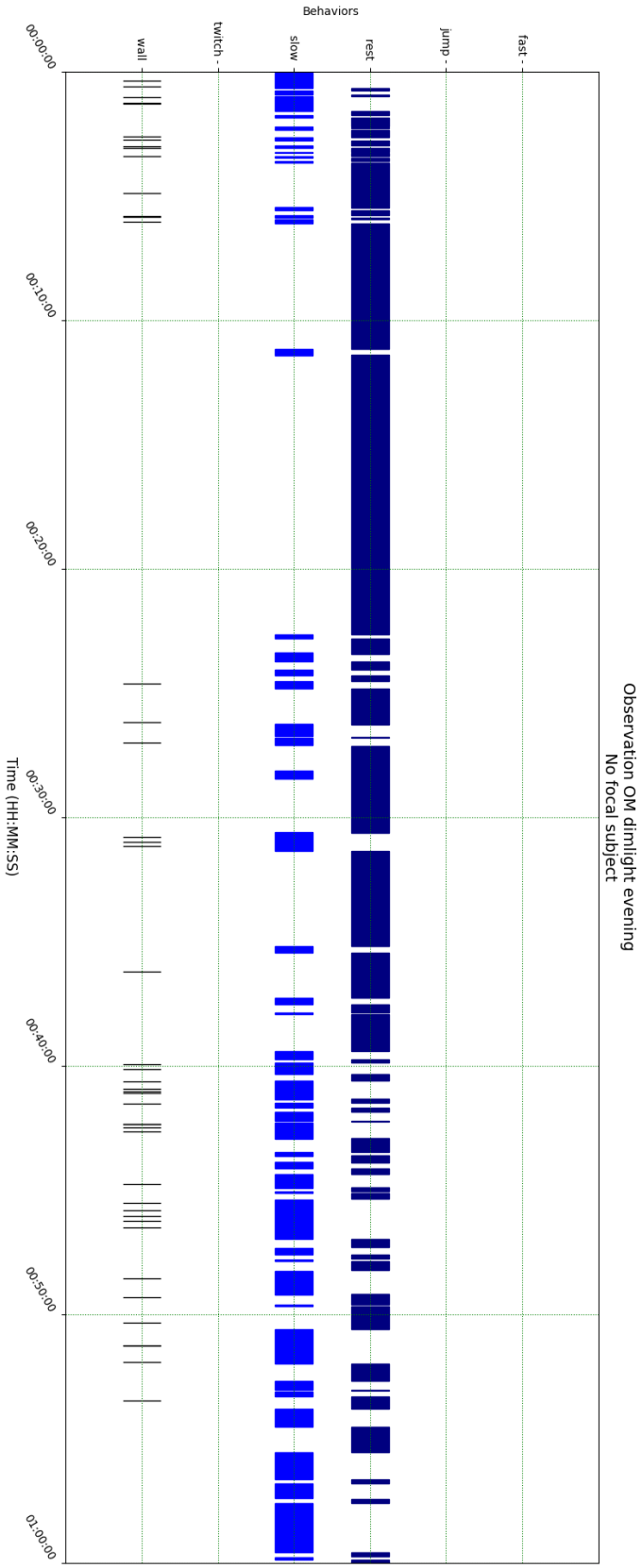

Sup-figure 25: Ethogram of the evening experimental phase

Ethogram of 60 minutes in the evening from 19:30 to 20:30.
Behaviour was coded with single events like touching the wall and longer occurring events like slow and resting phases. For a full description of the seen behaviour, see Table 2. Occurring events in numbers, see table 4.

Immunocytochemistry in Hek293 cell culture

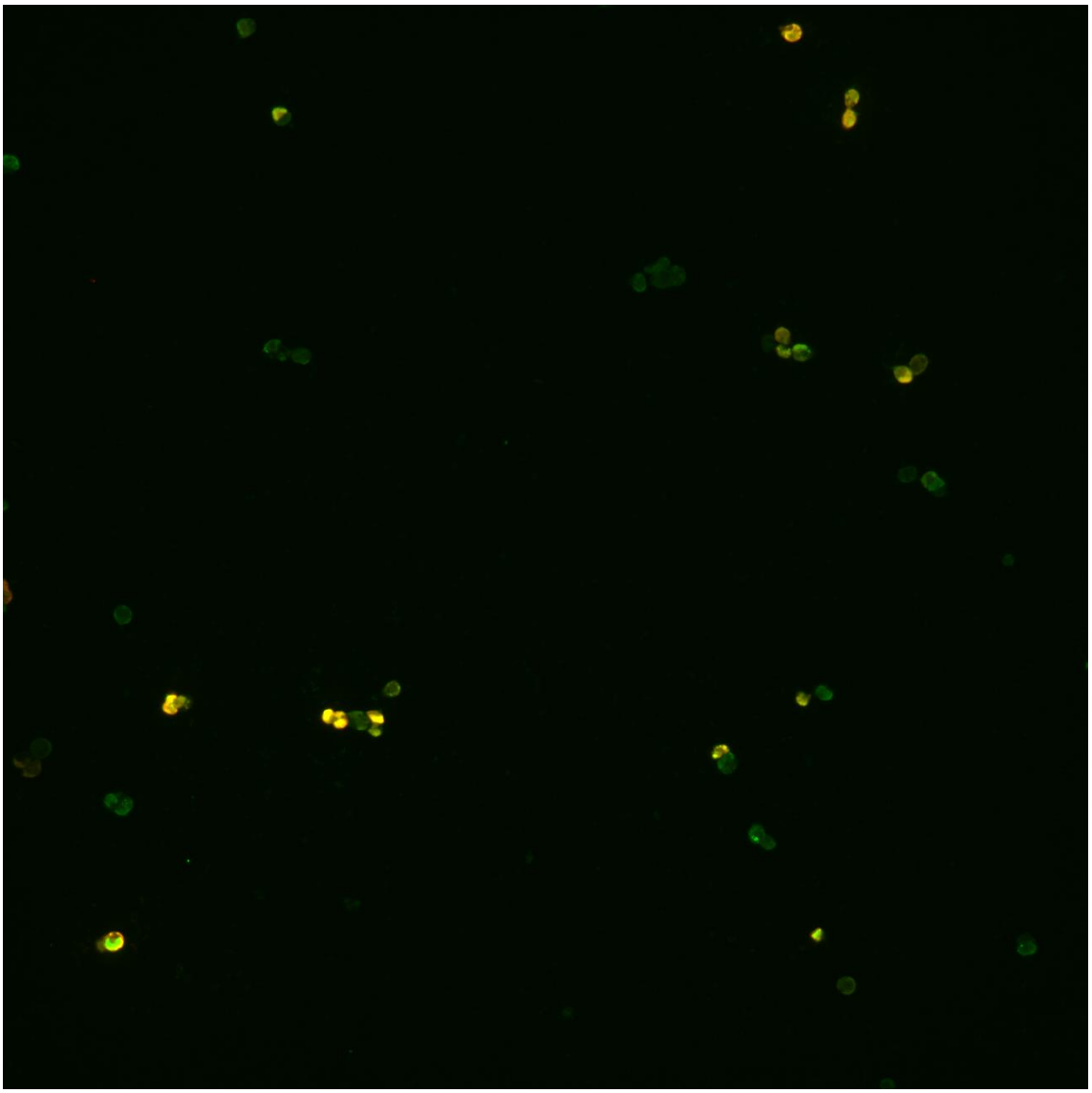

Sup-figure 26: Transfection experiment

Hek293 cells were transfected with vectorDNA (cFos sequence rainbow trout) and analysed based on the co-localization of vector induced pFlag with vectorDNA in the cell nuclei.
The image was taken with an epifluorescence microscope (Leica DM6) using a 20x (NA 1.40) Plan Apochromat objective. These were partially merged into projections from multiple individual images. The pixel size is 2048x2048.
With a wider overview with multiple cells in the view finder, we can see that the transfection was very low, with a rate of less than 30%.

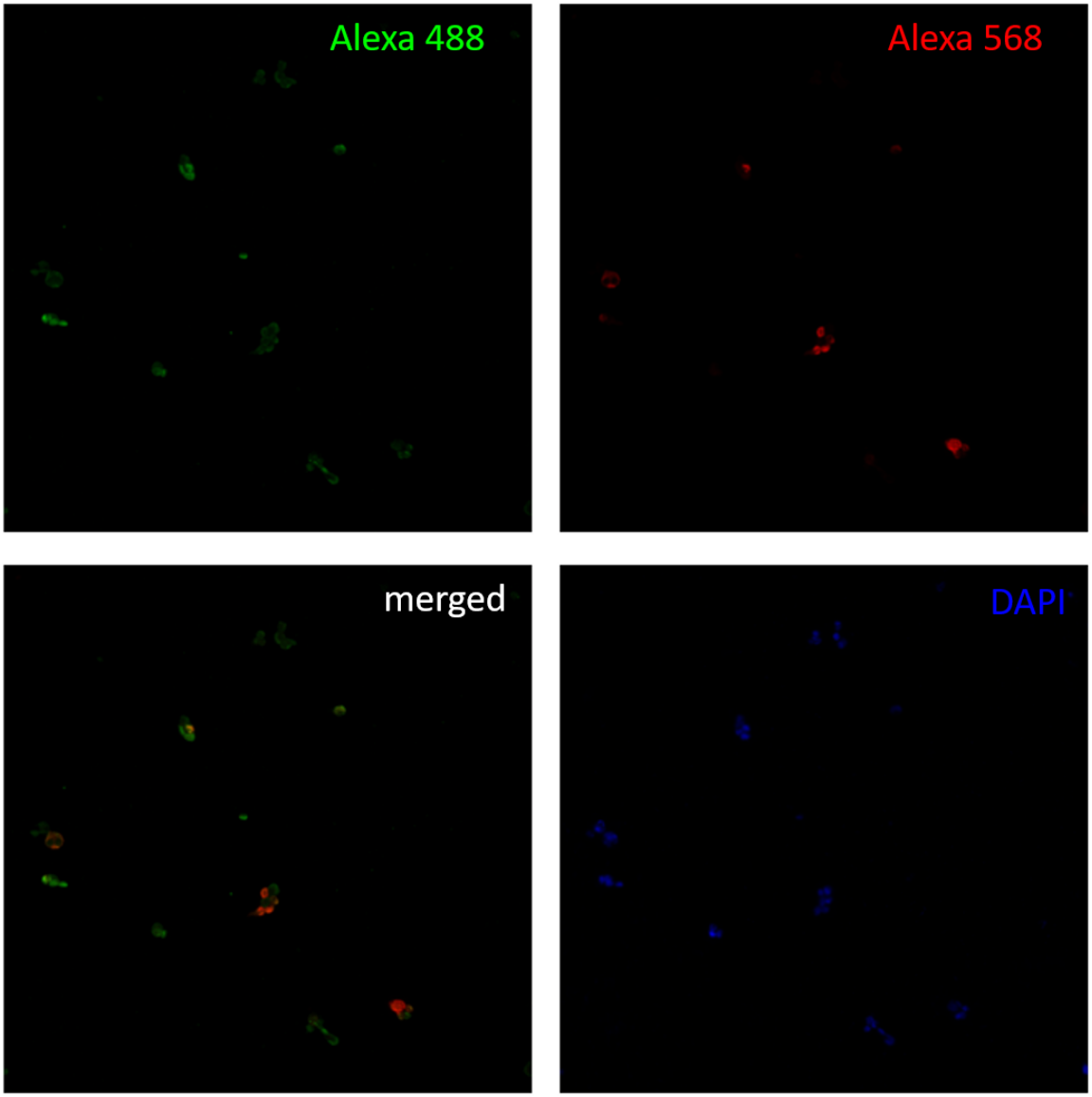

Sup-figure 27: Secondary antibody control in Hek293 cells

Secondary antibodies (gt@ms IgG Alexa488-conjugated and gt@rb IgG Alexa568-conjugated) controls show less fluorescence and no co-localisation like in the main experiments.
The secondary antibody control shows that the labelling observed is only due to binding the secondary antibody to the primary antibody. This control is done by replacing the primary antibody with the same amount of normal serum.

Western blots: original data

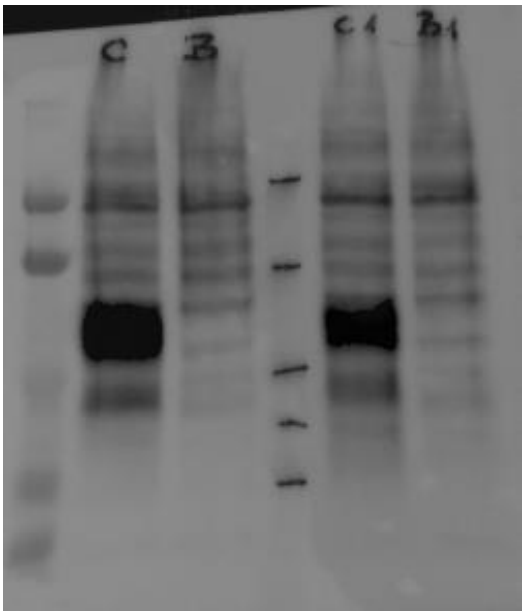

Sup-figure 28: Original from Figure 19

In the protein lane titled “C”, the Hek cells were transfected with the cFos sequence of a rainbow trout. And the lane titled “B”, the Hek cells were transfected with an Amino-terminal FLAG-BAP fusion protein.

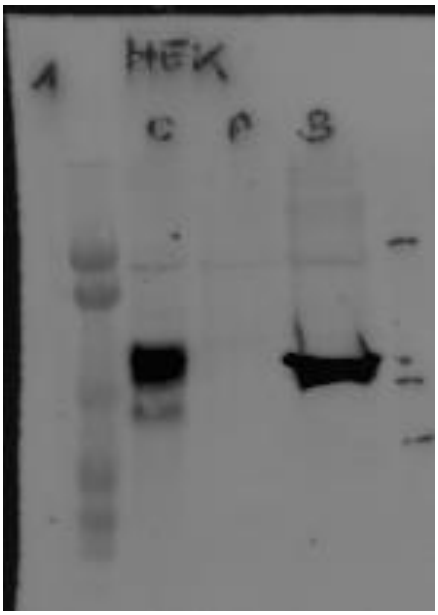

Sup-figure 29: Original from Figure 20

In the protein lane titled “C”, the Hek cells were transfected with the cFos sequence of a rainbow trout. The lane titled “P”, the Hek cells were transfected with an empty pFLAG-CMV™-5.1 Expression Vector. In the lane titled “B”, the Hek cells were transfected with an Amino-terminal FLAG-BAP Fusion Protein.

Table 8.1 Devices

Device	Company / manufacturer
Analogue HD Monitoring Set: 8 channel Video Recorder	Abus Security Tech Germany
Analogue Kamera HD Monitoring Set: 8-Kanal Video Rekorder	ABUS Security Tech Germany
Axio Scan.Z1	Zeiss, Oberkochen, Germany
Bipolar Operational Power Supply/Amplifier BOP 100-4M 4 88 D	KEPCO
Camera MC 170 HD	Leica, Wetzlar, Germany
ChemiDoc MP Imaging System	BioRad
CHROMABOND SPE vacuum chamber 12 positions	MACHEREY-NAGEL
Compound Binocular microscope OBE 112	KERN
Cryostat CM 1860	Leica, Wetzlar, Germany
DM 6	Leica, Wetzlar, Germany
External filter CristalProfi e402 greenline	JBL
Heating plate Typ 12801	Medax
Laptop Dell Latitude 5580	DELL
Magnetrührer mit Heizplatte VMS-A	VWR Avantor
Mini Rocker-Shaker MR 1	BioSan
Mini-PROTEAN Tetra System	BioRad
Multiskan™ GO Microplate Spectrophotometer	Thermo Scientific
Oven	Heraeus
Platform shaker Titramax 1000	Heidolph
PowerPac HC	BioRad
Scale PCB	Kern
Spektralphotometer 6300PC	VWR®
Stereo microscope MDG41	Leica, Wetzlar, Germany
three-axis fluxgate magnetometer	Institut Dr. Foerster GmbH, Reutlingen, Germany
Tube Revolver Rotator	Thermo Scientific™
Ultraschall-Homogenisator	Fisherbrand™
Ultrasonic cleaning Sonorex RK-31	Bandelin
Vacuum pump-system	VWR®

Water bath WNB 10	Memmert
Zentrifuge 5417 R	Eppendorf

Table 8.2 Chemicals and reagents

Name	Company / manufacturer
3,0 mm Premium Pellets	Forellenfutter AG
3'3-diaminobenzidine tetrahydochlorid	CarlRoth
Acetic acid	CarlRoth
Agar-Agar	CarlRoth
Ammonium chloride	CarlRoth
Ammonium nickel(II) sulfate hexahydrate	Sigma Aldrich
Ammonium persulfate (APS 10%)	CarlRoth
Cobalt(II) chloride hexahydrate	CarlRoth
D(+)-Saccharose	CarlRoth
di-Potassium hydrogen phosphate	VWR Chemicals
di-Sodium hydrogen phosphate dihydrate	VWR Chemicals
Elma lab clean A25	AllPax
Ethyl acetate	VWR Chemicals
Ethyl-3-aminobenzoat –methansulfonat (MS-222)	Sigma Aldrich
Ethylenediamine tetraacetic acid	CarlRoth
Glucose oxidase	CarlRoth
Glycerin	Sigma Aldrich
Hydrochloric acid	VWR Chemicals
ISO 2-Propanol	Sigma Aldrich
Milk Pulver	Saliter
Neo-Clear™	Sigma Aldrich
Osmose ReMineral+	Dennerle
Paraformaldehyde	CarlRoth
Potassium chloride	VWR Chemicals
Potassium dihydrogen orthophosphate	Fisher Chemicals
ROTI®Mount	CarlRoth
Sodium acetate	CarlRoth

Sodium azide	CarlRoth
Sodium chloride	CarlRoth
Sodium dihydrogen phosphate dihydrate	VWR Chemicals
Sodium hypochlorite	CarlRoth
TEMED	CarlRoth
Tris	CarlRoth
Tri-Sodium citrate dihydrate	VWR Chemicals
Triton X-100	CarlRoth
Penicillin G Sodium salt	Sigma Aldrich
Poly-L-lysine solution	Sigma Aldrich

Table 8.3 Materials

Name	Company / manufacturer
12-well plates	Sarstedt
1cm round coverslips	CarlRoth
6-well plates	Sarstedt
Artemia Sieve Combination	HOBBY
Cell scrapers	Avantor
Centrifuge tubes (Falcon), PP, 15 ml	Brand
Centrifuge tubes (Falcon), PP, 50 ml	Brand
Dumont #5 - Fine Forceps	Fine science tools FST
Dumont #5 Forceps	Fine science tools FST
Dumont #7 - Fine Forceps	Fine science tools FST
Dumont #7b Forceps	Fine science tools FST
Eppendorf Pipette Research plus 0,5 – 10 µL	Eppendorf
Eppendorf Pipette Research plus 100 – 1,000 µL	Eppendorf
Eppendorf Pipette Research plus 2 – 20 µL	Eppendorf
Eppendorf Pipette Research plus 20 – 200 µL	Eppendorf
Epredia™ SuperFrost Ultra Plus™ GOLD Adhesion Slides	Thermo fisher Scientific™
Glas beaker (different sizes)	Duran Schott
Gloves, NITRIL- (TOUCH N TUFF)	Ansell
Gloves, NITRIL- comfort	StarGuard

High precision cover glas 24x60mm	CarlRoth
Insect Pins	Fine science tools FST
Measuring cylinder (different sizes)	VWR®
Mini-PROTEAN Glass plates 1mm spacer	BioRad
Mini-PROTEAN short plates	BioRad
MX35 ultra Microtome Blade	Thermo fisher Scientific™
nitrocellulose membrane (pore size 0.2 µm)	Whatman PROTRAN
Parafilm PM-999	Bemis
Plastic measuring cup 1000ml	VITLAB
SIMAX reagent bottle (different sizes)	Kavalier
snap-cap bottles 8ml "ROLLRAND-SchnappdeckelGlas"	IDL GmbH & Co. KG
Solid glass Aquarium 60 x 30 x 30 cm	Marina
Solid Phase Extraction CHROMABOND column HR-X (45µm, fine-grained)	MACHEREY-NAGEL
Spring Scissors - 8mm Cutting Edge	Fine science tools FST
Sterile disposable scalpels	Swann-Morton
Surgical Scissors - Sharp-Blunt edges	Fine science tools FST
Tissue culture dishes 10mm	Sarstedt
Tissue culture dishes 6mm	Sarstedt
Tissue culture flasks 75cm^2 – vented	Sarstedt
Transferpette® S Multichannel Pipette 8-channel 30 - 300 µL	Brand
Vannas Spring Scissors – Titanium - curved	Fine science tools FST

Table 8.4 Primary antibodies

Antibodies	Dilution	Company / manufacturer	Cat. No.
Mouse anti cFos (mc)	1:100	Santa Cruz Biotechnology	sc-166940
Mouse anti Flag (mc)	1:2000	Sigma-Aldrich	F3165
Rabbit anti Flag (pc)	1:250	Invitrogen	PA1-984B

Table 8.5 secondary antibodies

Antibodies	Dilution	Company / manufacturer	Cat. No.
Goat anti-mouse IgG Alexa488-conjugated	1:600	Invitrogen	A28175
Goat anti-mouse IgG HRP-conjugated	1:2000	Sigma-Aldrich	A4416
Goat anti-rabbit IgG Alexa568-conjugated	1:600	Invitrogen	A-11011
Horse anti-mouse IgG biotin-conjugated	1:500	Biozol	VEC-PK-6102

Table 8.6 Tracer

Tracer	Company / manufacturer	Cat. No.
Dil-Färbemittel (1,1'-Dioctadecyl-3,3,3',3'-Tetramethylindocarbocyaninperchlorat ('DiI'; DiIC18(3))))	Invitrogen	D282

Table 8.7 Kits

Kit	Company / manufacturer	Cat. No.
Cortisol-free in Salvia ELISA Kit	Demeditec	DES6611
Pierce™ ECL Western Blotting-Substrate	Thermo Scientific™	32106
TGX Stain-FreeTM FastCastTM acrylamide Kit	Bio-Rad	#1610182
VECTASTAIN Elite ABC-HRP Kit, Peroxidase (Mouse IgG)	Biozol	VEC-PK-6102

Curriculum Vitae

Name	Laura Ziegenbalg
Geburtsdatum / Ort	31.08.1988 / Bremen

BILDUNG

2017 - 2023	Strukturierte Promotion „Molekulare Basis sensorischer Systeme“ (Universität Oldenburg) Institut für Biologie und Umweltwissenschaften, AG Sensorische Biologie der Tiere (Prof. Dr. Michael Winklhofer) Abschluss: Dr. rer. nat. (voraussichtlich im November 2023) Titel: Neurobehavioural correlates of magnetoreception in rainbow trout (Oncorhynchus mykiss)
2012 – 2015	Carl von Ossietzky Universität Oldenburg | Master of Science, Biologie Masterarbeit „Interaktion von räumlicher Quellentrennung und Vokalpaarung auf informelle Maskierung bei Wüstenrennmäusen (*Meriones unguiculatus*)“ (Note: 2,3)
2008 – 2012	Carl von Ossietzky Universität Oldenburg | Bachelor of Science, Biologie Bachelorarbeit “Versuche zur Magnetorientierung von Zugvögeln unter Störfeldbedingungen“(Note: 1,5)
2004 – 2007	Berufsbildende Schulen Osterholz-Scharmbeck Allg. Hochschulreife

ARBEITSERFAHRUNG

05/2016 – 08/2016	Mitarbeiterin in Forschungsprojekt von Max-Planck-Institut für Ornithologie in Kooperation mit dem Loro Parque (Teneriffa)
02/2016 – 04/2016	Culinari Feinkostladen (Barista, Verkauf von Lebensmitteln)
04/2015 – 01/2016	Büromanagement bei Geoservice Schaffert (Dipl.-Geologe)
05/2015 – 08/2015	Laborassistentin an der Carl von Ossietzky Universität Oldenburg (AG Zoophysiologie & Verhalten, Prof. Klump)
06/2013 – 09/ 2014	wissenschaftliche Hilfskraft / Vogelpflegerin Carl von Ossietzky Universität Oldenburg

Zugsaison: Frühjahr 2012 & Herbst 2013	Studentische Hilfskraft für verhaltensbiologische Versuche (Arbeitsgruppe Neurosensorik, Prof. Mouritsen)

SOZIALES ENGAGEMENT

2007 – 2008	Freiwilliges Soziales Jahr | The Mount Camphill Community, Wadhurst ,East Sussex
2004 – 2007	Freiwillige Mitarbeit im Sportsverein VfR Seebergen/Rautendorf

WISSENSCHAFTLICHE METHODEN

Verhalten	Horner-typ shuttle box – operante Konditionierungsverfahren
Immunhistologie	Gewebepräparation (olfaktorisches Epithelum, Retina, Gehirn) Perfusion an Fischen Fixierung, Einbettung und Erstellung von Gefrierschnitten klassische histologische Färbungen DAB und immuncytochemische Färbungen Gewebeklärung iDISCO (Gehirn (Regenbogenforelle, Zebrafisch) Applikation von fluoreszierenden Tracern
Zellkultur	Kultivierung von Hek293 Zellen Transfektionen
Biochemie	SDS-PAGE und Western-blotting Enzyme-linked Immunosorbent Assay (ELISA)
Mikroskopie-Techniken	Konfokales Fluoreszenzmikroskopie AxioScan Z.1 Zeiss Lightsheet Fluorescence Microscopy
andere	Magnetosomeextraction

BESONDERE KENNTNISSE

Projektmanagement	Weiterbildung im Bereich Projektmanagement (Dezember 2015)
Management	

	Betreuung von Abschlussarbeiten (B. Sc.) und eigenständig Forschungsmodule (Master)
	Organisationteam im Rahmen des Graduiertenkollegs „Molekulare Basis sensorischer Systeme“ (Prof. Dr. Karl Koch)
	Internationale “Sensory Systems in Health and Disease” Konferenz in Zusammenarbeit mit Daniele Dell’Orco (Universita di Verona)
Sprachen	Deutsch (Muttersprache)
	Englisch (fließend)
	Französisch (Basiswissen)
	Spanisch (Basiswissen)
EDV-Kenntnisse	MS Office (Word, Excel, Powerpoint)
	Bildbearbeitung (Adobe Photoshop, Adobe Illustrator, CorelDraw, ImageJ (Fiji))
	3D Zeichenprogrammen (SketchUp)
	Videoanalyse (BORIS)
	Datenverarbeitung und Statistik (Origin, SPSS)
	Zitierprogramme (Zotero)
	Content-Management-System für Websites (TYPO3)
	Raspberry pi

Danksagung

Ich möchte diese Gelegenheit nutzen, um meinen aufrichtigen Dank an all jene auszudrücken, die mich während der Erstellung meiner Promotionsarbeit unterstützt und inspiriert haben.

Mein ausdrückliches Dankeschön gilt meinem Doktorarbeit-Betreuer Prof Dr Michael Winklhofer. Ich danke Dir für Deine Hilfe und Ratschläge und besonders Dein Vertrauen in mich.
Der AG Biodiversität und Evolution der Tiere, insbesondere meiner Zweitprüferin Prof Dr Gabriele Gerlach, die mich mit dem nötigen Know-how anregte und mein erstes Tiermodell, den Zebrafisch (*Dario rerio*) zur Verfügung stellte, gilt mein Dank.

Bedanken möchte ich mich auch bei allen Mitarbeitern der AG Sensorische Biologie der Tiere für die angenehme Arbeitsatmosphäre und das freundliche Miteinander. Besonderer Dank gilt dabei Dr. Susanne Schwarze für die Unterstützung in meiner Anfangsphase, ohne Dich hätte ich nicht gewusst, wo ich beginnen sollte. Danke auch an meine lieben Kollegen Domna Zourelidou, Dr. Franziska Curdt, Dr. Lisa Spieker und Julia Brandt. Die vergangenen Jahre mit Euch kann ich nur mit Lachanfällen, gutem Essen, besseren Gesprächen und Wahnsinn zusammen fassen.

Weiterhin möchte ich mich bei allen Mitarbeitern der AG Neurobiologie des Sehens bedanken, besonderer Dank gilt dabei Hoto für die Lehre und Unterstützung während meiner Labortätigkeit. Ebenso bedanke ich mich für die Unterstützung und die Möglichkeit, die Labore der AG Biochemie zu nutzen. Für die zur Verfügungsstellung der geschirmten Versuchshütte möchte ich mich bei Prof Dr Henrik Mouritsen bedanken.
Danke an alle Mitglieder des GRK 1885: Molekulare Basis sensorischer Biologie für die stimulierenden Seminare und Ausflüge / Konferenzen, die wir gemeinsam geplant haben.

Ein besonderer Dank gilt meiner Familie und all meinen Freunden. Insbesondere möchte ich mich bei meinen Eltern bedanken, die mich immer unterstützen und stets ein offenes Ohr für mich haben.

Krissi für die dringend notwendigen Kaffeepausen, Jasmin für alle Gespräche und die geselligen Abende (oder eher Gossip Girl-Abende) und Dana, von Bachelor über Master in die Promotion, deine ständige Begleitung und alles darüber hinaus bleibt, dafür bin ich Euch allen von Herzen dankbar.

Erklärung gemäß § 12 Abs. 2 der Promotionsordnung

Hiermit erkläre ich gemäß § 12 Abschnitt 2 der gemeinsamen Promotionsordnung der Fakultät II, Fakultät V und Fakultät VI vom 18.03.2014, dass
(i) ich die Dissertation selbstständig verfasst habe und die benutzten Hilfsmittel verständig angegeben sind,
(ii) bisher wurde noch kein Teil der Dissertation veröffentlich, die jeweiligen Manuskripte sind unter der Rubrik „Publications“ anzufinden,
(iii) die Dissertation wird weder in Teilen noch in ihrer Gesamtheit einer anderen Hochschule zur Begutachtung in einem Promotionsverfahren vorgelegt,
(iv) der Grad eines Doktor der Naturwissenschaften (Dr. rer. Nat.) wird angestrebt
(v) der angestrebte Grad soll in der Promotionsurkunde in der männlichen Form als Doktor aufgeführt werden,
(vi) die Leitlinien guter wissenschaftlicher Praxis der Carl von Ossietzky Universität Oldenburg wurden befolgt, und
(vii) das im Zusammenhang mit dem Promotionsvorhaben keine kommerziellen Vermittlungs- oder Beratungsdienste (Promotionsberatung) in Anspruch genommen worden sind.

Oldenburg, der 27.09.2023

Laura Ziegenbalg